Ferdowsi University of Mashhad

ISSN 2008-9147

Numbers: 12

JCMR

Journal of Cell and Molecular Research

Volume 6, Number 2, Winter 2014

بسم الله الرحمن الرحيم

Issuance License No. 124/902-27.05.2008 from Ministry of Culture and Islamic Guidance
Scientific Research Issuance License No. 161675 from the Ministry of Science, Research and Technology, Iran

Journal of Cell and Molecular Research (JCMR)

Volume 6, Number 2, Winter 2014

JCMR Office: Department of Biology, Faculty of Sciences, Ferdowsi University of Mashhad, Mashhad, Iran.
Postal Code: 9177948953
P.O. Box: 917751436
Tel: +98-513-8804063
Fax: +98-513-8795162
E-mail: jcmr@um.ac.ir
Online Submission: http://jcmr.um.ac.ir

Table of Contents

The Editorial

The pluripotency feature of cancer cells; product of a harmony or an output of a disharmony

Hesam Dehghani[1,2,3]

1- *Embryonic and Stem Cell Biology and Biotechnology Research Group, Institute of Biotechnology, Ferdowsi University of Mashhad, Mashhad, Iran*
2- *Division of Biotechnology, Faculty of Veterinary Medicine, Ferdowsi University of Mashhad, Mashhad, Iran*
3- *Editorial Board Member of JCMR, JCMR Office, Department of Biology, Faculty of Sciences, Ferdowsi University of Mashhad, Mashhad, Iran*

Received 31 Jul 2014 Accepted 04 Sep 2014

Summary

Pluripotency is a central feature of stem and cancer cells. This feature enables cancer cells to self-renew and trans-differentiate. In this editorial, it is hypothesized that in cancer cells synchronized events rather than segmented procedures may lead to pluripotency.

***Keywords*:** Pluripotency, Stem cells, Cancer cells

The state of pluripotency is operationally defined by self-renewal and a capacity to differentiate into multiple lineages. However, numerous features have also been discovered that contribute to pluripotency and immortality. These features include high level of transcription, open chromatin and nuclear organization, re-expression of telomerase, activation of c-myc network, activity of specific transcription factors, and utilization of certain cell signaling pathways. In certain pluripotent states like what is existent in primordial germ cells, some other features like migratory behavior has also been observed.

Recent findings indicate that cancer cells and pluripotent cells (embryonic stem cells, adult stem cells, and primordial germ cells in some in vitro conditions) possess and use similar features. It seems that features of open organization of chromatin and increased level of transcription are shared between cancer and pluripotent cells (Dehghani et al., 2005, Efroni et al., 2008, Gaspar-Maia et al., 2011). Similarly, the increased activity of stemness transcription factors has been documented in both cancer and stem cells (Apostolou et al., 2012, Liu et al., 2013). On the other hand, the myc regulatory network frequently known for its involvement in cancer is also characterized to be a major player of pluripotency (Hurlin et al., 2013, Hirasaki et al., 2013, Chappell et al., 2013, Hann et al., 2014). With these similarities in mind and considering that cancer cells partially fulfill the requirements for the operational definition of stem cells, ability to self-renew and trans-differentiation into different cells (Sabe et al., 2011, Barneda-Zahonero et al., 2012, Shekhani et al., 2013), the important question that arises is that if the pluripotency feature is necessary for the cancerous nature of cancer cells, and whether this feature ever contributes to the pathogenesis of cancer.

Becoming a cancer cell is a much more coordinated and synchronized phenomenon that could be justified only by segmented cellular events such as mutations, cell-cycle control defects, and disengagement of apoptotic mechanisms. Inspired by Gottfried Wilhelm von Leibniz, the 17th century philosopher, there could be a pre-established synchronization and harmony among different features in order to reach a specific state of activity or a specific nature like cancer. Perhaps it is a harmony and synchronization between different features that provides a new identity for cancer cells. This is in prominent contrast to the idea that it is a disharmony and dysregulation that brings about cancer. If after all cancer is the result of a harmony of selected cellular features and abilities, there will be no doubt that the stemness and pluripotency is one of the most central features of cancer, which is actively regulated in sync with other cellular features.

∗Corresponding author E-mail:
Member of Editorial Board, JCMR
dehghani@um.ac.ir

References:

1. Apostolou P., et al. (2012) Cancer stem cells stemness transcription factors expression correlates with breast cancer disease stage. Current Stem Cell Research Therapy 7(6): p. 415-9.
2. Barneda-Zahonero, B., et al. (2012) Epigenetic regulation of B lymphocyte differentiation, transdifferentiation, and reprogramming. Computer Functional Genomics 564381.
3. Chappell J. and Dalton S. (2013) Roles for MYC in the establishment and maintenance of pluripotency. Cold Spring Harb Perspect Med 3(12): a014381.
4. Dehghani H., Dellaire G. and Bazett-Jones D.P. (2005) Organization of chromatin in the interphase mammalian cell. Micron 36(2): p. 95-108.
5. Efroni S., et al. (2008) Global transcription in pluripotent embryonic stem cells. Cell Stem Cell 2(5): p. 437-47.
6. Gaspar-Maia A., et al. (2011) Open chromatin in pluripotency and reprogramming. Nature Reviews Molecular Cell Biology 12(1): p. 36-47.
7. Hann S. R. (2014) MYC Cofactors: Molecular Switches Controlling Diverse Biological Outcomes. Cold Spring Harb Perspect Med. 17:4(9) a014399
8. Hirasaki M., et al. (2013) Striking similarity in the gene expression levels of individual Myc module members among ESCs, EpiSCs, and partial iPSCs. PLoS One 8(12): e83769.
9. Hurlin P. J. (2013) Control of vertebrate development by MYC. Cold Spring HarbPerspect Med,. 3(9): a014332.
10. Liu A., Yu X. and Liu S. (2013) Pluripotency transcription factors and cancer stem cells: small genes make a big difference. Clinical Journal of Cancer 32(9): p. 483-7.
11. Sabe H. (2011) Cancer early dissemination: cancerous epithelial-mesenchymal transdifferentiation and transforming growth factor beta signalling. Journal of Biochemistry 149(6): 633-9.
12. Shekhani M. T., et al. (2013) Cancer stem cells and tumor transdifferentiation: implications for novel therapeutic strategies. American Journal of Stem Cells 2(1): 52-61.

Research Article

Optimizing microRNA quantification in serum samples

Sedigheh Gharbi[1], Fatemh Mirzadeh[1], Shahriar Khatrei[3], Mohammad Reza Soroush[3], Mahmood Tavallaie[4], Mohammad Reza Nourani[5], Mehdi Sahmsara[2*], Seyyed Javad Mowla[1*]

1. *Department of Molecular Genetics, Faculty of Biological Sciences, Tarbiat Modares University, Tehran, Iran*
2. *National Institute of Genetic Engineering and Biotechnology, Tehran, Iran*
3. *Janbazan Medical and Engineering Research Center (JMERC), Tehran, Iran*
4. *Genetic Research Center, Baqiyatallah University of Medical Sciences, Tehran, Iran,*
5. *Chemical Injury Research Center (CIRC), Baqiyatallah University of Medical Sciences, Tehran, Iran*

Received 29 Jan 2014 Accepted 21 March 2014

Abstract

MicroRNAs constitute a group of small non-coding RNAs that negatively regulate gene expression. Aside from their contribution to biological and pathological pathways, altered expression of microRNAs have been reported in bio-fluid samples, such as serum etc. To employ serum's microRNAs as potential biomarkers, it is crucial to develop an efficient method for microRNA quantification, avoiding pre-analytical and analytical variations which could affect the accuracy of data analysis. Here, we optimized a real-time PCR quantification procedure for microRNA detection in serum samples. Serum total RNA was extracted using two different RNA isolation methods, one based on phenol-chloroform and the other based on silica column. To investigate a potential PCR inhibitory effect, different RNA amounts were subjected to reverse transcription. Moreover to assess the enzymatic efficiency, synthetic exogenous microRNAs was spiked into the mixture. To find a reliable internal control gene for normalizing the microRNA quantification, the amounts of 8 candidate non-coding RNAs including SNORD38B, SNORD49A, U6, 5S rRNA, miR-423-5p, miR-191, miR-16 and miR-103 were assessed on serum samples. Altogether, our data demonstrated that the silica-based method was more efficient for microRNA recovery. Furthermore, increasing the input volume of the extracted RNA would dramatically increase inhibitors' amounts which could end up in a larger Cq values. Therefore, the best input volume of RNA turned out to be 1.5 microliter/reaction. Among the 8 aforementioned internal controls, U6, SNORD38B and SNORD49A showed low levels of expression, and were undetectable in some samples. Amongst the others, 5s rRNA, had the biggest standard deviation which could significantly affect data analysis. MiR-103 with the least variations appeared to be the best normalizer gene.

Keywords: MicroRNA recovery, Real-time PCR quantification, Normalizer gene

Introduction

microRNAs (miRNAs) are a group of ~20 nucleotides non-coding RNAs that negatively regulate gene expression of their targets (Bartel, 2004). More than 60% of human protein-coding genes contain miRNA binding sites in their 3'UTR (Friedman et al., 2009). By direct binding to their mRNA targets, miRNAs play important roles in most cellular and developmental processes, and hence have been implicated in a large number of human diseases (Kloosterman and Plasterk, 2006). In parallel to their contribution to biological pathways, miRNA could be also easily detected in biofluid samples such as serum, urine, saliva (Ajit, 2012). The ease of tracing them in biofluid samples, along with their unique signature of expression in various diseases have made microRNAs a new generation of biomarkers (Etheridge et al., 2011). Although the exact function of secreted miRNAs is not fully understood (Chen et al., 2012), but recent findings indicate that cells can uptake secreted miRNAs as exogenous signals to fine-tune their interior regulatory network (Kosaka and Ochiya, 2011; Mittelbrunn and Sanchez-Madrid, 2012; Wang et al., 2010). It is also demonstrated that specific patterns of cell-free miRNAs are related to different pathological states (Brase et al., 2010; Fan

∗Corresponding authors E-mail:
sjmowla@modares.ac.ir
shamsa@nigeb.ac.ir

et al., 2013; Taylor and Gercel-Taylor, 2008).

Due to growing propensity toward using cell free miRNAs as biomarkers it is critical to develop an efficient method for miRNAs evaluation to avoid pre analytical and analytical pitfalls while working with serum samples (Gilad et al., 2008; McDonald et al., 2011). One of the most important sources of pre-analytical variations is RNA extraction step (Eldh et al., 2012; McDonald et al., 2011) because of low concentration of RNA and abundance of proteins in serum samples, it is of great importance to choose a reliable RNA isolation method, otherwise loss of RNA load and co purification of PCR inhibitors could cause considerable deviation of the result and misleading data (Kroh et al., 2010; Mraz et al., 2009).

Although technical variations are inevitable, finding and applying a suitable internal control gene to normalize qPCR data would be an appropriate way to minimize analytical variations. Successful biomarker discovery projects are dependent on controlling for these sources of pre-analytical and analytical variations. To address aforementioned pitfalls, two conventional methods for serum RNAs recovery were compared. Moreover to minimize the effect of serum derived inhibitors the optimal starting volume of extracted RNA in cDNA synthesis step was evaluated. Furthermore, we showed the importance of a reliable normalizer gene for miRNA qPCR analysis.

Materials and methods

Blood collection and plasma preparation

Whole blood samples were collected from 20 healthy donors and directly drawn into serum separator tube (BD Vacutainer, Plymouth, UK). They were incubated for 1 hour at room temperature and then centrifuged for 15 min in 2500g. The clear supernatant was harvested in nuclease free tubes and stored in -80^{o}C until further investigations.

RNA extraction

Each serum samples was divided into two 200 µl portions. One was subjected to phenol-chloroform RNA extraction, using Trizol LS reagent (Invitrogen, USA). The other aliquot was used in silica column based RNA extraction, using miRNeasy mini kit (Qiagen, Germany). All Serum samples were completely thawed on ice and then, 20 fmol of synthetic Caenorhabditis elegans miRNA was spiked into the mixture. Extraction procedure was performed according to the manufacturer's instruction for both RNA isolation methods. In column based method, before adding Qiazol, MS2 RNA (Roche Applied Science) was added to each sample at the final concentration of 1 µg µl-1 to increase the yield of miRNA extraction. Adding this carrier would increase the final recovery of miRNA during extraction.

Reverse transcription

Synthetic spiked-in miRNA, miR-21 and 5s rRNA were reverse transcribed by commercially available primers (exiqon) and The miRCURY locked nucleic acid universal cDNA synthesis kit (exiqon, Denmark). In order to minimize PCR inhibitory effect of the serum derived RNA, several volume of RNA sample input were tested including 0.5, 2, 1, 1.5, 3 and 6 µl of RNA were reverse transcribed in a 10-µl reaction volume. Other reagents were applied according to the company's protocol. A non-template reaction, containing only exogenous synthetic spiked-in miRNA (a high quality RNA provided by exiqon), was considered as a control to determine the exact cDNA synthesis efficiency and also monitor PCR inhibitory effect.

cDNA for miRNA profiling, was synthesized using miRCURY locked nucleic acid universal cDNA synthesis kit following manufacturer's instruction.

Real-time PCR

Quantification of the synthetic spiked-in miRNA, miR-21 and 5s rRNA was done in 20-µl PCR reaction using the miRCURY SYBR Green kit and specific primer mix (exiqon, Denmark) through ABI 7500 Instrument (7500 Applied Biosystems, USA). All reactions were performed in duplicates. LinReg software was used to evaluate the PCR reactions efficiency.

Table 1. Statistical values of 8 candidates reference genes

Column1	min	max	std	average
SNORD49A	36.61	40	1.54	38.26
miR-423-5p	30.58	33.95	1.02	32.21
miR-103	27.64	30.2	0.74	28.73
miR-191	30.08	33.05	0.97	31.68
SNORD38B	35.76	40	1.90	37.51
miR-16	26.68	30.23	1.02	27.67
5s rRNA	20.07	34.15	3.21	26.63
u6 snRNA	32.98	40	2.13	36.13

We used the miRCURY LNA human miRNA Real-time PCR panel I and miRCURY SYBR Green kit for miRNA profiling experiments on serum RNA, with LightCycler instrument (Light Cycler 480, Roche Company, Germany). q-PCR data of 7 candidate reference genes including SNORD38B, SNORD49A, U6, miR-423-5p, miR-191, miR-16 and miR-103, provided in panel I and also of 5s rRNA (not provided in panel and was obtained using a separate reaction on samples), were use for finding an eligible internal control in serum (table 1).

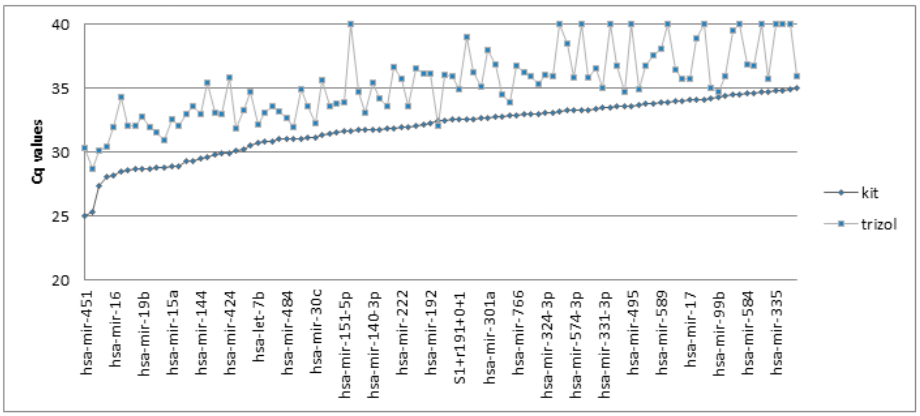

Fig. 1 Comparison of raw Cq values of 100 highly expressed microRNAs in two differentially extracted RNA samples groups

Statistical analysis

Standard deviations and student t test p values were calculated by GraphPad software and MS EXCEL. P values less than 0.01 considered to be significant.

Results

Pre-analytical optimization

Optimizing RNA recovery

One of the most challenging steps of miRNA quantification in serum samples is RNA extraction which is also considered as a source of pre-analytical variations. In addition to small RNAs loss during isolation step, potential PCR inhibitors could be introduced into the extracted RNA. After reviewing several related publications, we decided to test two frequently used isolation methods; first, extraction with Trizol® LS reagent which is based on phenolchloroform method and second isolation by miRNeasy mini kit that depends on silica filter column. The ability of two different RNA isolation methods for miRNAs recovery was investigated through qPCR. Our results showed superior recovery of miRNAs by the kit, with an average reduction in Ct values of 3.329 on all types of miRNAs, including those which are highly expressed (miR-21; miR-16) or those with very low amounts of endogenous transcripts (miR-192; miR423-5p). qPCR profiling on 20 normal samples showed that out of 380 miRNAs, included on panel I, only 68 miRNAs were detected in RNA samples, purified by Trizol (Cq <35 was included in analysis). Surprisingly this amount increased to 114 miRs in the kit purified RNAs. Comparison of raw Cq values of 100 highly expressed miRNAs in two differentially extracted RNA samples groups is shown in figure 1.

Evaluating the presence of inhibitors

Considering the low (minute) amount of secreted miRNA in serum samples, it is tempting to maximize the amount of input RNA used per reactions to compensate for such a low RNA yield. However, our data revealed that increasing the input amount of RNA could dramatically increase inhibitor amounts and end up in a larger Cq value. For example, miR-21's Cq value which was 28 for 1.5-µl RNA input reactions, increased to 40 when 3-µl RNA input was applied in the cDNA synthesis step.

Considering the Cq value of spiked-in in the non-template reaction as baseline we concluded that the volume of 1.5 µl RNA input has the minimum PCR inhibitory effect among five different examined volumes (fig 2). Moreover our analysis on two endogenous noncoding RNAs (5s rRNA and miR-21) was in accordance with spiked-in data (fig 3).

Analytical considerations

To find a reliable internal control gene, 8 non-coding RNA candidates available on panel I qPCR, were assessed on serum samples. Some of these genes including U6, SNORD38B and SNORD49A showed low level of expression which lead to their exclusion from further analysis. Statistical assessment on the remaining candidates indicate that miR-103 with the lowest standard deviation is the best normalizer gene. Surprisingly 5s rRNA, a frequently used internal control in miRNA studies, had the largest standard deviation. To have better insight on internal control effect on data analysis, we normalized miR-143 expression using miR-103

and 5s rRNA on 10 individuals (Fig. 3). As shown in the graph, normalizing Mir-143 expression using 5s rRNA gives a mean value of 8.7 while this value decreased to 4.1 when normalized by miR-103 (p value <0.0001). This large amount of variation could significantly affect the level of expression. Our other finding was in agreement with this statement that 5s rRNA cannot be a reliable internal control gene. As when we used an expired cDNA synthesis kit to evaluate robustness of 5s rRNA for evaluating the enzymatic efficiency, Cq values of 5s rRNA were near the mean range, while none of other targeted miRNAs were detected.

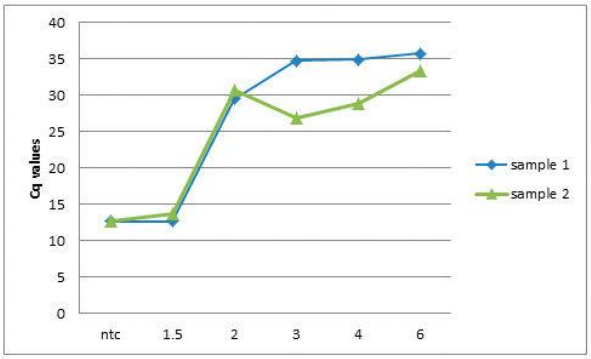

Fig. 2 Comparison of different volume of RNA sample input to find the volume with minimum inhibitory effect.

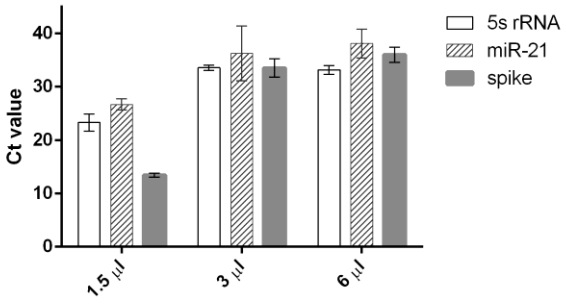

Figure 3. Comparison of Cq value of 3 targetes in 3 different volumes

Discussion

Recent studies introduce serum miRNAs as promising non-invasive biomarkers for varied biological and pathological conditions. Despite the accessibility and their ease of use, miRNAs quantification in bio-fluid are subjected to many technical challenges which should be addressed prior to starting the procedure.

The small amount of secreted RNA in serum samples make it critical to choose a robust RNA extraction method to ensure recovery of maximum RNA load. Herein, we demonstrate that silica column based RNA isolation methods are more efficient than the widely used phenol-chloroform methods. Moreover, organic particles are carried over during isolation step and high level of protein inhibitors in serum samples; make it crucial to evaluate the best starting input volume for minimizing inhibitory effects. Finally To achieve reliable and also reproducible qPCR data, non-biological variations, resulting from technical inconsistencies should be corrected using an appropriate reference gene, although finding a suitable reference gene for miRNA quantification in bio-fluid samples is a problematic step. Our findings revealed that non-miRNA reference genes like U6 and 5s rRNA could not be considered as powerful normalizers. Aside from large standard deviations they could not represent the actual efficacy of enzymatic reactions. This could be due to minute amount of miRNA compared to abundant RNA fraction of 5s rRNA in serum samples. Therefor the discrepancy in frequency of these two groups of non-coding RNAs (miRNA and rRNAs) leaves 5s rRNA out of potential miRNAs normalizer genes.

Acknowledgment

The authors are grateful to all the participants who took part in the study. This research was financially supported by Janbazan Medical and Engineering Research Center (JMERC).

References:

1- Ajit S. K. (2012) Circulating microRNAs as biomarkers, therapeutic targets, and signaling molecules. Sensors (Basel) 12:3359-3369.

2- Bartel D. P. (2004) MicroRNAs: genomics, biogenesis, mechanism, and function. Cell 116:281-297.

3- Brase J., Wuttig D., Kuner R. and Sultmann H. (2010) Serum microRNAs as non-invasive biomarkers for cancer. Molecular Cancer 9: 306

4- Chen X., Liang H., Zhang J., Zen K. and Zhang C. Y. (2012) Secreted microRNAs: a new form of intercellular communication. Trends in cell biology 22:125-132.

5- Eldh M., Lotvall J., Malmhall C. and Ekstrom K. (2012) Importance of RNA isolation methods for analysis of exosomal RNA: evaluation of different methods. Molecular immunology 50:278-286.

6- Etheridge A., Lee I., Hood L., Galas D. and Wang K. (2011) Extracellular microRNA: a new source of biomarkers. Mutation research 717:85-90.

7- Fan K. L., Zhang H. F., Shen J., Zhang Q. and Li X. L. (2013) Circulating microRNAs levels in Chinese heart failure patients caused by dilated

cardiomyopathy. Indian heart journal 65:12-16.

8- Friedman R. C., Farh K. K., Burge C. B. and Bartel D. P. (2009) Most mammalian mRNAs are conserved targets of microRNAs. Genome research 19:92-105.

9- Gilad S., Meiri E., Yogev Y., Benjamin S., Lebanony D., Yerushalmi N., Benjamin H., Kushnir M., Cholakh H., Melamed N., Bentwich Z., Hod M., Goren Y. and Chajut A. (2008) Serum microRNAs are promising novel biomarkers. PloS one 3:e3148.

10- Kloosterman W. P. and Plasterk R. H. (2006) The diverse functions of microRNAs in animal development and disease. Developmental cell 11:441-450.

11- Kosaka N. and Ochiya T. (2011) Unraveling the Mystery of Cancer by Secretory microRNA: Horizontal microRNA Transfer between Living Cells. Frontiers in genetics 2:97.

12- Kroh E. M., Parkin R. K., Mitchell P. S. and Tewari M. (2010) Analysis of circulating microRNA biomarkers in plasma and serum using quantitative reverse transcription-PCR (qRT-PCR). Methods 50:298-301.

13- McDonald J. S., Milosevic D., Reddi H. V., Grebe S. K. and Algeciras-Schimnich A. (2011) Analysis of circulating microRNA: preanalytical and analytical challenges. Clinical chemistry 57:833-840.

14- Mittelbrunn M. and Sanchez-Madrid F. (2012) Intercellular communication: diverse structures for exchange of genetic information. Nature reviews. Molecular cell biology 13:328-335.

15- Mraz M., Malinova K., Mayer J. and Pospisilova S. (2009) MicroRNA isolation and stability in stored RNA samples. Biochemical and biophysical research communications 390:1-4.

16- Taylor D. D. and Gercel-Taylor C. (2008) MicroRNA signatures of tumor-derived exosomes as diagnostic biomarkers of ovarian cancer. Gynecologic oncology 110:13-21.

17- Wang K., Zhang S., Weber J., Baxter D. and Galas D. J. (2010) Export of microRNAs and microRNA-protective protein by mammalian cells. Nucleic acids research 38:7248-7259.

Journal of Cell and Molecular Research (2014) 6 (2), 57-63

Research Article

The Application of Organotypic Brain Slice Culture to Study Microglial Differentiation by *Lycopersicon esculentum* and *Sambucus nigra* Lectin Histochemistry

Roya Lari[1] and Peter D. Kitchener[2]

1. *Department of Biology, Faculty of Sciences, Ferdowsi University of Mashhad, Mashhad, Iran*
2. *Department of Anatomy and Cell Biology, University of Melbourne, Parkville, Victoria 3010*

Received 07 Aug 2014 Accepted 12 Sep 2014

Abstract

Microglial cells are the subset of macrophages in the central nervous system (CNS). Changes in the CNS such as injury or developmental events cause morphological and physiological changes in microglial cells. In this study organotypic brain slice cultures under serum free condition were used to investigate the morphology and lectin histochemistry of microglia and macrophages in the CNS *in vitro*. Microglial cells exhibited dramatic morphological changes in the organotypic brain slice culture. Immediately after slicing microglias were seen to have the same morphology as they do in the intact brain: they had small cell bodies from which radiated several highly ramified processes. After 1 day *in vitro* (DIV) all microglia transformed into an active form with round soma and no processes. At 5 days *in vitro*, and especially at 9 days *in vitro*, many of the microglia had tended to return to the ramified phenotype. The expression of different carbohydrates was examined at the 0, 1, 5 and 9 days *in vitro* time periods by employing *Lycopersicon esculentum* tomato lectin (LEA lectin) and *Sambucus nigra* (SNA). Microglial cells with different morphology intensely stained with the LEA. SNA stained the ramified microglia only after they re-ramified at 5 DIV and 9 DIV. The results of this study confirmed that the expression of carbohydrate structures in these cells would undergo changes corresponding to the changes in morphology.

Keywords: Microglia, Macrophage, phagocyte, Lectin, in vitro

Introduction

Microglial cells are the subset of macrophages in the central nervous system (Guillemin and Brew, 2004). Changes in the CNS such as injury or developmental events cause morphological and physiological changes in microglia. Morphologically three types of microglia can be considered which are ramified, amoeboid, and intermediate (Rezaie et al., 2004). Resting or ramified microglial cells are found in normal, healthy CNS and they have an immune survival role (Czapiga and Colton, 1999). Any kinds of infection or damage can activate the microglias with change to round shapes as well as up-regulates their cell-surface antigens and contain a high proportion of hydrolytic enzymes contributing to their activated phagocytic properties (Kaur et al., 2007; Ling and Wong, 1993).

Microglial cells are labelled by many of the same antibodies as monocytes. For example, both microglia and macrophages are recognised by monoclonal antibodies against CD68, CD45,CD11c and CD 11b (Fischer and Reichmann, 2001; Rezaie et al., 1999). In addition to antibodies directed against proteins expressed by macrophages and microglia, lectins have become increasingly used to examine these cells. A variety of lectins have been shown to bind to both microglia and macrophages in the CNS (Colton et al., 1992; Czapiga and Colton, 1999). The changes of carbohydrates in cell surface have been shown to play an important role in immune defence (Boyzo et al., 2003; Mackowiak et al., 2007; Suzuki et al., 2005). Further characterization of carbohydrate structures might enable the identification of structures uniquely associated with particular macrophage and microglial phenotypes and functions.

In this study the differentiation of microglia *in vitro* and characterizing aspects of cell surface's carbohydrates has been examined by using *Sambucus nigra* Agglutinin (SNA) also called Elderberry bark lectin and *Lycopersicon esculentum* agglutinin (LEA) lectin. SNA lectin binds preferentially to sialic acid attached to terminal galactose in α-2-6 and to a lesser degree

∗Corresponding authors E-mail: royalari@gmail.com

α-2-3 linkage. LEA lectin is composed of single polypeptide that can bind poly N-acetyl lactosamine oligomers (Acarin et al., 1994). We have detected expression of these different carbohydrate structures in microglia and macrophages over nine days of organotypic culture of neonatal brain slices and also in intact brains of neonatal rats. It was hypothesised that the expression of carbohydrate structures in these cells would undergo changes corresponding to the changes in cell morphology.

Materials and methods

Organotypic brain slice culturing

Brain slicing

Sparge Dawley rat pups age between postnatal days (P) 0 to 8 days old were used for brain slicing as it has been described before (Lari et al., 2012). Briefly, in a laminar flow hood rat pups were sacrificed by decapitation. The brain where quickly desiccated from the head in the ice-cold slicing buffer and attached to a chuck with super glue. Warm agar (37-40°C) swirled around the brain to provide support for the brain during the cutting of 250 μm thick slices on a Leica VT 1000 vibratome.

Brain culture

After cutting, the agar was gently removed from around the slices. 1 ml of cold (4°C) culture medium (see below) was placed in the wells of 6-well tray. Sterile Millicell-CM 30mm-diameter transparent culture inserts (Millipore) were used for brain slice culture. A glass Pasteur pipette was used to gently transfer the brain slices to the inserted membrane. Usually, two slices were placed in each membrane. The slices were kept in 4°C in sterile serum free Minimum Essential Medium (Sigma M-3024) (MEM) for the next two hours, and then refreshed with a change of the serum free MEM from cold 4°C C to warm 37°C. The cultures were placed in an incubator at 37°C in a 5% CO_2 95% O_2 atmosphere. The MEM was changed every two days. The cultured tissue was kept in an incubator for 1 day, 5 days or 9 days.

Cultured tissue fixation

Culture brain slices were fixed with Bouins fixative by replacing the medium inside the culture dish with Bouins fixative overnight in room temperature. To avoid over fixation the Bouins was then replaced with 70% ethanol.

Agar embedding of slice cultures

To prepare the cultured tissues for paraffin embeds warm agar in liquid form was added to the insert containing the tissues. After 30 minutes in room temperature the agar sets to solid form, thus supporting the tissue during the processing. A scalpel was used to gently cut around the membrane and agar freeing it from plastic insert. The agar with tissues inside it put in 70% ethanol and then processes for paraffin embedding. These brain slices were embedded in one of two different ways, either "flat", to enable sections of the entire face (*en face*) of the slice to be cut, or "edge on", to allow cross sections of the brain slices to be cut. Sections cut at 6 μm were floated onto 0.1% gelatin coated slides.

Perfusion-fixation the brain

Two P13 rats were deeply anesthetized (100 mg/kg Nembutal i.p.), and their hearts exposed by thoractomy. Under the fume hood and at the room temperature a cannula connected to the constant pressure perfusion apparatus was inserted into the left ventricle and the right atrium was cut to serve as an outlet. Blood and plasma proteins were removed by perfusing the animals with 0.1 M PBS for 2-3 minutes. The brains and livers were fixed by perfusion of Bouins fixative for 1-2 minutes. The tissues were removed and kept in the Bouins fixative overnight.

Lectin histochemistry

Lectin staining of paraffin sections

Paraffin sections of the cultured brain slice tissues that were 0 DIV, 1 DIV, 5 DIV and 9 DIV were de-waxed in Histolene and hydrated from absolute ethanol to 70% ethanol and then into PBS. Sections were incubated with biotinylated *Lycopersicon esculentum* agglutinin (LEA) and *Sambucus nigra* Agglutinin (SNA) lectins (vector Laboratories, Inc.CA). Lectin was made up at a diluted of 1:3000 in fish gelatin blocker solution. After 24-48 hours they washed (4x5 times) in 0.1M PBS (0.1 M and pH 7.4). Lectin binding that remained after the washes was visualized by the avidin-biotin-HRP localization of biotinylated lectins. A 1:100 dilute solution of Avidin -Biotin Complex (ABC; vector Laboratories, CA) was made up in 0.1M PBS and applied to the sections for 12-24 hours. The sections were washed again (4x5 times in PBS) and reacted with 0.05% of diaminobenzadine (DAB) and 0.01% hydrogen peroxide (H_2O_2) in PBS.

Microscopy and imaging

Lectins stained sections were viewed with bright–field and Nomaski (DIC) microscopy (Zeiss Axioskop II). Micrographs were obtained with a Nikon digital SLR attached to the lightpath of the microscope; acquired images were adjusted for brightness and contrast using the Adobe Photoshop® software.

Results

General changes in brain slices during culture in vitro

In order to investigate microglial morphology LEA lectin was considered as a reliable type of lectin for microglial and macrophages (Velasco et al.; 1995, Acarin et al., 1994). In addition to macrophages and microglia, LEA also binds to endothelium, but it was considered that there would be no ambiguity in the identification of endothelium versus macrophages and microglia in the brain tissues.

Once cut and placed into culture (day 0), many of the microglial cells appeared with the typical morphology of resting microglia - they were highly ramified with small cell bodies. The thin cytoplasmic processes were multi-branches that tend to all directions (Fig. 1A). Many of the ramified cells located in the middle of the *en face* slices. The cross sections of the slices revealed that the branches were oriented in various directions (data not shown). At this time also some macrophages with round or oval cell body were observed, these were seen in the *en face* sections to be located mostly towards the in the edge of the slices.

After one day *in vitro* (1 DIV) some macrophage-like cells had started to migrate from the slices onto the membrane, which gave the edges of the slices an uneven appearance. These cells were apparently evenly distributed in the *en face* sections and cross sections of the brain slices. At this time dramatic changes had occurred in the LEA positive cells. All the LEA positive cells exhibited the active morphology of cells classified as ameboid microglia, with round or irregular cell body and no, or few, short cytoplasmic processes (Fig. 1C). These processes were probably due to the phagocytic action of the cells at that time.

After 5 DIV the slices adhered to the membrane and in the edge tended to flatten due to migration of cells (some clearly had a macrophage-like in morphology). At this time a large portion of microglial cells was developed towards a more ramified appearance, although round or ovaloid cells without any processes were still present (Fig. 1D and E). Labelled macrophages at 5 DIV appeared to have weaker LEA reactivity than at 0 DIV and they appeared to be smaller and had smaller nuclei than macrophage cells seen at 1DIV, but a few big macrophages still could be observed (Fig. 1E). Most of the macrophages were located around the edge of the slides and appeared less labelled than 0 DIV and 1 DIV. The ramified cells had short branches and stained less intensely than the macrophages (Fig. 1D). Most of the ramified cells were located in the middle of the slice.

At 9 DIV further development towards ramification had taken place. Few ovaloid cells could be seen around the edges (Fig. 1G). The tissues were flatter and strongly adhered to the membrane. Although adherence is believed to be due to the proliferation and growth of astrocytes that extend their presses into the insert membrane (Stoppini et al., 1991), the 9DIV specimens in this study revealed cellular processes in the insert membrane that were stained with lectins. Therefore, growth of microglial or endothelial processes into the membrane is also a possibility. Majorities of cells were highly ramified with long multi-branches processes that looked to eyes longer and thicker than 0 DIV. Microglial cell bodies were small with multi-branch cytoplasmic processes projecting in all directions (Fig. 1F). A few macrophages also reacted with LEA; these were located around the edge of the slices. Almost no blood vessels were detectable. In sections from perfusion-fixed P13 rat brain all the microglial type cells had small cell body and were highly ramified with branches in all directions (Fig. 1H). In addition to ramified microglias, there were very few highly stained macrophages in the P13 brain with round or oval cell body with no cytoplasmic processes (Fig. 1I). The macrophages mostly located around the ventricle and also in the sub-cortical white matter.

***Sambucus nigra* Agglutinin (SNA)**

This lectin appeared to label cytoplasmic side of macrophages evenly (Fig. 2B). At 0 DIV there was little evidence of binding to microglia (Fig. 2A), but blood vessels were strongly and evenly stained (Fig. 2B). At 1 DIV this lectin intensely stained some organelle of cells (Fig. 2C). The blood vessels were also labelled with the SNA. In contrast with 0 DIV most of the blood vessels had beaded appearance. It appeared that there was a general staining of the extra-cellular regions. After 5 DIV some ramified cells weakly reacted with SNA (Fig. 2D). Many macrophages were labelled with SNA as well and some of them had few cytoplasmic processes (Fig. 2E).

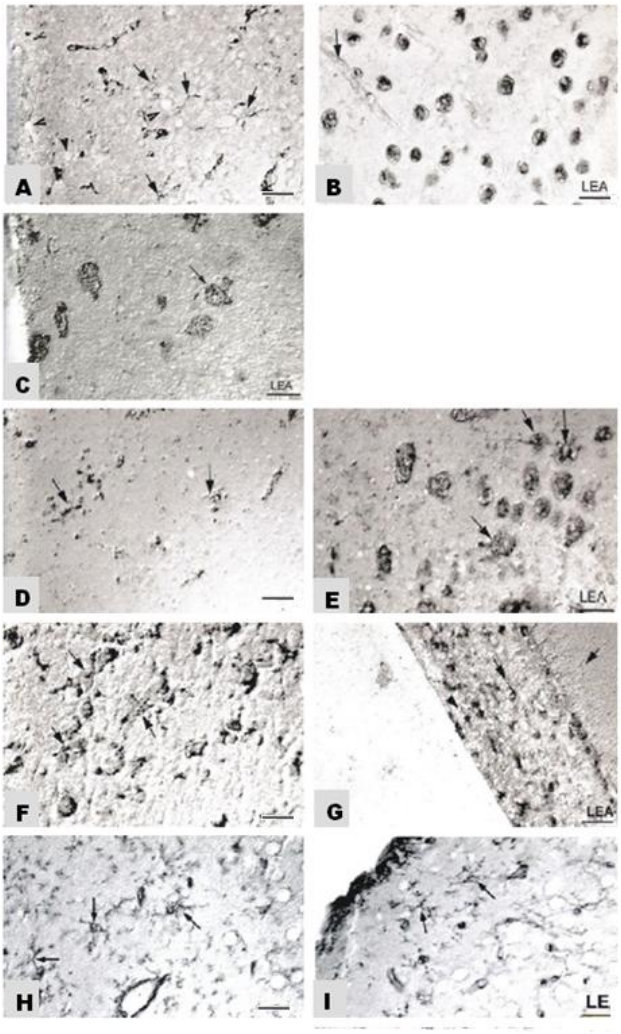

Fig. 1 Microglial changes in brain slices culture in vitro: brain slices fixed at different time points in and stained for LEA.
Slices at 0 DIV (A) and (B); (A) Ramified microglia stained with LEA exhibiting long thin processes (long arrows). Neuronal cell bodies were unstained (arrowheads). (B) LEA positive macrophages: reactivity was observed in the cytoplasm and plasm membrane. LEA also labels blood vessels (arrow). (C) At 1 DIV LEA stained activated microglial.
Slices at 5 DIV (D) and (E); (D) LEA stained ramified cells with short-branched processes. (E) LEA positive macrophages, some with a few cytoplasmic processes (arrow) and some without any processes. Slices at 9 DIV (F) and (G): (F) LEA stained highly ramified microglia with long multi-branched processes (arrows) (G) a cross section of LEA stained ramified microglia. These cells were distributed throughout the depth of the slice extended and cytoplasmic process in different directions -some eventually growing into the insert membrane (arrow). Perfused-fixed P13 brain (H) and (I): (H) LEA positive microglial cells in the sub cortical grey matter (arrows) (I) Macrophages with round or oval cell bodies with no or a few cytoplasm process and darkly stained with LEA(big arrow head). Blood vessels also stained. Scale bar: 25 µm in all panels.

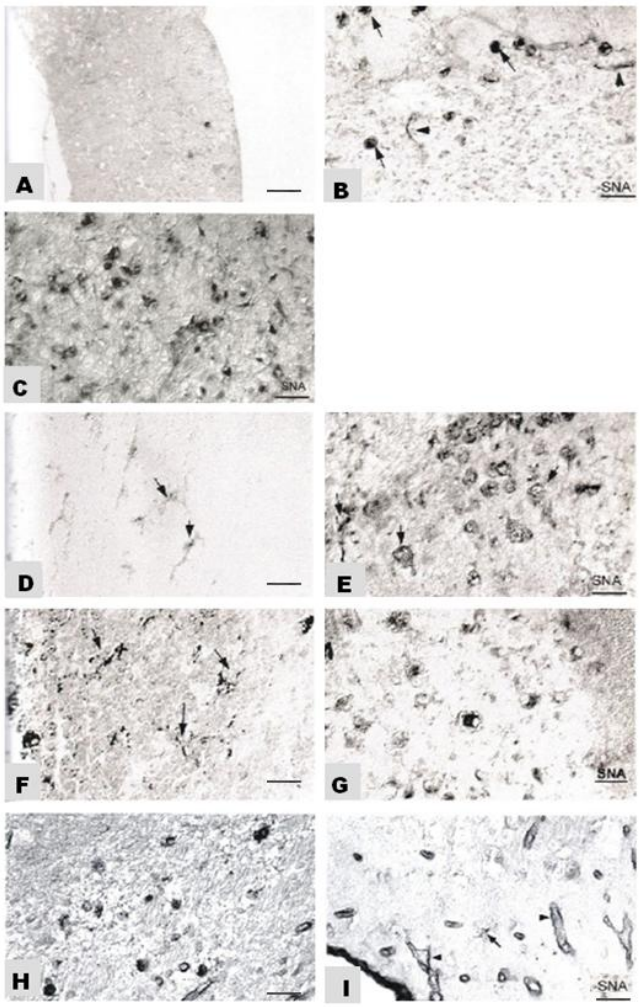

Fig. 2. SNA staining of microglial and macrophages in organotypic brain slice cultures**.**
Slices at 0 DIV (A) and (B); (A) Cross-section of the brain slice revealing some ramified cells that were faintly stained with SNA. (B) SNA appeared to label macrophages (long arrow) and strongly stained blood vessels (arrowhead) as well as some staining of entities in most or all cells giving the impressioof a general background staining. (C) At 1 DIV SNA strongly stained some parts of cells. Slices at 5 DIV (D) and (E); ramified cells weekly reacted with SNA (arrows). Many macrophages were labelled with SNA as well. Slices at 9 DIV (F) and (G): (F) 9 DIV SNA had a weak reaction with a few ramified cells (arrows) (G) some macrophages stained with SNA. In perfused-fixed P13 brain (H) and (I) SNA stained some macrophages and blood vessels but no ramified cells. Scale bar: 50 µm in panel A, 25 µm in all other panels.

SNA also barely labelled the blood vessels and some background cells. At 9 DIV although the background was highly stained, SNA had a weak reaction with some ramified type cells and also some macrophages (Fig. 2G). The macrophages were the same size as macrophages in 0 DIV. This lectin in P13 brain only labeled a few macrophages around the ventricle and in the cortex (Fig. 2H). No ramified microglia reacted with SNA. These results are summarised in table 1. Some macrophages and

blood vessels labeled with SNA lectin at P13 (Fig. 2H and I).

Table 1. Summary of lectins staining in normal brain and culture

Lectins		P13 brain	0 DIV	1 DIV	5 DIV	9 DIV
LEA	R.microglia	++	++	_	++	++
	macrophages	+++	+++	+++	+++	_
SNA	R. microglia	_	_	_	++	++
	macrophages	+++	+++	+++	+++	++

Discussion

The organotypic brain slice culture used for investigating microglial function change was first described by (Hailer et al., 1996), but the few subsequent studies that have employed this method have not significantly extended this initial description of microglial activation and re-ramification. Most of the histochemical changes in microglia and macrophages of the CNS have been on the fixed intact brain or mixed glial primary cultures (Ananth et al., 2003; Song et al., 2006).

In the current study, the brains of rats age between 0 to 8 were used because at this age, there is a peak in the density and the ramification of microglia (Navascues et al., 2000), thus this age brain can support (or is at least permissive to) the development of microglia. During the slicing procedure, the brain was dissected out quickly in the 4°C hyperosmotic buffer to minimize cell swelling glutamate-mediated toxicity. Also, calcium free condition Mg^{2+} was added to minimize mediated toxicity and in result, reduces the cell death in culture. The serum free conditions were used to prevent serum stimulation on activating microglia and also possibly to limit the proliferation of astrocytes (Czapiga and Colton, 1999). The common use of fetal serum on microglial cultures appears to maintain these cells in an activated state (Czapiga and Colton, 1999).

The detection of poly N-acetyl lactosamine residues by LEA lectin resulted in staining of both macrophages and ramified microglia in the intact and cultured brain (Billiards et al., 2006; Rezaie et al., 2005). Previous studies have demonstrated N-acetyl lactosamine associated with glycoproteins in the cell surface and lysosomal membrane (Carlsson and Fukuda, 1990). The cytoplasm of macrophages would be expected to contain numerous secretory granules and lysosomes with high level of N-acetyl lactosamine due to their phagocytic action in removing dead cells (Acarin et al., 1994). It can be the reason that macrophages and the activated microglia invariably exhibited more intense staining that the ramified microglia. Endothelial cells in blood vessels also stained with LEA lectin, in sections from intact and from cultured brains. However, the blood vessel labelling appeared to change over time in the cultures: at 0 DIV blood vessels similar to normal brains evenly stained with LEA but after 1 DIV and at 5 DIV they had lumpy appearance. After 9 DIV only a few blood vessels labelled with the LEA. One possible explanation for these changes could be the blood vessels were degenerating, or reorganising, in the organotypic brain slice culture after a few days - presumably due to the loss of blood flow within.

SNA has been reported to label microglia in meningoencephalitis (Lutsik et al., 1991) and in Alzheimer's disease (Zambenedetti et al., 1998). Sialic acid has also been reported to play an important role in the activation of macrophages by facilitating attachment of bacteria to macrophages (Maganti et al., 1998). It has been reported that the level of sialoglucoconjugated was changed in several diseases such as cancer, diabetes and rheumatoid arthritis (Alturfan et al., 2007; de Castro et al., 2008; Holzhauser and Faillard, 1988; Maruhama et al., 1983). As SNA did not label microglia at day 0 and also in the P13 brain, but it strongly interacted with re ramified microglia in day 5 and day 9. These results indicated that re-ramification increased the expression the level of sialic acid attached to terminal galactose in α-2-6 or α-2-3. Therefore, SNA could be a modulator for stress on ramified microglia cells.

Sialic acid is known to involve in neural plasticity in the adult CNS. It changes in hormonal patterns, adaptations to pain and stress, and aspects of learning and memory (Rutishauser, 2008) and also it has role in microglia-neuron interactions (Wielgat and Braszko, 2012). Therefore, increasing the level of sialic acid after re-ramification of microglia may play a key role in repair of adult CNS tissue.

References:

1- Rutishauser U. (2008) Polysialic acid in the plasticity of the developing and adult vertebrate nervous system. Nat Rev Neurosci 9: 26-35.

2- Acarin L., Vela J. M., Gonzalez B. and Castellano B. (1994) Demonstration of poly-N-acetyl lactosamine residues in ameboid and ramified microglial cells in rat brain by tomato lectin binding. J Histochem Cytochem 42:1033-1041.

3- Alturfan A. A., Uslu E., Alturfan E. E., Hatemi G., Fresko I. and Kokoglu E. (2007)

Increased serum sialic acid levels in primary osteoarthritis and inactive rheumatoid arthritis. Tohoku J Exp Med 213:241-248.

4- Ananth C., Gopalakrishnakone P. and Kaur C. (2003) Induction of inducible nitric oxide synthase expression in activated microglia following domoic acid (DA)-induced neurotoxicity in the rat hippocampus. Neurosci Lett 338:49-52.

5- Billiards S. S., Haynes R. L., Folkerth R. D., Trachtenberg F. L., Liu L. G., Volpe J. J. and Kinney H. C. (2006) Development of microglia in the cerebral white matter of the human fetus and infant. The Journal of comparative neurology 497:199-208.

6- Boyzo A., Ayala J., Gutierrez R. and Hernandez R. J. (2003) Neuraminidase activity in different regions of the seizing epileptic and non-epileptic brain. Brain Res 964:211-217.

7- Carlsson S. R. and Fukuda M. (1990) The polylactosaminoglycans of human lysosomal membrane glycoproteins lamp-1 and lamp-2. Localization on the peptide backbones. The Journal of biological chemistry 265:20488-20495.

8- Colton C. A., Abel C., Patchett J., Keri J. and Yao J. (1992) Lectin staining of cultured CNS microglia. J Histochem Cytochem 40:505-512.

9- Czapiga M. and Colton C. A. (1999) Function of microglia in organotypic slice cultures. J Neurosci Res 56:644-651.

10- de Castro J., Rodriguez M. C., Martinez-Zorzano V. S., Hernandez-Hernandez A., Llanillo M. and Sanchez-Yague J. (2008) Erythrocyte and platelet phospholipid fatty acids as markers of advanced non-small cell lung cancer: comparison with serum levels of sialic acid, TPS and Cyfra 21-1. Cancer Invest 26:407-418.

11- Fischer H. G. and Reichmann G. (2001) Brain dendritic cells and macrophages/microglia in central nervous system inflammation. J Immunol 166:2717-2726.

12- Guillemin G. J. and Brew B. J. (2004) Microglia, macrophages, perivascular macrophages, and pericytes: a review of function and identification. J Leukoc Biol 75:388-397.

13- Hailer N. P., Jarhult J. D. and Nitsch R. (1996) Resting microglial cells in vitro: analysis of morphology and adhesion molecule expression in organotypic hippocampal slice cultures. Glia 18:319-331.

14- Holzhauser R. and Faillard H. (1988) Sialic acids in human lymphocytes. Qualitative and quantitative alterations in cancer cases. Carbohydr Res 183:89-95.

15- Kaur C., Dheen S. T. and Ling E. A. (2007) From blood to brain: amoeboid microglial cell, a nascent macrophage and its functions in developing brain. Acta pharmacologica Sinica 28:1087-1096.

16- Lari R., Khan J. A. and Kitchener P. D. (2012) Organotypic brain slice culture promotes the transformation of haemopoietic Journal of Cell and Molecular Research 4:11-17.

17- Ling E. A. and Wong W. C. (1993) The origin and nature of ramified and amoeboid microglia: a historical review and current concepts. Glia 7:9-18.

18- Lutsik B. D., Iashchewnko A. M. and Lutsik A. D. (1991) Lectin-peroxidase markers of the microglia in paraffin sections. Arkhiv patologii 53:60-63.

19- Mackowiak M., Chocyk A., Markowicz-Kula K. and Wedzony K. (2007) Acute activation of CB1 cannabinoid receptors transiently decreases PSA-NCAM expression in the dentate gyrus of the rat hippocampus. Brain Res 1148:43-52.

20- Maganti S., Pierce M. M., Hoffmaster A. and Rodgers F. G. (1998) The role of sialic acid in opsonin-dependent and opsonin-independent adhesion of Listeria monocytogenes to murine peritoneal macrophages. Infection and immunity 66:620-626.

21- Maruhama Y., Hikichi I., Saito F., Hashimoto T., Kaneko H., Takahashi K. and Kaito I. (1983) Low density lipoprotein-sialic acids in patients with non-insulin dependent diabetes mellitus. Tohoku J Exp Med 141:199-205.

22- Navascues J., Calvente R., Marin-Teva J. L. and Cuadros M. A. (2000) Entry, dispersion and differentiation of microglia in the developing central nervous system. Anais da Academia Brasileira de Ciencias 72:91-102.

23- Rezaie P., Bohl J. and Ulfig N. (2004) Anomalous alterations affecting microglia in the central nervous system of a fetus at 12 weeks of gestation: case report. Acta Neuropathol 107:176-180.

24- Rezaie P., Dean A., Male D. and Ulfig N. (2005) Microglia in the cerebral wall of the human telencephalon at second trimester. Cereb Cortex 15:938-949.

25- Rezaie P., Patel K. and Male D. K. (1999) Microglia in the human fetal spinal cord--patterns of distribution, morphology and phenotype. Brain Res Dev Brain Res 115:71-81.

26- Song Y., Morikawa S., Morita M., Inubushi T., Takada T., Torii R., Kitamura Y., Taniguchi T. and Tooyama I. (2006) Comparison of MR images and histochemical localization of intra-arterially administered microglia surrounding beta-amyloid deposits in the rat brain. Histology and histopathology 21:705-711.

27- Suzuki M., Nakayama J., Suzuki A., Angata K., Chen S., Sakai K., Hagihara K., Yamaguchi Y.

and Fukuda M. (2005) Polysialic acid facilitates tumor invasion by glioma cells. Glycobiology 15:887-894.

28- Wielgat P. and Braszko J. J. (2012) The participation of sialic acids in microglia-neuron interactions. Cell Immunol 273:17-22.

29- Zambenedetti P., Giordano R. and Zatta P. (1998) Histochemical localization of glycoconjugates on microglial cells in Alzheimer's disease brain samples by using Abrus precatorius, Maackia amurensis, Momordica charantia, and *Sambucus nigra* lectins. Exp Neurol 153:167-171.

Journal of Cell and Molecular Research (2014) 6 (2), 64-68

Research Article

Analysis of IFN-γ (+874 A/T) and IL-10 (-1082 G/A) genes polymorphisms with risk of schizophrenia.

Dor Mohammad Kordi-Tamandani[1] , Maryam Najafi[1], Azizoallah Mojahed[2], Ali Shahraki[1]

1. Department of Biology, University of Sistan and Baluchestan, Zahedan, Iran.
2. Department of Clinical psychology ,Zahedan University of Medical Sciences, Zahedan, Iran

Received 27 Apr 2014 Accepted 01 Jun 2014

Abstract

Schizophrenia is a sophisticated mental disability which has affected nearly1.1% of people all over the world. According to recent researches, the key proteins triggered in the immune system are cytokines which might also be taking part in the pathogenesis of schizophrenia. The aim of this study was to evaluate the relationship between the -1082G/A and +874T/A polymorphisms of IL-10 and IFN-γ genes, respectively, in patients with schizophrenia. Total of 94 schizophrenic patients and 97 individuals as control samples were enrolled in this study. All samples were genotyped by amplification mutation refractory system-polymerase chain reaction (ARMS PCR) for candidate SNPs in IFN-γ and IL-10 genes. No significant association was found among various genotypes of IFN-γ and IL-10 in selected SNPs with risk of schizophrenia. As well as there was no significant variation in allelic frequency of IFN-γ and IL-10 genes with the risk of disease**.** These data suggest that the -1082G/A of IL-10 and +874T/A IFNγ genes are not involved in the development of schizophrenia risk. To validate this data, more studies in diverse populations with larger sample size are required.

***Keywords*:** Schizophrenia**,** IFN-γ, IL-10, gene, polymorphism

Introduction

Schizophrenia is a heterogeneous disorder disclosed by a interruption in cognition and emotion along with negative (abolition, alogia, apathy, poor social functioning) and positive (hallucinations, delusions) symptoms with a worldwide incidence of 1.1% (Rubinov and Bullmore, 2013). Regarding to the macrophage-T cell theory of psychiatric disorders, immune cells (macrophages and T cells) are activated in bipolar disorders and schizophrenia. This hypothesis believed that chronically activated macrophages, microglia and T cells synthesize inflammatory compounds like cytokines that destabilize the brain and lead to schizophrenia (Smith and Maes, 1995) . This possibility that polymorphism of a specific cytokine exhibits susceptible genes for schizophrenia development after infection or ischemia-related insults during the neurodevelopmental process has been proved in vast studies (Paul-Samojedny et al., 2010),(Paul-Samojedny et al., 2011). One of these cytokines that shows alternation in schizophrenia is IL-10 that is located on chromosome 1q31-32, a region previously reported to be linked to schizophrenia in genetic studies ,and is expressed by a variety of cells, such as monocytes, macrophages, microglia, astrocytes, T, B and mast cells (Ekelund et al., 2001),(Peng et al., 2008). IL-10 have various effecs on B and T cells such as initiating B cell differentiation and growth, inhibition the Th1 immune cytokines such as IFN-γ, IL-2 respectively. Also it induces alternative activation of myeloid cells and suppresses lymphocyte effector functions. Morever it was shown recently, that IL-10 prevents glutamate and N-methyl-D-aspartate (NMDA)-mediated cell death in vitro and exerts inhibition of IL-6-mediated excitotoxicity. (Itoh and Hirohata, 1995),(Fiorentino et al., 1991),(Blazevski et al., 2013),(Jun et al., 2003) . The promoter region of this gene has three major putative SNPs; 1082G/A, 819 T/C and -592 C/A. The -1082G/A SNP has known as a higher IL-10-producing allele than others, as well as -G in comparison to A allele has more effect on expression of this anti-inflammatory cytokine (Paul-Samojedny et al., 2010). There is evidence of increased concentration of this Th2 cytokine in the serum of patients with schizophrenia compared to the group of healthy

Corresponding authors E-mail:
** dor_kordi @yahoo.com*

(Yu L, 2004 Nov 1),(Ozbey et al., 2009).

Another cytokine express changes in schizophrenia is IFN-γ which is secreted by CD4+ T helper cell, CD8+ cytotoxic lymphocytes, NK cells, B cells, professional antigen-presenting cells (APCs) such as microglia. This pro-inflammatory cytokine that is located on choromosome 12q14 is provital in stimulation of Th1 cytokines and inhibition of Th2 clonal expansion.Furthermore this cytokine prevents of synapse formation, induces class I major histocompatibility complex (MHC) antigen expression on both neuronal and glial cells and also induces MHC class II expression on microglia, some population of astrocytes, and endothelial cells, enhances the function of microglia by increasing the production of some cytokines, nitric oxide, as well as free radicals (Paul-Samojedny et al., 2011),(Kim et al., 2012) .Vast investigations assigned that expression of this Th1 cytokine was significantly reduced due to the functional IFN-γ (+874 A/T) SNP in patients with schizophrenia compared with normal controls (Freudenreich O, 2010 Apr 30). The presence of genotype A/A is linked with low cytokine production, whereas genotype A/T is linked to medium cytokine production, and genotype T/T to high cytokine production, respectively (Pravica et al., 2000). A clear Th2 shift in schizophrenia, may be indicating a possible deregulation of the balance between Th1/Th2 cytokines (Chiang SS, 2013 May). Our present study examines the IFN-γ (+874 A/T) and IL-10 (-1082 G/A) genes polymorphisms with risk of schizophrenia.

Materials and Methods

Patients were randomly assigned to control and experimental groups.This case-control study was conducted on 94 newly diagnosed and untreated patients with schizophrenia (mean age: 47.53 ± 10.801) and (average of onset age: 20.79 ± 8.729) who were admitted to Azadi and EmamHossein Hospitals during 2010 and 2011 in Tehran, Iran. The control group consisted of 98 subjects with a median age of 46.70+11.716 years who was detached from any signs of neuropsychiatric disorders. All steps of this study were approved by the ethical committee of the university and informed consents were obtained from all patients and healthy in individuals. The demographic characteristics of the participants have been cited in table 1.

DNA isolation and polymerase chain reaction (PCR)

DNA was extracted from EDTA-collected peripheral whole blood with a method which previously described by Kordi-Tamandani et al (2012) (Kordi-Tamandani et al., 2012).

Table 1: The socio-demographic characteristics of the case and control groups

Variables	Cases	Controls	*P value
Age	47.53± 10.801	46.70± 11.716	p>0.05
Age of onset	20.79± 8.729	-	
Sex			
Females	26	29	p>0.05
Males	67	70	
Smoking status			
Non-smokers	-	54	P<0.001
Smokers	93	45	
Educational level			
Illiteracy	3	-	
Primary school	8	1	
Guidance	16	5	
High school	53	28	
AD	2	26	P<0.001
BA	8	27	
MA	1	10	
Missing data	3	2	
Marital status			
Single	60	29	
Married	17	63	P<0.001
Divorced	17	4	

Polymorphisms were analyzed by using amplification mutation refractory system-polymerase chain reaction (ARMS PCR), at positions -597 (rs1800872) in the promoter of the IL10 and +874 IFN-γ genes, the primers have been listed in Table 2. The PCR reaction for these SNPs was carried out in a final volume of 25 µL containing 100 ng genomic DNA, 0.3 mm/L of each primer, 1.5 U Taq DNA polymerase, 2 mm/L $MgCl_2$, 0.25 mm/L dNTPs and 1X PCR buffer. The amplification conditions for IL10 gene were as follows: 94 °C for 5 min, then 35 cycles of 94 °C for 30 Sec, 64 °C for 45 Sec, and 72 °C for 90 Sec, followed by a single cycle of final extension at 72 °C for 10 min. For IFN-γ +874A/T, the reaction was denatured initially at 94 °C for 4 min followed by 35 cycles of denaturation at 94 °C for 30 sec, annealing at 48 °C for 30 sec and extension at 72 °C for 30 sec. This response was followed by a final extension step at 72 °C for10 minutes. Finally, PCR products were visualized by 2% agarose gel electrophoresis stained by ethidium bromide. Primer design program was Primer 3.

Statistical data analyses

The association between polymorphism in IFN-γ and IL-10 genes with the risk of schizophrenia

estimated by computing Odds ratio (OR) and 95% confidence intervals (95% CI) using Epi-Info software (Epi-Info, version3, Center for Disease Control and prevention, Atlanta, GA, USA) and SPSS statistical software version 16 (SPSS, Chicago, IL).

Table 2. The list of primers sequence

Gene		primer	
IFN-γ +874 A/T	Generic primer	5'-TCAACAAAGCTGATACTCCA-3'	262bp
	Primer T (sense)	5'-TTCTTACAACACAAAATCAAATCT-3'	
	Primer A (sense)	5'-TTCTTACAACACAAAATCAAATCA-3'	
	Sense:	5'-GCCTTCCCAACCATTCCCTTA-3'	429bp
	Antisense:	5'-TCACGGATTTCTGTTGTGTTTC-3'	
IL10-1082 G / A	Generic primer (antisense)	5'-CAGCCCTTCCATTTTACTTC-3'	550bp
	Primer G (sense)	5'-TACTAAGGCTTCTTTGGGAG-3'	
	Primer A (sense)	5'-CATCTAAGGCTTCTTTGGGAA-3'	550bp

Results

As given in Tables (3&4), TT genotype of IFN-γ was not significant in schizophrenia disorder (OR=4, 95% CI, 0.17-261.5). Also, for AT and combined AT+TT genotypes of IFN-γ have been detected great risk of disease (OR=1.25. 95% CI, 0.20-8.75; OR=1.28, 95% CI, 0.21-8.95) respectively. Analysis of the IL-10 1082G/A genotyping have been highlighted that GA and combined GA +AA genotypes increased the risk of schizophrenia (OR= 0.63, 95% CI, 0.05-5.66; OR=0.64, 95% CI, 0.05-5.72) respectively, but not significant. The allele frequency at T+874A of IFN-γ and G-1082A IL-10 has not demonstrated significant difference between patients and healthy subjects. These data suggest that IL-10 and IFN-γ polymorphism may not confer a susceptibility to the development of schizophrenia at least in the iranian population. Immunological studies in schizophrenia indicated that a shift from Th1 to Th2 immune reactivity has been found to be the most common characteristic immune finding in patients with schizophrenia. A possible mechanisms in the pathogenesis of schizophrenia is that IL-10 is a Th2 cytokine and IFN- γ is a Th1 cytokine that are closely associated with the works of the central nervous system through immunologic, neurochemical, neuroendocrine, and stress-related behavioral activities. Present study has not found any association between IL-10 -1082G/A and IFN-γ +874A/T gene polymorphism with risk of schizophrenia in a sample of the Iranian population. Considering that these two genes do not work alone but functions through a network system and reciprocal interaction with other cytokines, we could suggest that the putative role of IL-10 and IFN-γ influencing the development of schizophrenia would have a complex regulatory function rather than a genetic component. The power of study is important if the negative result comes out.

Table3. Allele frequency (%) among individual SCZ cases and healthy controls

Genes	Cases (%)	Controls (%)	P value
IFN-γ +874 A/T			0.84
T	93(50%)	95(48/47%)	
A	93(50%)	101(51/53%)	
IL10-1082 G / A			0.92
G	92(48/94%)	95(48/97%)	
A	96(51/06%)	99(51/03%)	

Table 4. Genotype frequency of IL10-1082 G /A and IFN-γ +874 A/T in SCZ cases and healthy controls.

SNP	Case	Control	OR	95%cl	P value
IFN-γ					
AA	3(3.22%)	4(4/08%)	Ref	Ref	Ref
AT	87(93.55%)	93(94/90%)	1.25	0.20-8.75	0.92
TT	3(3.22%)	1(1/02%)	4	0.17-261.5	0.68
AT+TT	90(96.77%)	94(95/92%)	1.28	0.21-8.95	0.94
IL10-1082 G /					
AA	3(3/19%)	2(2/13%)	Ref	Ref	Ref
GA	90(95/74%)	95(97/94%)	0.63	0.05-5.66	0.96
GG	1(1/1%)	0	-	-	0
GA+AA	93(98/94%)	97(1 00%)	0.64	0.05-5.72	0.97

Discussion

Several studies have tried to replicate this association in various populations with conflicting results. Samojedny et al (2010) has highlighted that the presence of one or two allele G at position -1082 of IL-10 correlates with increasing risk of paranoid schizophrenia in the Polish population (Paul-Samojedny et al., 2010). In line our data, Ozbey et al (2009) have reported that there is not any association between polymorphism -1082 G/A at the promoter of IL-10 and the risk of schizophrenia (SCZ) in Turkish population (Ozbey et al., 2009). As well as, Yu et al (2004) results have not shown any significant association between IL-10 1082G/A gene polymorphism and progress of SCZ in Chinese population.(Yu L, 2004 Nov 1) A certain study in Spanish population has not uncovered a significant link between the -1082 G/A polymorphic site of the IL-10 gene and risk of schizophrenia (Almoguera B, 2011 Jun 9). These suggest that the contribution of the IL-10 gene promoter polymorphism to the development of schizophrenia may vary among different ethnic groups. Data are sparse regarding the effect of IFN-γ (+874T/A) polymorphism on the development of SCZ. An investigation of the Korean population has been detected a significant difference in genotype distributions and allele frequencies of the IFN-γ +874A/T gene between patients with bipolar disorders and healthy controls (Yoon HK, 2012 Feb). Paul-Samojedny et al (2011) has reported significant difference of IFN-γ (+874T/A) polymorphism between males and female groups in a Polish population (Paul-Samojedny et al., 2011). Frydecka et al (2013) indicated that IL-2, IL-6, IFN-gamma and TGF-beta gene polymorphisms are not linked to the risk of schizophrenia in a sample of Polish population.(Frydecka. et al., 2013) Although, Kim HJ et al (2012) has reported that IFN-γ polymorphisms may be associated with schizophrenia risk in Korean population In conclusion, It seems that the IFN-Gamma (+874 A/T) and IL-10 (-1082 G/A) genotypes studied here do not fully account for the development of SCZ.(Kim et al., 2012) More analyses, with larger sample sizes in various populations are required for more exposing the role of IFN-γ (+874 A/T) and IL-10 (-1082 G /A) in the risk for SCZ.

Acknowledgments

The authors wish to thank the University of Sistan and Baluchestan for financially supporting this project through grants to DMK.

References:

1. Almoguera B. R., Lopez-Castroman A. R., Dorado J., Lopez-Rodriguez P., Fernandez-Navarro R., Baca-García P., Fernandez-Piqueras J., Dal-Ré R., Abad-Santos F., Llerena A., Ayuso C. (2011) ATA homozigosity in the IL-10 gene promoter is a risk factor for schizophrenia in Spanish females: a case control study. BMC Med Genet 12: 2312-2381.
2. Blazevski J., Petkovic F., Momcilovic M., Jevtic B., Miljkovic D. and Mostarica Stojkovic M. (2013) High interleukin-10 expression within the central nervous system may be important for initiation of recovery of Dark Agouti rats from experimental autoimmune encephalomyelitis. Immunobiology 218:1192-1199.
3. Chiang S. S., Schwarz M., Mueller N. (2013) Is T-helper type 2 shift schizophrenia-specific? Primary results from a comparison of related psychiatric disorders and healthy controls. Psychiatry Clin Neurosci 67:228-236.
4. Ekelund J., Hovatta I., Parker A., Paunio T., Varilo T., Martin R., Suhonen J., Ellonen P., Chan G., Sinsheimer J. S., Sobel E., Juvonen H., Arajarvi R., Partonen T., Suvisaari J., Lonnqvist J., Meyer J. and Peltonen L. (2001) Chromosome 1 loci in Finnish schizophrenia families. Human molecular genetics 10:1611-1617.
5. Fiorentino D. F., Zlotnik A., Vieira P., Mosmann T. R., Howard M., Moore K. W. and O'Garra A. (1991) IL-10 acts on the antigen-presenting cell to inhibit cytokine production by Th1 cells. Journal of immunology 146:3444-3451.
6. Freudenreich O. B. M., Henderson D. C., Evins A. E., Fan X.,Walsh J. P., Goff D. C. (2010) Analysis of peripheral immune activation in schizophrenia using quantitative reverse-transcription polymerase chain reaction (RT-PCR). Psychiatry Res 176:(2-3), 99–102.
7. Frydecka. D., Beszlej. A., Karabon. L., Pawlak-Adamska. E., Tomkiewicz. A., Partyka. A., Misiak. B., Piotrowski. P., Zagdanska. M. and Kiejna A. (2013) IL-2, IL-6, IFN-gamma and TGF-beta genetic polymorphism with respect to susceptibility to schizophrenia. European Psychiatry, 28.
8. Itoh K. and Hirohata S. (1995) The role of IL-10 in human B cell activation,

proliferation, and differentiation. Journal of immunology 154:4341-4350.
9. Jun T. Y., Pae C. U., Kim K. S., Han H. and Serretti A. (2003) Interleukin-10 gene promoter polymorphism is not associated with schizophrenia in the Korean population. Psychiatry and clinical neurosciences 57:153-159.
10. Kim H. J., Eom C. Y., Kwon J., Joo J., Lee S., Nah S. S., Kim I. C., Jang I. S., Chung Y. H., Kim S. I., Chung J. H. and Choi J. S. (2012) Roles of interferon-gamma and its target genes in schizophrenia: Proteomics-based reverse genetics from mouse to human. Proteomics 12:1815-1829.
11. Kordi-Tamandani D. M., Sahranavard R. and Torkamanzehi A. (2012) DNA methylation and expression profiles of the brain-derived neurotrophic factor (BDNF) and dopamine transporter (DAT1) genes in patients with schizophrenia. Molecular biology reports 39:10889-10893.
12. Ozbey U., Tug E. and Namli M. (2009) Interleukin-10 gene promoter polymorphism in patients with schizophrenia in a region of East Turkey. The world journal of biological psychiatry : the official journal of the World Federation of Societies of Biological Psychiatry 10:461-468.
13. Paul-Samojedny M., Kowalczyk M., Suchanek R., Owczarek A., Fila-Danilow A., Szczygiel A. and Kowalski J. (2010) Functional polymorphism in the interleukin-6 and interleukin-10 genes in patients with paranoid schizophrenia--a case-control study. Journal of molecular neuroscience : MN 42:112-119.
14. Paul-Samojedny M., Owczarek A., Suchanek R., Kowalczyk M., Fila-Danilow A., Borkowska P., Kucia K. and Kowalski J. (2011) Association study of interferon gamma (IFN-gamma) +874T/A gene polymorphism in patients with paranoid schizophrenia. Journal of molecular neuroscience : MN 43:309-315.
15. Peng H. Y., Ku Y. C., Shu B. C. and Lung F. W. (2008) Association between Interleukin-10 Gene Promoter Haplotype and Schizophrenia in a Han-Chinese Study. International journal of biomedical science : IJBS 4:185-191.
16. Pravica V., Perrey C., Stevens A., Lee J. H. and Hutchinson I. V. (2000) A single nucleotide polymorphism in the first intron of the human IFN-gamma gene: absolute correlation with a polymorphic CA microsatellite marker of high IFN-gamma production. Human immunology 61:863-866.
17. Rubinov M. and Bullmore E. (2013) Schizophrenia and abnormal brain network hubs. Dialogues in clinical neuroscience 15:339-349.
18. Smith R. S. and Maes M. (1995) The macrophage-T-lymphocyte theory of schizophrenia: additional evidence. Medical hypotheses 45:135-141.
19. 19- Yoon HK K. Y. (2012 Feb) The T allele of the interferon-gamma +874A/T polymorphism is associated with bipolar disorder. Nord J Psychiatry. 66:14-18.
20. Yu L Y. M., Zhao J,Shi YY,Zhao XZ,Yang JD,Liu ZJ,Gu NF,Feng GY,He L. (2004 Nov 1) An association between polymorphisms of the interleukin-10 gene promoter and schizophrenia in the Chinese population. Schizophr Res. 71:179-183.
21. Genetic diversity and involvement in bread spoilage of *Bacillus* strains isolated from flour and ropy bread. Letters in applied microbiology 37: 169-173.
22. Sun F., Wu, D., Qiu, Z., Jin, M. and Li, J. (2010) Development of real-time PCR systems based on SYBR Green for the specific detection and quantification of *Klebsiella pneumoniae* in infant formula. Food Control 21: 487-491.
23. Wehrle E., Didier, A., Moravek, M., Dietrich, R. and Märtlbauer, E. (2010) Detection of *Bacillus cereus* with enteropathogenic potential by multiplex real-time PCR based on SYBR green I. Molecular and cellular probes 24: 124-130.

Journal of Cell and Molecular Research (2014) 6 (2), 69-75

Research Article

A comparative investigation on efficiency of bacteriophage lambda and M13 based vectors for delivering and expression of transgene in eukaryote cells

Elham Abedheydari[1], Mohammad Khalaj-Kondori*[1], Mohammad-Ali Hosseinpour-Faizi[1], Morteza Kosari-Nasab[2]

1. Department of Animal Biology, Faculty of Natural Science, University of Tabriz, Tabriz, Iran
2. Drug Applied Research Center, Tabriz University of Medical Sciences, PO Box 51656-65811, Tabriz, Iran.

Received 23Jul2014 Accepted 27Aug 2014

Abstract

Gene delivery might be affected by several tribulations based on carrier/vector applied. Bacteriophages lambda and M13 have different genome conformations; linear double-stranded and circular single-stranded respectively. Therefore, it might be expected that these two common classes of gene delivery vehicles will have different capacity for gene delivery and expression in eukaryote cells. To address the possible effects of linear double-stranded and circular single-stranded genome conformations of bacteriophages lambda and M13 on the transgene expression, the transfection efficacy of two vectors based on lambda and M13 were compared in AGS cell line. The GFP encoding sequence was inserted into the Lambda ZAP-CMV XR vector which resulted in λ-ZAP-CMV-GFP construct. The construct was then in vitro packaged using Gigapack® III Gold packaging extract and λ-GFP phage particles were obtained. The λ-GFP phage particles were then used for in vivo excisioning which resulted in M13-CMV-Script-GFP construct. 10^{11} copy of λ-ZAP-CMV-GFP or M13-CMV-Script-GFP constructs were transfected into AGS cells using lipofectamine 2000. Transfection efficiencies were analyzed by FACS. Results showed that linear double-stranded λ-ZAP-CMV-GFP was efficient than single-stranded form of M13-CMV-Script-GFP while its double-stranded form was efficient than the linear double-stranded λ-ZAP-CMV-GFP construct for transgene delivery and expression. Moreover the GFP signals resulted from transfections by single-stranded form of M13-CMV-Script-GFP construct faded more quickly in comparison to others. These findings highlight that genome conformation of gene carriers might be an important factor when seeking for an appropriate gene carrier/vehicle.

***Keywords*:** :Gene delivery; Phage-mediated gene transfection; Vector conformation

Introduction

Bacteriophages are bacterial viruses that infects specifically bacterial cells, however, they have been considered as a class of gene delivery vehicles for eukaryotes by ever-increasing number of researchers (Larocca et al., 1999; Larocca et al., 2001; Piersanti et al., 2004; Lankes et al., 2007; Khalaj-kondori et al., 2010). Among bacteriophages, M13 and lambda are the most studied and exploited ones in molecular biology. These bacterial viruses have several striking features including no tropism for eukaryotic cells, safety, physical stability at various harsh conditions, inexpensive mass production, ease of genome manipulation, nanostructured size and availability of diverse approaches for their specific targeting which have made them attractive for researches of different fields (Poul and Marks, 1999; Larocca and Baird, 2001; Olofsson et al., 2001; Larocca et al., 2002; Catherine et al., 2004). Lambda is a head and tailed bacteriophage with a double-stranded genome of ~48 kb. It has an icosahedral capsid of ~55 nm in diameter surrounding its genome and a fibrous tail of ~145 nm in length (Kaiser, 1966; Zanghi et al., 2005).While, M13 is a filamentous bacteriophage with a ~6.4 kb circular single-stranded genome surrounded by a proteinaceous coat (Petrenko et al., 1996; Calendar and Abedon, 2005).

There are several steps that may affect the efficacy of gene delivery procedure when using bacteriophages as gene delivery vectors/carriers.First of all, as for any other gene delivery vehicles, phage particles should be internalized into target cells, and then they must bypass the cytoplasmic barriers e.g. degradative enzymes of the cytoplasm as well as trafficking-associated problems of transgene toward the cell nucleus (Larocca and

Corresponding authors E-mail:
* *E-mail: khalaj@tabrizu.ac.ir*

Baird, 2001). Surface modifications of phage particles through phage display and chemical coupling technologies have been partly overcome these problems. It has been shown that bacteriophages M13 and lambda targeted to mammalian cells by displaying or coupling of host derived ligands on their surfaces can result in expression of the transgene in the target cells (Larocca et al., 2001; Sapinoro et al., 2008; Khalaj-Kondori et al., 2011; Kim et al., 2012). Moreover, displaying of different peptides such as NLS on the surface of bacteriophages and application of proteasome inhibitors indicated an exciting role on efficient intracellular trafficking of phage based vectors (Akuta et al., 2002; Volcy and Dewhurst, 2009). Nevertheless it seems that entering to the nucleus is not sufficient by itself, since several studies indicated that despite displaying of targeting ligands on the phages surface, relatively a small fraction of transfected cells was expressing the transgene.

The final step in a gene delivery attempt is transcription of the transgene and subsequent translation of mRNA to the functional protein. Recently it was reported that phagemid particles bearing inverted self-complementary sequences with capacity of converting to double-stranded DNA can result in higher level of transgene expression than those containing single-stranded DNA (Prieto and Sánchez, 2007). This finding suggests that the bacteriophage genome structure and conformation might be implicated on the processes such as transcription and translation even after successful entering into the nucleus.

In the present study, effects of single-stranded circular conformation of a vector, as seen in M13-based gene carriers, at transgene delivery and expression efficacy were compared to that of double-stranded linear vector conformation such as λ-based ones. To achieve this purpose, the sequence encoding for GFP was inserted into the Lambda ZAP®-CMV XR vector to obtain λ-ZAP-CMV-GFP construct as a vector with double-stranded linear conformation. Then λ-ZAP-CMV-GFP vector was used for obtaining M13-CMV-Script-GFP construct as a vector with single-stranded circular conformation. Finally, efficacy of the two constructs in delivery and expression of GFP transgene in AGS cell line was studied by florescence activated cell sorting (FACS) analysis.

Materials and Methods

Construction of λ-ZAP-CMV-GFP vector and in vitro packaging

λ-ZAP-CMV-GFP vector was constructed according to a previous report (Khalaj-kondori et al., 2010). In brief, the sequence coding for GFP was obtained by PCR using a primer pairs, forward: 5'-GTAGAATTCCGCCACCATGGTGAGCA -3', reverse; 5'-GACCTCGAGTTACTTGTACAGTTCGTCCATG C-3' and pEGFP-N1 plasmid (BD Biosciences Clontech) as template. The PCR product was purified, digested with EcoRI and XhoI (Fermentas, Lithuania) and ligated to the Lambda ZAP-CMV XR vector (figure 1a) (Stratagene La Jolla, CA) digested with the same enzymes. To obtain λ-GFP particles, the ligation product was in vitro packaged using Gigapack® III Gold packaging extract (Stratagene La Jolla, CA) and used to transfect E.coli XL1-Blue MRF´ strain (Stratagene La Jolla, CA). The melted and cooled to 48°C NZY Top agar was added on transfected E.coli XL1-Blue MRF´ cells and immediately plated on prewarmed NZY agar plates. After 12 hours incubation at 37ºC, the recombinant plaques appeared were confirmed by plaque-PCR and amplified.

Amplification of λ-GFP particles

XL1-blue MRF´ cells were cultured in 10 ml of LB broth supplemented with 10 mM MgSO4 and 0.2% (W/V) maltose. The culture was infected by λ-GFP at a multiplicity of infection (MOI) of 1:20 and incubated at 37°C with vigorous agitation until lysis observed. Upon lysis, chloroform was added to a 5% (v/v) final concentration, mixed well and incubated for 15 minutes at room temperature. Then cell debris was removed by centrifugation for 10 minutes at 500×g. DNase I and RNase A (Fermentase) were added to a final concentration of 1µg/ml to eliminate nucleic acids. To precipitate the phage particles, polyethylene glycol 8000 and NaCl were added to a final concentration of 10% (W/V) and 1M respectively and incubated in ice for 60 minutes. Phage particles were collected by centrifugation at 11000×g, 4°C for 10 minutes. Phage pellet was resuspended in SM buffer and tittered

Construction of M13-CMV-Script-GFP vector and M13-GFP particles

Inserts cloned into the Lambda ZAP-CMV XR vector can be excised out of the phage in the form of the kanamycin-resistant pCMV-Script® EX phagemid (figure 1b) vector. So, M13-CMV-Script-GFPvector wasprepared by in vivo excision. In vivo excision was achieved according to the instruction manual of Lambda ZAP®-CMV XR Library Construction Kit (Stratagene). Briefly, 200 µl of XL1-Blue MRF´cells at an OD_{600} of 1 were

coinfected with 250 µl of λ-GFP particles (10^5particles) and 1 µl of Ex Assist helper phage (10^6pfu/µl) and the mixture was incubated at 37°C for 15 minutes to allow the phage to attach to the cells. Then 3 ml of LB broth was added to the mixture and incubated for 3 hours at 37°C with shaking. The mixture was heated at 70°C for 20 minutes and cell debris was pelleted at 1000×g for 15 minutes. The supernatant contains M13-CMV-Script-GFP phagemid packaged as filamentous phage particles (M13-GFP particles). XLOLR cells (Stratagene) were infected with M13-GFP particles and plated on NZY agar containing 30mg/ml kanamycin. Colonies appeared were confirmed by colony-PCR.

Amplification of M13-GFP particles

A 10 ml of 2xYT containing 50mg/ml kanamycin was inoculated with a confirmed single colony of XLOLR and incubated for one hour at 37°C. R408 helper phage (Sratagene) was added to the culture at a MOI of 10 and incubated for 18 hours. The culture was spinned for 10 minutes at 6000×g and Polyethylene glycol 8000 and NaCl were added into the supernatant in a final concentration of 10% and 1M respectively followed by incubation for 60 minutes on ice. The precipitated M13-GFP particles were collected by centrifugation at 17000×g, 4°C for 20 minutes. The pellete was resuspended in SM buffer and tittered.

DNA extraction

The λ-ZAP-CMV-GFP and M13-CMV-Script-GFP constructs were extracted from λ-GFP and M13-GFP particles respectively. M13-GFP and λ-GFP particles were obtained as mentioned above. Phenol-chloroform (1:1 v/v) was added to the phage particles in SM buffer and filliped to destruct the capsid followed by centrifugation 12000×g, 4°C for 10 minutes. The procedure was repeated for 2 times and followed by another round of chloroform extraction. DNA was precipitated by adding one volume of ice cold isopropanol and collected by centrifugation at 12000×g, 4°C for 10 minutes. Moreover replicative form of the M13-CMV-Script-GFP construct was obtained by plasmid minipreparation method. DNA was quantified by Picodrop and evaluated on 1% agarose gel.

Transfection of AGS cells and FACS analysis

AGS cells were seeded into 24-well plates containing RPMI 1640 with 10% FBS at 4×104 cells/well 24 h prior to transfection. Cells were transfected by 1011 copy of λ-ZAP-CMV-GFP, single-strand or double stranded forms of M13-CMV-Script-GFP constructs using Lipofectamine 2000 (Invitrogene). After 24 and 48 hours incubation, cells were removed from the wells with trypsin–EDTA (Gibco BRL), pelleted and incubated with 5% paraformaldehyde in PBS for 20 min. The cells were washed with PBS and resuspended in PBS containing 0.01% sodium azide and analyzed by FACS (Becton Dickinson Biosciences, San Diego, CA). Transfection efficiency was measured as the percentage of total cells that were GFP positive as detected by FACS analysis. Transfections were done in duplicate and performed three times.

Results and discussion

Preparation and confirmation of constructs

The sequence encoding for GFP was PCR amplified using pEGFP-N1 as template and inserted into the Lambda ZAP-CMV XR vector (figure 1a) to obtain λ-ZAP-CMV-GFP construct. The construct was in vitro packaged and used for transfection of E.coli XL1-Blue MRF´ cells. Plaques appeared were confirmed by plaque-PCR assay. The positive plaques represent λ-GFP particles containing λ-ZAP-CMV-GFP construct.

We obtained M13-CMV-Script-GFP construct from λ-ZAP-CMV-GFP construct by in vivo excision. In vivo excision was resulted in M13-GFP phagemid particles containing the M13-CMV-Script-GFP construct. To plate the excised M13-GFP phagemid, XLOLR cells were infected and colonies appeared were analyzed and confirmed by colony-PCR (figure 2).

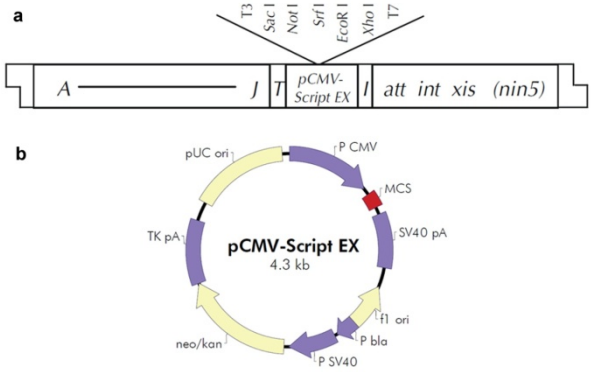

Figrure 1. Map and elements of (a) the Lambda ZAP-CMV XR vector and (b) the pCMV-Script® EX phagemid vector

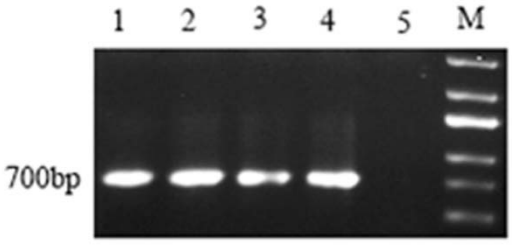

Figure 2. Screening of XLOLR colonies by Colony-PCR.

Lanes 1, 2 and 3; colony-PCR of three well separated colonies, lanes 4 and 5; positive and negative controls respectively, M; size marker.

The Lambda ZAP-CMV XR vector has been designed to allow in vivo excision and recircularization of any cloned insert contained within the lambda vector in the form of the pCMV-Script® EX phagemid vector by the same excision mechanism used with the Lambda ZAP vectors (Stratagene, 2007). This means that the gene inserted would be in the same context of regulatory and vector backbone sequence elements both in lambda and phagemid constructs. This is important because it might eliminate any possible effects of vector backbone sequence on the insert gene expression. In other words, we used this strategy to lower as much as possible any vector sequence-related effects that might affect the transgene expression.

Equaling the copy number of constructs

For comparative study of the efficacy of structurally different constructs in transgene delivery and expression it is needed that different constructs used for transfection have the equal copy numbers. To achieve equal copy numbers, the molecular weight for one molecule of each construct in µg was multiplied by 10^{11} to obtain the µg of each construct needed for each transfection reaction. We chose the copy number 10^{11} for all tests, because it yields 800 ng of λ-ZAP-CMV-GFP construct being in the best DNA concentration range that might be transfected using lipofectamine 2000 for 24-well platform. It should be noted that during M13-GFP phagemid amplification not only the phagemid will amplify but the helper phage R408 amplification will occur as well. Fortunately, the helper phage R408 has been designed to amplify 50 folds less than the phagemid(Stratagene, 2007). Amplification proportion of phagemid to helper phage R408 was tested on gel electrophoresis (figure 3). So, we applied a correction coefficient of one-fifty for calculation of the phagemid copy number. Table 1 summarizes the calculations and represents the micrograms of each construct per one transfection reaction.

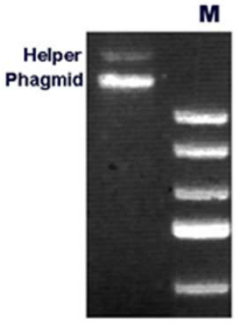

Figure 3. Gel electrophoresis showing the amplification proportion of phagemid to helper phage R408. After phagmid amplification, DNA was purified and electrophoresed on 1% agarose gel. M; size marker.

Table 1. Calculations for equaling the copy number of λ-ZAP-CMV-GFP and M13-CMV-Script-GFP constructs for one transfection reaction.

Construct	Size(kb)	Molecular weight (µg)	Conc. (ng/µl)	Copy No./ µl	Vol. (µl)
λ-ZAP-CMV-GFP	~42.7	4.68005×10^{-11}	830	0.1773×10^{11}	5.640
M13-CMV-Script-GFP	~5	2.74008×10^{-12}	158	0.56×10^{11}	1.76

Transgene expression analysis

To reveal potential effects of vector conformation and structure on transgene delivery and expression, AGS cells were transfected by the same copy numbers of single-stranded circular M13-CMV-Script-GFP and double-stranded linear λ-ZAP-CMV-GFP constructs using lipofectamine 2000. Moreover, double-stranded circular form of the M13-CMV-Script-GFP construct was used as positive control. Transgene delivery and expression efficiencies were evaluated at both individual and total cell population levels. To achieve these, we took advantage of GFP reporter system which is capable to report gene expression accurately even in the level of individual cells (Soboleski et al., 2005). Figure 4 depicts the results obtained from FACS analysis of AGS cells transfected by the above-mentioned constructs. FACS analysis showed that transfections by single-stranded circular M13-CMV-Script-GFP resulted in 36.8% and 25.5% GFP positive cells in 24 and 48 hours post transfection assays respectively. Whereas transfections by double-stranded λ-ZAP-CMV-GFP resulted in 23.3% and 37.3% GFP positive cells in 24 and 48 hours post transfection assays respectively (figure 4a). Mean Fluorescence Intensity (MFI) analysis (figure 4b) also revealed that the MFI of GFP positive cells in 24 and 48 hours post transfection tests of the single-stranded circular M13-CMV-Script-GFP construct was 4.86 and 4.07 respectively. Furthermore, the MFI of GFP positive cells in 24 and 48 hours post transfection tests of double-stranded linear λ-ZAP-CMV-GFP construct was 3.76 and 5.01 respectively. Moreover, the transfections by control construct resulted in 32.6% GFP positive cells with MFI of 7.00 in 48 hours post transfection assays (Figure 4a and b).

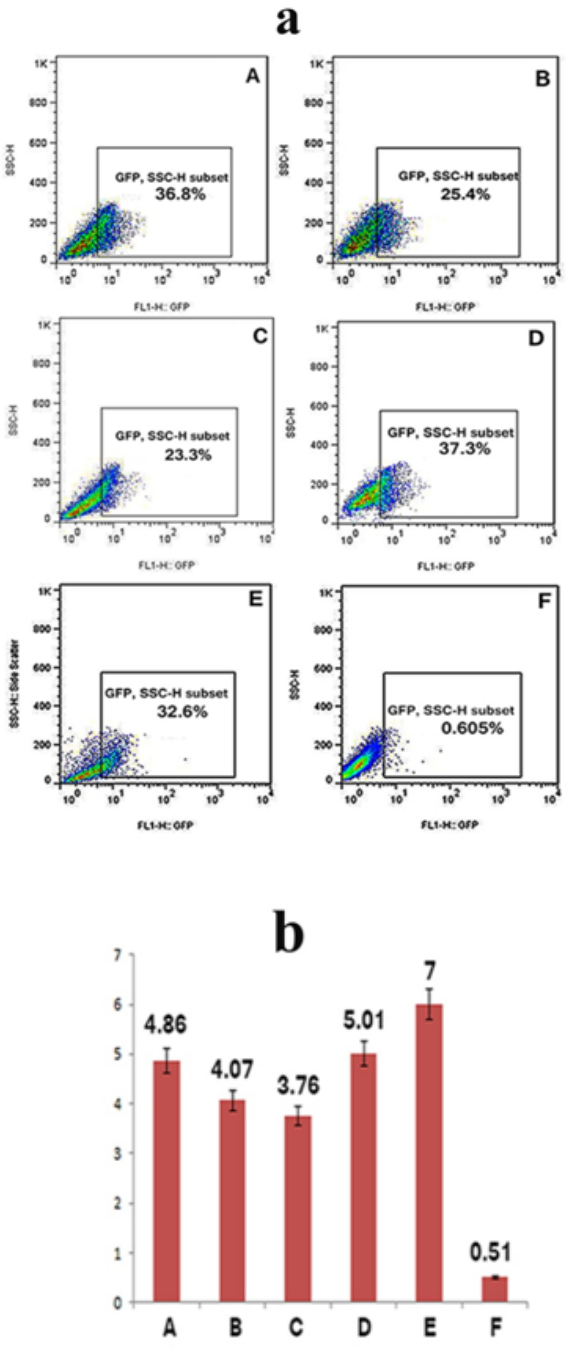

Figure 4. FACS analysis of GFP transgene expression in AGS cell line. AGS cells were seeded in 24 well plates and transfected with 10^{11} copies of λ-ZAP-CMV-GFP and M13-CMV-Script-GFP constructs. 10^{11} copies of double-stranded form ofM13-CMV-Script-GFP construct were usedascontrol to allow comparisons. After 6 hours the medium wasexchanged and cells were incubated until 24 hours or 48 hours. Finally cells were removed from the plate, fixed by paraformaldehyde 2% and resuspended in sodium azide 0.01% and analyzed by FACS. Panel **a** shows GFP positive cells obtained from transfection of AGS cells with 10^{11} copies of A) single-stranded M13-CMV-Script-GFP construct analyzed after 24 hours B) the same construct analyzed after 48 hours, C) double -stranded λ-ZAP-CMV-GFP construct analyzed after 24 hours, D) the same construct after 48 hours and E) double-stranded M13-CMV-Script-GFP construct analyzed after 48 hours. F) no construct. Panel **b** shows the Mean Fluorescence Intensity (MFI) of GFP positive cells of corresponding wells of panel a. All tests have been repeated tree times.

It is worth noting that none of the constructs are able to amplify in the AGS cells, hence the GFP expression level will be depend on merely the copy number and conformation/structure of the construct molecules available for transcription apparatus of the transfected cell. Comparison of the percentage of GFP positive cells achieved at the 24 hours post transfection assays showed that those transfections mediated by single-stranded circular M13-CMV-Script-GFP result in more GFP positive cells (36.8%) than those of the double-stranded λ-ZAP-CMV-GFP (23.3%) construct. This finding implies at first glance that the single-stranded circular conformation might be more efficient than the linear double-stranded conformation for transgene delivery and expression. However, this finding was not true when comparisons were made for the results of 48 hours post transfection assays because those transfections mediated by double-stranded λ-ZAP-CMV-GFP resulted in more GFP positive cells (37.3%) than those of the single-stranded circular M13-CMV-Script-GFP (25.4%) construct. In other words, the percentage of GFP positive cells achieved by transfections mediated by single-stranded circular M13-CMV-Script-GFP construct was decreased over time while that for double-stranded λ-ZAP-CMV-GFP was increased. This finding was true for MFI comparisons too. The MFI of GFP positive cells in 24 hours post transfection assays (3.76) of λ-ZAP-CMV-GFP construct was less than that of 48 hours post transfection assays (5.01). Moreover, the MFI of GFP positive cells achieved in 24 hours post transfection assays (4.76) for M13-CMV-Script-GFP construct was higher than that of 48 hours post transfection assays (4.07). Comparing the results of control to the results of both test constructs revealed that those for the control construct was more close to the results of λ-ZAP-CMV-GFP than those of the M13-CMV-Script-GFP in 48 hours post transfection assays. This might be explained by existence of double-stranded structure in both control and λ-ZAP-CMV-GFP constructs. In other words, it implies that having double-stranded structure might be more critical for a construct to be stable in the transfected cell, because whilst higher percentage and MFI of GFP positive cells in 24 hours post transfection assays mediated by M13-CMV-Script-GFP construct they diminished in 48 hours post transfection assays.

What obvious is from plenty of phage-mediated gene transfer studies to eukaryote cells

(Larocca et al., 1998; Larocca et al., 1999; Di Giovine et al.,2001; Larocca et al., 2001; Urbanelli et al., 2001; Burg et al., 2002; Prieto and Sánchez, 2007) as well as the present study is that constructs having single-stranded circular conformation such as M13-CMV-Script-GFP can mediate transgene expression. However, the mechanism by which this type of constructs is recognized by transcription machinery of eukaryote cells is not clear. This fact raises some questions which need more research to be answered including; are single-stranded circular constructs recognized by eukaryote cell transcription machinery? Can eukaryote cells convert single-stranded constructs to the double-stranded circular conformation? Our 24 hours post transfection assays showed that probably the transcription machinery of eukaryote cells are able to recognize single-stranded circular constructs, hence the GFP positive cells as well as their MFI observed for M13-CMV-Script-GFP were higher than those for 48 hours post transfection assays. Moreover, a research by Michael and coworkers showed that it might be possible converting single-stranded circular constructs to double-stranded form. They transfected many tumor cell lines by EGF-targeted phagemid particles in the presence of genotoxic agents such as camptothecin and obtained expression efficiency up to 30%. Moreover camptothecin treatment resulted in increased stable GFP expression up to 120 hours (Burg et al., 2002). A possible mechanism for this observation might be induction of DNA damage repair system which converts single-stranded DNA to double-stranded form which in its turn may increase the transgene expression efficacy. In addition, other researchers increased transgene expression by designing a construct capable of transforming to double-stranded form. They designed phagemid vectors bearing inverted self-complementary sequences for their expression cassette capable of converting the single strand genome of fF to dsDNA structure in HEK 293T cells (Prieto and Sánchez, 2007).

In conclusion, the results of present study highlights that the double-stranded structure and conformation of vector is critical for proper and stable expression of the transgene. So when one intended to use a carrier such as a bacteriophage for delivering a transgene to eukaryote cells/tissues it might be important to choose a carrier with double-stranded genome such as bacteriophage lambda. However, single-stranded bacteriophages such as M13 also might be of important options if designing a strategy which helps to convert single-stranded structure to double-stranded conformation.

Acknowledgments

This work was supported by the research deputy of University of Tabriz.

References:

1. Burg M. A., Jensen-Pergakes K., Gonzalez A. M., Ravey P., Baird A. and Larocca D. (2002) Enhanced phagemid particle gene transfer in camptothecin-treated carcinoma cells. Cancer Researc 62:4, 977-81.
2. Calendar R. and Abedon S. T. (2005) The bacteriophages. Oxford University Press. UK.
3. Catherine D., Clark J., March J. B. (2004) Bacteriophage lambda is a highly stable DNA vaccine delivery vehicle. Vaccine. 22: 2413-9.
4. Di Giovine M., Salone B., Martina Y., Amati V., Zambruno G., Cundari E. and Saggio I. (2001) Binding properties, cell delivery, and gene transfer of adenoviral penton base displaying bacteriophage. Virology 282: 102-12.
5. Kaiser A. (1966) On the internal structure of bacteriophage lambda. J Gen Physiol 49: 171-8.
6. Khalaj-Kondori M., Sadeghizadeh M., Behmanesh M., Saggio I. and Monaci P. (2011) Chemical coupling as a potent strategy for preparation of targeted bacteriophage-derived gene nanocarriers into eukaryotic cells. Journal of Gene Medicine 13: 622–31.
7. Khalaj-kondori M., Sadeghizadeh M. and Behmanesh M. (2010) Bacteriophage lambda-mediated gene transfer into human AGS cell line. ICBEE 176-9.
8. Kim A., Shin T-H., Shin S-M., Pham C. D., Choi D-K., Kwon M-H. and Kim Y-S. (2012) Cellular internalization mechanism and intracellular trafficking of filamentous M13 phages displaying a cell-penetrating transbody and TAT peptide. PloS one 7: e51813.
9. Lambda ZAP ® -CMV XR Library Construction Kit. In: Stratagene (2007) editor. United States and Canada, Stratagene.
10. Lankes H.A., Zanghi C.N., Santos K., Capella C. Duke C.M. and Dewhurst S. (2007) In vivo gene delivery and expression by bacteriophage lambda vectors. Journal of Applied Microbiology 102:1337–49.
11. Larocca D., Kassner P., Witte A., Ladner R., Pierce G. and Baird A. (1999) Gene transfer to mammalian cells using genetically targeted filamentous bacteriophages. FASEB 6: 727–34.

12. Larocca D., Jensen-Pergakes K., Burg M. and Baird A. (2001) Receptor-targeted gene delivery using multivalent phagemid particles. Molecular Therapy 3: 476–84.
13. Larocca D. and Baird A. (2001) Receptor-mediated gene transfer by phage-display vectors: applications in functional genomics and gene therapy. Drug Discovery Today 6: 793-801.
14. Larocca D., Brug M., Jensen-Pergakes K., Prenn R. E., Maria G. A. and Baird A. (2002) Evolving phage vectors for cell targeted gene delivery. Current Pharmacology and biotechnology 3: 45-57.
15. Larocca D., Jensen-Pergakes K., Burg M. A. and Baird A. (2001) Receptor-targeted gene delivery using multivalent phagemid particles. Molecular Therapy 3: 476-84.
16. Larocca D., Witte A., Johnson W., Pierce G. F. and Baird A. (1998) Targeting bacteriophage to mammalian cell surface receptors for gene delivery. Human Gene Therapy 9: 2393-9.
17. Larocca D., Kassner P. D., Witte A., Ladner R. C., Pierce G. F. and Baird A. (1999) Gene transfer to mammalian cells using genetically targeted filamentous bacteriophage. FASEB Journal 13: 727-34.
18. Olofsson L., Ankarloo J., Andersson P. O. and Nicholls I. A. (2001) Filamentous bacteriophage stability in non-aqueous media. ChemBiol 8: 661-71.
19. Petrenko V., Smith G., Gong X. and Quinn T. (1996) A library of organic landscapes on filamentous phage. Protein Engineering 9: 797-801.
20. Piersanti S., Cherubini G., Martina Y., Salone B., Avitabile D., Grosso F. et al. (2004) Mammalian cell transduction and internalization properties of lambda phage displaying the full-length adenoviral penton base or its central domain. Journal of Molecular Medicine 82: 467–76.
21. Poul M. A. and Marks J. D. (1999) Targeted gene delivery to mammalian cells by filamentous Bacteriophage. Molecular Biology 288: 203-11.
22. Prieto Y. and Sánchez O. (2007) Self-complementary sequences induce the formation of double-stranded filamentous phages. BiochimBiophysActa 1770: 1081-4.
23. Sapinoro R., Volcy K., Rodrigo W., Schlesinger J. J. and Dewhurst S. (2008) Fc receptor-mediated, antibody-dependent enhancement of bacteriophage lambda-mediated gene transfer in mammalian cells. Virology 373: 274-86.
24. Soboleski M. R., Oaks J. and Halford W. P. (2005) Green fluorescent protein is a quantitative reporter of gene expression in individual eukaryotic cells. FASEB Journal 19: 440-2.
25. Akuta T., Eguchi A., Okuyama H., Senda T., Inokuchi H., Suzuki Y., et al. (2002) Enhancement of phage-mediated gene transfer by nuclear localization signal. Biochemistry and Biophysic Research Communication 297: 779–86.
26. Urbanelli L., Ronchini C., Fontana L., Menard S., Orlandi R. and Monaci P. (2001) Targeted gene transduction of mammalian cells expressing the HER2/neu receptor by filamentous phage. Journal of Molecular Biology 13: 965-76.
27. Volcy K. and Dewhurst S. (2009) Proteasome inhibitors enhance bacteriophage lambda (λ) mediated gene transfer in mammalian cells. Virology 384: 77-87.
28. Zanghi C. N., Lankes H. A., Bradel-Tretheway B., Wegman J. and Dewhurst S. (2005) A simple method for displaying recalcitrant proteins on the surface of bacteriophage lambda. Nucleic Acids Research 33: e160-e.

Journal of Cell and Molecular Research (2014) 6 (2), 76-82

Research Article

Neuronal differentiation of mouse amnion membrane derived stem cells in response to neonatal brain medium.

Sheida Shahraki[1], Hanieh Jalali[2*], Kazem Parivar[1], Nasim Hayati Roudbari[1], Mohammad Nabiuni[3], Zahra Heidari[2]

1. *Department of Biology, Science and Research Branch, Islamic Azad University, Tehran, Iran*
2. *Department of Developmetal Biology, Faculty of Biological Science, Kharazmi University, Tehran, Iran*
3. *Department of Cell and Molecular Biology, Faculty of Biological Science, Kharazmi University, Tehran, Iran*

Received 22 Jul 2014 Accepted 27 Aug 2014

Abstract

Amniotic membrane derived stem cells have considerable advantages for being used in regenerative medicine and their anti-inflammatory effects, growth factor secretion and differentiation potential, have made them suitable candidates for nervous system stem cell therapy. The developing and neonatal brain contains a spectrum of growth factors to direct development of endogenous and donor cells. Using an *in vitro* model, we have investigated the plasticity and potential of mouse amnion membrane stem cells to be differentiated into neural cells in response to neonatal mice brain extracted medium. Mouse amniotic membrane stem cells were isolated from embryonic membrane and confirmed by flow cytometric analysis for their surface markers. Harvested stem cells were cultured in neonatal brain derived medium for 21 days and neural differentiation of cells was explored using immunohistochemistry and flowcytometry analysis. Isolated amnion membrane stem cells showed high rate of viability and proliferation and also expressed stem cell markers such CD105 and CD90. Amnion stem cells presented neural characters such as morphological changes and development of axon like appendixes as well as *Nestin* and *Map-2* expression when came in contact with brain tissue. In conclusion, the current investigation showed that amnion membrane derived stem cells are potent cells for responding to environmental signals promoting them to neural fate and could be used in regenerative medicine of neurodegenerative disorders.

***Keywords*:** fetal tissue, neuron, regeneration, stem cell

Introduction

The amniotic membrane is a fetal derived tissue, which composes of three layers: a single epithelial layer, a thick basement membrane, and an avascular mesenchymal layer (Dobreva et al., 2010). Subpopulations of stem cells exist in both the epithelial and mesenchymal layers, which term as amniotic epithelial cells (AECs) and amniotic mesenchymal cells (AMCs) (Toda et al., 2007). Amniotic membrane stem cells (AMSCs) have considerable advantages with regard to cellular therapy; they easily obtain from fetal placenta and their isolation lack any ethical problems, also millions of them can be harvested from each term amniotic membrane, which is important to prevent potential immune responses arising from cells of several unrelated donors (Pratama et al., 2011). Amniotic membrane derived stem cells don't express HLA class I and II and have low risk of rejection in transplantation procedures (Akle et al., 1981; Banas et al., 2008). They are not tumorogenic because of low telomerase activity (Miki et al., 2005) and do not form teratomas upon transplantation into the testes of SCID mice (Ilancheran et al., 2007). Amniotic membrane cells express pluripotency markers such as Oct-4, Sox-2 and Nanog (Izumi et al., 2009), also they are positively expressed mesenchymal stem cells markers, such as CD105 and CD90, and negatively expressed hematopoietic markers, such as CD45 (Kim et al., 2014). AMSCs have capacity to differentiate into three germ layer cells such as myocytes, osteocytes, adipocytes, pancreatic cells, hepatocytes, as well, as well as neural and glial cells (Broughton et al., 2012; Toda et al., 2007).

A developing and neonatal brain contains various growth factors that direct development of endogenous cells and have similar effects on donor cells in transplantation studies; in fact, neural and non-neural stem cell populations are capable of responding to this complex environment, to differentiate into neural cell types (Marcus et al.,

Corresponding authors E-mail:
std_jalali@khu.ac.ir

2008a). This suggests that a developing brain could be considered as neuronal environment to assess the plasticity and function of stem cells.

Using an *in vitro* model, we investigated the plasticity and potential of mouse AMSCs to differentiate into neural cells in response to neonatal mice brain medium (mBM) and the aim of this investigation was to explore the effects of brain environment on the fate of amnion derived stem cells.

Materials and Methods

Cell isolation and primary culture

Mouse amniotic membrane stem cells isolation and culture were performed as described previously (Marcus et al., 2008b). Briefly, amniotic membranes were collected from 13-16 days old NMRI strain mouse embryos in sterile condition and after cutting into small pieces, were digested twice in 0.05% trypsin-EDTA (Gibco, UK) for 10 minutes at 37°C. Following trypsin inactivation with fetal bovine serum (FBS) (Gibco, UK), centrifuge was performed at 1500 rpm for 5 minutes and cell pellet was transferred to culture plates containing Modified Eagle's Medium (DMEM), (Sigma-Aldrich, USA), 10% FBS and 1% Streptomycin-penicillin (Gibco, UK) in a humidified atmosphere of 95% and 5% CO_2 at 37 ^oC.

Preparation of mouse brain medium

Mouse brain medium was prepared from neonatal mice. Briefly, 1-2 old days animals were anesthetized in CO_2 chamber under sterile condition and each brain was homogenized to obtain 1ml mBM. The brains were discarded using thin surgical forceps and then transferred to cold PBS (Gibco, UK). After 3 times washing, tissues were cut and homogenized in DMEM medium and centrifuged at 1500 rpm for 20 minutes. Supernatant was collected and was filtered using 0.2 µm filters and kept at -70 °C. All concerns of animal welfare were considered during mating and surgery.

Treatment of AMSCs with mBM and neural differentiation analysis

Amniotic membrane derived stem cells were counted using tripan blue (Gibco, UK) and 10^4 cells/ml were plated in 24 well cell culture plates. To eliminate the serum effects on neural differentiation, FBS concentration reduced to 1%. Twenty-four hours after cell seeding, the cell culture media was replaced with fresh medium containing 50-300 µl/ml of brain derived medium; experiments were lasted for 21 days and medium was changed every 3 days. Neural differentiation was investigated in 7^{th} and 21^{th} days, on the basis of morphological and immunological properties.

Immunocytochemistry analysis

The cells were fixed using 4% paraformaldehyde for 30 minutes, permeabilized with Triton X-100 (0.4%) for 10 minutes, blocked with 5% goat serum (Gibco, UK) and processed for immunocytochemistry using primary anti-mouse Map-2 antibody produced in rabbit (Abcam, USA). Goat anti-rabbit FITC conjugated antibody (Abcam, UK) was used as secondary antibody and cell nuclei were labeled with Propidium iodide (PI) (Sigma-Aldrich, USA).

Flowcytometric surface marker expression analysis

For flow cytometry analysis, the cells were stained with a specific antibody, as described previously (Park et al., 2012). In brief, cultured AMSCs were harvested using 0.25% trypsin/EDTA, and then washed with PBS and permabilized with Triton X-100 for 30 minutes. Blocking was done with goat serum for 20 minutes, and then the cells were incubated with mouse anti CD90, CD105, CD45 (all from eBioscience, USA) and Nestin primary antibodies (Abcam, USA) for overnight. After washing with PBS, cells were incubated secondary antibody for 45 minutes. Fluorescein-activated cell sorting (FACS) was performed to measure the percentage of antigen expressing cells both in control and treated samples.

Statistical analysis

All experiments were performed at least for three times and the statistical analysis was performed using SPSS.16 software.

Results

Cell harvesting from amnion membrane

Amniotic membranes, isolated from 13-16 days old embryos, were used for stem cell isolation and compared to membranes isolated from 17-19 days embryos. Cell counting showed that membrane from younger embryo was a more appropriate source for cell harvesting and the amount of isolated cells was significantly higher in comparison to the older embryos. Measurement of the viability rate of isolated cells with trypan blue staining showed that 92% of the cells were viable 3 days after enzymatic cell isolation; indicating non-damaging procedure for cell isolation.

Morphological analysis under light microscope showed the presence of 2 types of cells, which was related to the presence of both epithelial and mesenchymal stem cells in amniotic membrane (Figure 1).

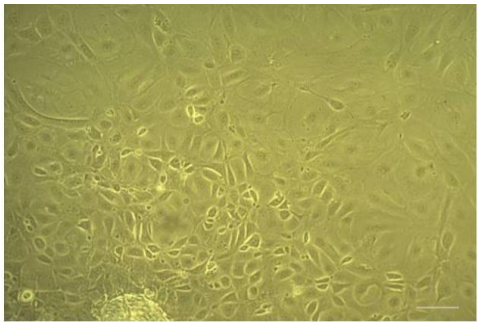

Figure 1. Stem cells isolated from mouse amniotic membrane. Both epithelial and mesenchymal like cells are present in the cell population derived from amniotic membrane. Observation under light invert microscope (200 ×).

Characterization of amnion membrane derived stem cells

To characterize the amniotic stem cells specific surface markers, flowcytometry was performed and results showed 95.71% of CD105, 88.17% of CD90 (Figures 2A and 2B) and low rate expression of the hematopoietic marker CD45 (Figure 2C).

Effect of 150-300 µl/ml of BEM on AMSCs

Treatment of AMSCs with 150, 200 and 300 µl/ml of mBM showed high concentration of medium had cytotoxic effects on AMSCs. Observation of mBM treated AMSCs under an invert microscope showed their cell death after mBM addition to the cell culture medium especially at 300 and 200 µl/ml concentrations. Although the cell death rate in 150 µl/ml of mBM was lower in comparison to higher doses, any neural differentiation was not obvious through 21 days of 150 µl/ml mBM treatment (Figure 3).

Effect of 50 µl/ml of mBM on AMSCs

Investigation of AMSCs treated with 50 µl/ml of mBM showed this concentration of mBM had significant effect on neural fate of the cells. Results from flowcytometry analysis showed decline in Nestin expression in AMSCs, 88.52% and 11.5% in third and seventh days after treatment, respectively (Figure 4).

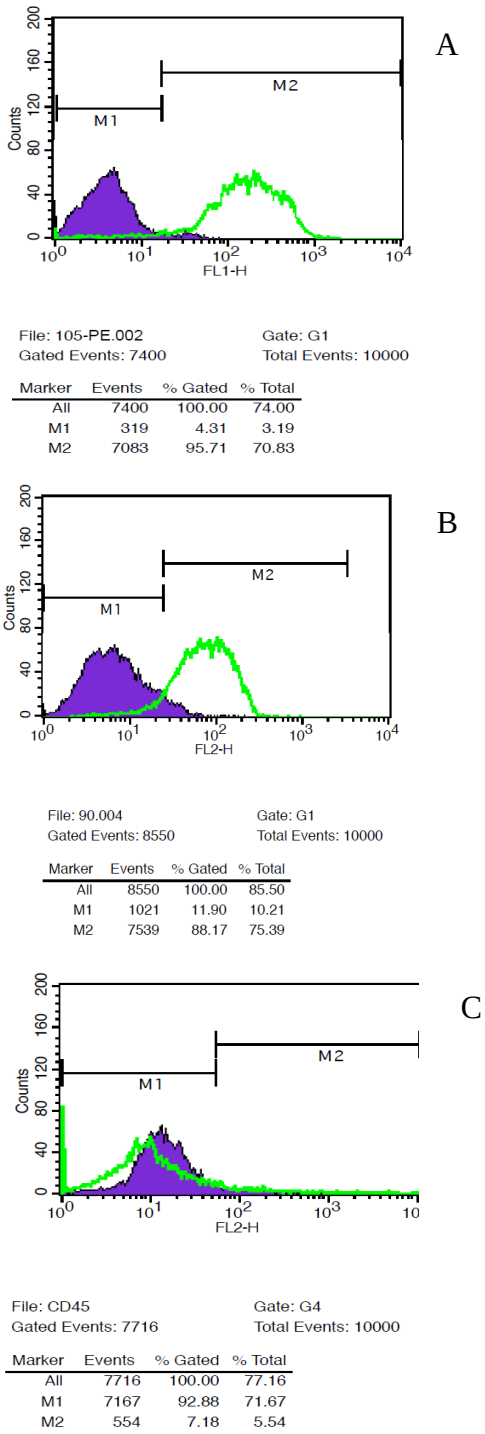

Figure 2. Flowcytometry analysis showing expression of A) CD105, B) CD90 and C) CD45 cell surface markers on AMSCs.

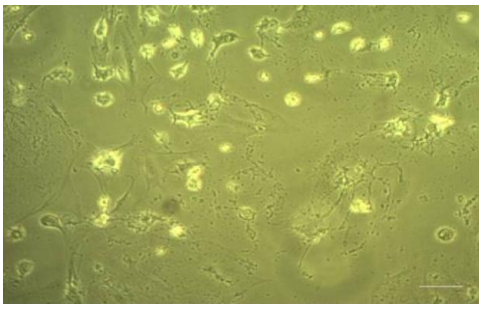

Figure 3. Cytotoxic effect of high dose of brain derived medium on amniotic stem cells. AMSCs underwent broad cell lysis under treatment with 150-300 µl/ml mBM. Observation under light invert microscope (200 ×).

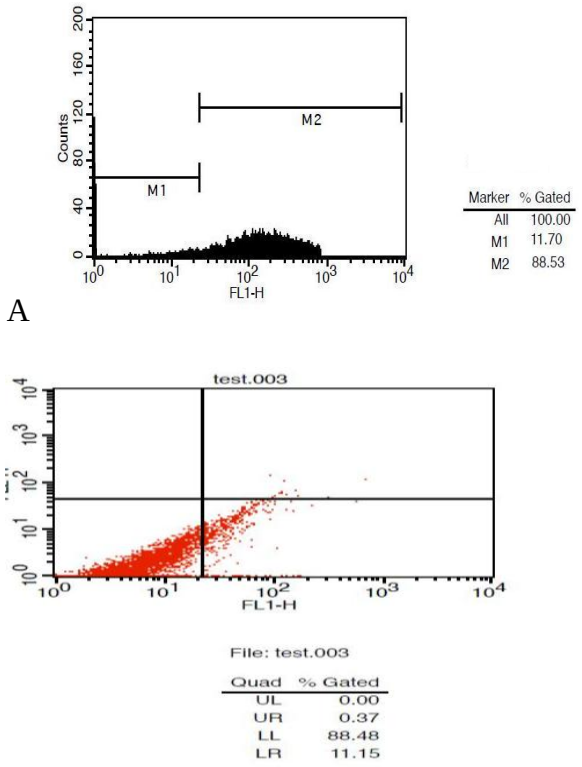

Figure 4. Flowcytometry analysis showing expression of Nestin in AMSCs. Nestin expression was measured 3 (A-M2) and 7 (B- LR) days after neural differentiation of AMSCs which represented 88.53% and 11.15% of Nestin expression in cells, respectively.

In addition to changes in Nestin expression, 7 days after mBM treatment, AMSCs started to neural related morphological changes and axon like process developed gradually. Twenty-one days after treatment, neuronal related changes of AMSCs was significant in comparison to untreated AMSCs that was accompanied with high rate of Map-2 expression on the basis of results obtained from immunohistochemistry analysis (Figiures 5 and 6).

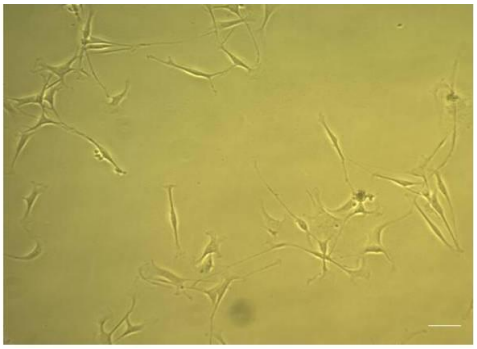

Figure 5. Differentiation of AMSCs toward neural cells in the presence of BEM. Neural related changes such long bipolar or multipolar process and some cell to cell contacts are evident in figure. Observation under light invert microscope (200 ×).

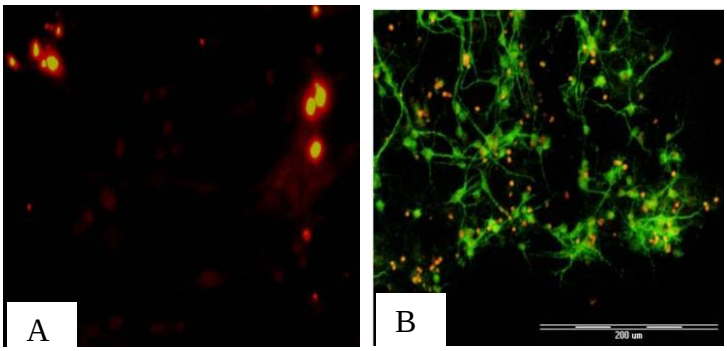

Figure 6. Immunoflurescent assay representing the negative Map-2 expression in A (undifferentiated AMSCs, in the absence of mBM), and positive Map-2 expression in B (differentiated AMSCs, in the presence of mBM). Map-2 expression is obvious in stained cells (green) and nuclei are stained with PI (red). Observation under immunofleurecent microscope.

Discussion

Amniotic membrane derived stem cells have characteristics of neural cells and express some markers for neuronal and glial cells (Toda et al., 2007). Amnion membrane cells differentiate into functional neurons in spinal cord injury models (Sankar and Muthusamy, 2003). Intra-cerebral grafting of amnion derived cells in a mouse model of Parkinson' disease showed that human amniotic cells had an advantage to use in Parkinson' disease because they synthesize and release dopamine, acetylcholine, catecholamine and neurotrophic factors, such as nerve growth factor, neurotrophin-3, and brain-derived neurotrophic factor (Kakishita et al., 2000; Sakuragawa et al., 1997). Amniotic mesenchymal cells exhibited the phenotype of neuroglial progenitor cell and when subjected to a

neural cell differentiating protocol, extended long bipolar or multipolar processes (Sakuragawa et al., 2004).

Although brain assumed as impotent tissue for regeneration, it provides a neurogenic cues, influencing the fate of inherent or extrinsic cells. Several studies have showed inductive effects of developing or adult brain on neural and non-neural stem cells; for example adult bone marrow stromal cells (Kopen et al., 1999) and human umbilical cord blood cells (Zigova et al., 2002), acquired neural and glial fates subsequent to transplantation into the rodent brains. Neural cells transplanted to developing brain of rats populated large areas of the CNS and underwent region specific differentiation and appropriate for their final location (Campbell et al., 1995; Fishell, 1995).

In the current study we investigated the neural differentiation of AMSCs in response to brain tissue as well as the ability of the neonatal brain environment to promote neural fate in mouse amniotic membrane derived stem cells witch obtained results demonstrated the mouse brain medium may contain factors to promote neural fate in AMSCs. Characterization of mouse amniotic membrane derived stem cells demonstrated the expression of amniotic membrane specific markers such CD105 and CD90 and absence of hematopoietic cells specific factor CD45, in a manner conforming to previous studies(Roubelakis et al., 2012). In *in vitro* studies, neural differentiation of stem cells and also the survival of differentiated neurons, depends on the presence of inducing and growth factors (Mao and Lee, 2005) and amniotic membrane stem cells have been differentiated into neural cells in the presence of different neural inducing factors such as bFGF, RA and EGF (Niknejad et al., 2010). In current study all inducing factors were absent in the culture medium of AMSCs and they underwent treatment with pure mBM; moreover, to eliminate the inhibitory effect of serum on neural differentiation (Kawasaki et al., 2000), the serum in the medium was decreased to minimum amount. Conducted co-culture of AMSCs and brain derived medium promoted AMSCs towards morphological changes related to neural fate and developing the axon-like processes. Expression analysis showed early expression of Nestin and its reduction throughout the first days of experiment which was accordance the fact that Nestin supports survival and proliferation of stem/progenitor cells (Park et al., 2010), and upon differentiation becomes dowenregulated (Michalczyk and Ziman, 2005). As in postmitotic terminally differentiated neurons Map-2 is highly enriched in the dendritic compartments and primarily this protein is associated with neurons (Sanchez et al., 2000), we investigated its expression in neural differentiated AMSCs which confirmed last stage of neural development in AMSCs cultured in vicinity of brain medium. These results were comparable to the effects of inducing factors on the neuronal differentiation of amniotic membrane derived cells (Tamagawa et al., 2008).

Results from different studies on rodent brains have showed that early in postnatal life, the brain continues to undergo extensive development of different growth and neurotrophic factors such as fibroblast growth factors, BDNF, NT-3, and NGF which are important self-renewal or inducing factors for neural development (Friedman et al., 1991; Kopen et al., 1999; Maisonpierre et al., 1990). Neural related changes in AMSCs co-cultured with mBM may be explained with the presence of such factors which influenced on their fate and promoted them towards neural development. Though AMSCs synthesize and release some neurotrophic factors such as nerve growth factor, neurotrophin-3, and brain-derived neurotrophic factor (Kong et al., 2008), which could have self-inducing effects on them, non neural differentiation related changes observed in mBM untreated AMSCs which declines the hypothesis of differentiation of AMSCs because of their self- produced factors.

Conclusion

In conclusion, results from this study showed the amniotic membrane derived stem cells are potent to respond to environmental signals promoting them to neural fate. AMSCs are easily isolated from the amnion membrane and provide an accessible source of autologous cells for transplantation approaches, so they could be useful vehicles for treating a variety of central nervous system to replace damaged cells in response to proper intra-tissue factors. Anti- inflammatory effects, growth factor secretion and differentiation potential are characters that make them suitable candidates for stem cell therapy of the nervous system.

Acknowledgment

This work was supported by Science and Research Branch, Islamic Azad University, Tehran, Iran.

Conflict of Interests

The authors declare no any conflict of interest.

References

1- Akle C. A., Adinolfi M., Welsh K. I., Leibowitz S. and McColl I. (1981) Immunogenicity of human amniotic epithelial cells after transplantation into volunteers. Lancet 2:1003-1005.

2- Banas R. A., Trumpower C., Bentlejewski C., Marshall V., Sing G. and Zeevi A. (2008) Immunogenicity and immunomodulatory effects of amnion-derived multipotent progenitor cells. Human immunology 69:321-328.

3- Broughton B. R., Lim R., Arumugam T. V., Drummond G. R., Wallace E. M. and Sobey C. G. (2012) Post-stroke inflammation and the potential efficacy of novel stem cell therapies: focus on amnion epithelial cells. Frontiers in cellular neuroscience 6:66.

4- Campbell K., Olsson M. and Bjorklund A. (1995) Regional incorporation and site-specific differentiation of striatal precursors transplanted to the embryonic forebrain ventricle. Neuron 15:1259-1273.

5- Dobreva M. P., Pereira P. N., Deprest J. and Zwijsen A. (2010) On the origin of amniotic stem cells: of mice and men. The International journal of developmental biology 54:761-777.

6- Fishell G. (1995) Striatal precursors adopt cortical identities in response to local cues. Development 121:803-812.

7- Friedman W. J., Olson L. and Persson H. (1991) Cells that Express Brain-Derived Neurotrophic Factor mRNA in the Developing Postnatal Rat Brain. The European journal of neuroscience 3:688-697.

8- Ilancheran S., Michalska A., Peh G., Wallace E. M., Pera M. and Manuelpillai U. (2007) Stem cells derived from human fetal membranes display multilineage differentiation potential. Biology of reproduction 77:577-588.

9- Izumi M., Pazin B. J., Minervini C. F., Gerlach J., Ross M. A., Stolz D. B., Turner M. E., Thompson R. L. and Miki T. (2009) Quantitative comparison of stem cell marker-positive cells in fetal and term human amnion. Journal of reproductive immunology 81:39-43.

10- Kakishita K., Elwan M. A., Nakao N., Itakura T. and Sakuragawa N. (2000) Human amniotic epithelial cells produce dopamine and survive after implantation into the striatum of a rat model of Parkinson's disease: a potential source of donor for transplantation therapy. Experimental neurology 165:27-34.

11- Kawasaki H., Mizuseki K., Nishikawa S., Kaneko S., Kuwana Y., Nakanishi S., Nishikawa S. I. and Sasai Y. (2000) Induction of midbrain dopaminergic neurons from ES cells by stromal cell-derived inducing activity. Neuron 28:31-40.

12- Kim E. Y., Lee K. B. and Kim M. K. (2014) The potential of mesenchymal stem cells derived from amniotic membrane and amniotic fluid for neuronal regenerative therapy. BMB reports 47:135-140.

13- Kong X. Y., Cai Z., Pan L., Zhang L., Shu J., Dong Y. L., Yang N., Li Q., Huang X. J. and Zuo P. P. (2008) Transplantation of human amniotic cells exerts neuroprotection in MPTP-induced Parkinson disease mice. Brain research 1205:108-115.

14- Kopen G. C., Prockop D. J. and Phinney D. G. (1999) Marrow stromal cells migrate throughout forebrain and cerebellum, and they differentiate into astrocytes after injection into neonatal mouse brains. Proceedings of the National Academy of Sciences of the United States of America 96:10711-10716.

15- Maisonpierre P. C., Belluscio L., Friedman B., Alderson R. F., Wiegand S. J., Furth M. E., Lindsay R. M. and Yancopoulos G. D. (1990) NT-3, BDNF, and NGF in the developing rat nervous system: parallel as well as reciprocal patterns of expression. Neuron 5:501-509.

16- Mao Y. and Lee A. W. (2005) A novel role for Gab2 in bFGF-mediated cell survival during retinoic acid-induced neuronal differentiation. The Journal of cell biology 170:305-316.

17- Marcus A. J., Coyne T. M., Black I. B. and Woodbury D. (2008a) Fate of amnion-derived stem cells transplanted to the fetal rat brain: migration, survival and differentiation. Journal of cellular and molecular medicine 12:1256-1264.

18- Marcus A. J., Coyne T. M., Rauch J., Woodbury D. and Black I. B. (2008b) Isolation, characterization, and differentiation of stem cells derived from the rat amniotic membrane. Differentiation; research in biological diversity 76:130-144.

19- Michalczyk K. and Ziman M. (2005) Nestin structure and predicted function in cellular cytoskeletal organisation. Histology and histopathology 20:665-671.

20- Miki T., Lehmann T., Cai H., Stolz D. B. and Strom S. C. (2005) Stem cell characteristics of amniotic epithelial cells. Stem Cells 23:1549-1559.

21- Niknejad H., Peirovi H., Ahmadiani A., Ghanavi J. and Jorjani M. (2010) Differentiation factors that influence neuronal markers expression in vitro from human amniotic epithelial cells. European cells & materials 19:22-29.

22- Park D., Xiang A. P., Mao F. F., Zhang L., Di C. G., Liu X. M., Shao Y., Ma B. F., Lee J. H., Ha K. S., Walton N. and Lahn B. T. (2010) Nestin

is required for the proper self-renewal of neural stem cells. Stem Cells 28:2162-2171.

23- Park S. B., Seo M. S., Kim H. S. and Kang K. S. (2012) Isolation and characterization of canine amniotic membrane-derived multipotent stem cells. PloS one 7:e44693.

24- Pratama G., Vaghjiani V., Tee J. Y., Liu Y. H., Chan J., Tan C., Murthi P., Gargett C. and Manuelpillai U. (2011) Changes in culture expanded human amniotic epithelial cells: implications for potential therapeutic applications. PloS one 6:e26136.

25- Roubelakis M. G., Trohatou O. and Anagnou N. P. (2012) Amniotic fluid and amniotic membrane stem cells: marker discovery. Stem cells international 2012:107836.

26- Sakuragawa N., Kakinuma K., Kikuchi A., Okano H., Uchida S., Kamo I., Kobayashi M. and Yokoyama Y. (2004) Human amnion mesenchyme cells express phenotypes of neuroglial progenitor cells. Journal of neuroscience research 78:208-214.

27- Sakuragawa N., Misawa H., Ohsugi K., Kakishita K., Ishii T., Thangavel R., Tohyama J., Elwan M., Yokoyama Y., Okuda O., Arai H., Ogino I. and Sato K. (1997) Evidence for active acetylcholine metabolism in human amniotic epithelial cells: applicable to intracerebral allografting for neurologic disease. Neuroscience letters 232:53-56.

28- Sanchez C., Diaz-Nido J. and Avila J. (2000) Phosphorylation of microtubule-associated protein 2 (MAP2) and its relevance for the regulation of the neuronal cytoskeleton function. Progress in neurobiology 61:133-168.

29- Sankar V. and Muthusamy R. (2003) Role of human amniotic epithelial cell transplantation in spinal cord injury repair research. Neuroscience 118:11-17.

30- Tamagawa T., Ishiwata I., Ishikawa H. and Nakamura Y. (2008) Induced in-vitro differentiation of neural-like cells from human amnion-derived fibroblast-like cells. Human cell 21:38-45.

31- Toda A., Okabe M., Yoshida T. and Nikaido T. (2007) The potential of amniotic membrane/amnion-derived cells for regeneration of various tissues. Journal of pharmacological sciences 105:215-228.

32- Zigova T., Song S., Willing A. E., Hudson J. E., Newman M. B., Saporta S., Sanchez-Ramos J. and Sanberg P. R. (2002) Human umbilical cord blood cells express neural antigens after transplantation into the developing rat brain. Cell transplantation 11:265-274.

Journal of Cell and Molecular Research (2014) 6 (2), 83-92

Research Article

Designing a SYBR Green Absolute Real time PCR Assay for Specific Detection and Quantification of *Bacillus subtilis* in Dough Used for Bread Making

Alireza Sadeghi[1], Seyed Ali Mortazavi[2,3],Ahmad Reza Bahrami[3,4*], Balal Sadeghi[5]and Maryam M. Matin[3,4]

1. Department of Food Science and Technology, Gorgan University of Agricultural Sciences and Natural Resources, Gorgan, Iran
2. Department of Food Science and Technology, Ferdowsi University of Mashhad, Mashhad, Iran
3. Cell and Molecular Biotechnology Research Group, Institute of Biotechnology, Ferdowsi University of Mashhad, Mashhad, Iran
4. Department of Biology, Faculty of Science, Ferdowsi University of Mashhad, Mashhad, Iran
5 . Current Address:Department of Food Hygiene and Public Health, Faculty of Veterinary Medicine, ShahidBahonar University of Kerman, Kerman, Iran

Received 06Sep2014 Accepted 18 Oct 2014

Abstract

In this present study, a SYBR green based real time PCR assay has been developed for specific detection and quantification of *Bacillus subtilis* in dough used for bread making. New primer pairs were designed to amplify a 212 base pair fragment of the *aprE* gene. Specificity of these primer pairs was confirmed with conventional and real time PCR methods. Standard curves constructed using the threshold cycle (C_T) versus copy numbers of *B. subtilis* showed good linearity for reference standards of cloned insert (R^2=0.999, slope=-3.035) and also induced contaminated dough (R^2=0.988, slope=-3.142), and the melting temperature (T_m=82.2 ^oC) was consistently specific for the amplicon. Limits of detection were 200 and 2000 colony forming units (CFUs) per ml or g of these samples, respectively. This real time PCR offers a fast tool with high sensitivity and specificity for detection and quantification of this rope-forming pathogen in dough used for bread making.

***Keywords*:** Real-time PCR, *Bacillussubtilis*, new primer pairs, contaminated dough

Introduction

Bacillus subtilis is a gram positive member of the genus*Bacillus*, which is rod shaped, catalase positive and has the ability to form a tough, protective endospore, allowing the organism to tolerate extreme environmental conditions (Jay et al., 2005; McMeekin, 2000). In recent years, many researchers have focused on this bacterium due to its association with foodborne illnesses and also as a consequence of its thermal tolerance, especially concerning its reported resistance to commercial baking conditions and spore forming ability in food products (Nicholson et al., 2000; PAVIC et al., 2005). The importance of *B. subtilis* in rope spoilage of bread has also been confirmed. Rope spoilage is the most important bacterial spoilage of bread that is usually caused by *Bacillus* spp., especially *B. subtilis*(Rosenkvist and Hansen, 1995; Sorokulova et al., 2003). Due to the large number of species and the often incomplete descriptions of a number of newly reported species within the genus *Bacillus*, it is very difficult to determine the species types and therefore some recent works have focused on optimizing more efficient culture independent methods and detection strategies to overcome this problem (Fernández-No et al., 2011; Liu, 2010; Sadeghi et al., 2012).

Rapid detection and quantification of microbial species are crucial to improve food safety by developing effective preventive and/or adjustment measures. During the past 30 years, tremendous insights have been gained on how microorganisms spread and cause various diseases (Justé et al., 2008; Martínez et al., 2011). As well as conventional PCR, the advent of SYBR green technology has offered the ability to simultaneously detect and quantify DNA from specific targets using rapid real time PCR (Levin, 2010). The use of shortened target DNA sequences in real time PCR results in more efficient amplification than standard PCR where amplicons are required to be at least

Corresponding authors E-mail:
* ar-bahrami@um.ac.ir

200 bp in length to allow detection by electrophoretic separation, and also allows reduced extension times (Fricker et al., 2007; Martínez et al., 2011).

In real time PCR, unlike in conventional PCR, the amplification is monitored continuously during the reaction, which permits the user to quantify the target faster. Real time PCR is performed in a closed tube system and requires no post-PCR manipulation of the samples, preventing PCR mix contamination. Real time PCR depends on the emission of an ultraviolet induced fluorescent signal that is proportional to the quantity of DNA that has been synthesized. The simplest, least expensive and most direct fluorescent system for real time PCR involves the incorporation of the SYBR green dye whose fluorescence under UV greatly increases when bound to the minor groove of double helical DNA. The quantification of the target amount in unknown samples can be estimated by generating a standard curve. The establishment of a standard curve using the quantitative real time PCR process is a key step in determining the copy number of a given target sequence. A perfect amplification reaction produces a standard curve with an efficiency of two, because the amount of target DNA should double during each cycle (Klein, 2002; Mackay, 2004; Postollec et al., 2011).

In the past decade, more researchers relied upon real time PCR studies using simple and less expensive SYBR green dye. A number of SYBR green real time PCR assays for detection and quantification of foodborne bacterial pathogens such as *Escherichia* (Jothikumar and Griffiths, 2002), *Mycobacterium*(O'Mahony and Hill, 2002), *Salmonella*, *Shigella*, *Yersinia*, *Campylobacter*, *Vibrio*, *Aeromonas*, *Staphylococcus*, *Clostridium* and *Bacillus*(Fukushima et al., 2003), *Salmonella* and *Listeria* (Jothikumar et al., 2003), *Campylobacter*(Inglis and Kalischuk, 2004), *Vibrio*(Panicker et al., 2004), *Salmonella*(Nam et al., 2005), *Enterobacter*(Liu et al., 2006), *Clostridium*(Fenicia et al., 2007), *Plesiomonas*(Gu and Levin, 2008), *Klebsiella*(Sun et al., 2010) and *Staphylococcus*(Fusco et al., 2011) have been reported.

The objective of this study was to develop and evaluate a SYBR green absolute real time PCR method for the specific detection and enumeration of *B. subtilis* in culture medium and dough samples used for bread making.

Materials and Methods

Bacterial species, induced contamination and DNA extraction

Bacterial species (*Bacillus subtilis* ATCC 6633, *Bacillus amyloliquefaciens* ATCC 23350, *Bacillus cereus* ATCC 11778, *Bacillus licheniformis*ATCC 9789, *Bacillus* spp., ATCC 21832, *Staphylococcus aureus* ATCC 6538, *Escherichiacoli* ATCC 25922 and*Lactobacillus* spp., ATCC 8001) used in this study were purchased from American Type Culture Collection as vacuum dried cultures. These species, after activation, were plated into nutrient agar (Merck, Germany), incubated for 24-48 hours at 30-37 ^{o}C and then pure bacterial colonies were obtained (Jay et al., 2005). Wheat flour was prepared from a local flour mills factory. Chemicals (Merck, Germany), conventional PCR reagents (Fermentas, Lithuania), designed primers (MWG, Germany), DNA Extraction DNeasy kit (Qiagen, Germany), GeneJET Plasmid Miniprep Extraction kit (Thermo Scientific, USA), S.N.A.P. Gel Purification kit (Invitrogen, USA), Maxima SYBR Green/Fluorescein qPCR Master Mix (Thermo Scientific, USA) and InsTAclone PCR Cloning kit (Thermo Scientific, USA) were also purchased and used.

Dough samples were prepared according to our previous study (Sadeghi et al., 2012). Then equal numbers of the mentioned bacterial species were used for contamination of the dough. 25g of dough was inoculated with bacteria at numbers of ca. 10^5 CFU/g of each species, separately (Blackburn, 2006; McMeekin, 2000).Qiagen genomic DNA extraction kit was used according to the manufacturer protocol to obtain genomic DNA from cultured cells. The extracted DNA from activated *B. subtilis* in nutrient broth culture was used as positive control in following PCR assays. Extraction of the total DNA from dough samples was performed as described by Merothe*t al.*(Meroth et al., 2003). The DNA extracted from artificially contaminated dough samples with related and unrelated species that may be naturally present in dough including *B. amyloliquefaciens*, *B. cereus*, *B. licheniformis,Bacillus* spp., *S.aureus*, *E.coli* and *Lactobacillus* spp., were also used as negative controls in PCR tests.

Primer design, specificity evaluation and conventional PCR setting

Forward primer (5'-ACCATTGCGGTAGGTGCG-3') and reverse primer (5'-GCGTTTGTCCAAGTCGGG-3') were designed according to the *aprE* gene sequence published in the GeneBank (AJ539133). The target

gene encodes subtilisin toxin precursor and is a highly conservative and specific gene of *B. subtilis*(Sadeghi et al., 2012). The design of primers was performed using Primer Premier 5 (Premier Biosoft, USA) according to the recommendations of software. Computer simulation of different combinations of all the primer pairs was performed in order to find the best combination for development of the real time PCR test and the primers were then tested for specificity using BLAST (http://www.blast.ncbi.nlm.nih.gov/Blast.cgi). Primer specificities were also assayed and assessed by cross reaction among mentioned related and unrelated bacterial species. Specificity of primer was further affirmed by carrying out melting peak analysis of real time PCR assays on the amplicon.

The conventional PCR tests were performed on a Corbett N15128 thermocycler (Australia). First the PCR was optimized for detection of *B. subtilis*. After evaluating the effects of different annealing temperatures (in the range of 50 to 60^{o}C), optimized PCR reaction (initial denaturation at 94^{o}C for 4 min, amplification for 35 cycles at 94^{o}C for 30 s, 54^{o}C for 45 s, 72^{o}C for 45 s and final extension of 7 min at 72^{o}C) was carried out in 20 µl final volume including 2 µl *Taq* polymerase with 2.5 units activity, 2.5 µl buffer 10x, 2.5 µl $MgCl_2$ at concentration of 25 mM, 0.5 µl of dNTPs mixture (10 Mm), 2 µl of each primer at concentration of 0.5 mM and 2 µl DNA with concentration of 100 ng per µl. Then PCR products were electrophoresed on 1.5% (w/v) agarose gel in TBE buffer with pH 8, stained by SYBR Safe DNA gel stain (Invitrogen, USA) and observed under UV light. Based on the *B. subtilis* target gene sequence, the amplified PCR products should be 212 bp. Finally, the PCR product was sent for sequencing to MWG Co. (Germany) and sequencing result was evaluated by BLASTN procedure with the available data in NCBI.

Constructing reference standard and generation of standard curve

The reference standards were constructed to detect *B. subtilis* with real time PCR. The 212 bp fragment of the *aprE* gene obtained using the designed primers was cloned. First this was achieved by amplifying the selected sequence of target gene using the conventional PCR and the presence of the specific amplified product was confirmed by electrophoresis. Purification of the amplified product was performed using the S.N.A.P. Gel Purification kit (Invitrogen, USA), according to manufacturer's recommendations. DNA manipulations were carried out according to standard protocols and instructions of InsTAclone PCR Cloning kit (Thermo Scientific, USA). These included ligation of the amplified 212 bp fragment of *B. subtilisaprE* gene with the TA cloning plasmid vector (pTZ57R/T), transformation of the construct into competent *E. coli* DH5α, screening of the positive clones and then plasmid DNA extraction by GeneJET Plasmid Miniprep kit (Thermo Scientific, USA) as illustrated in Fig. 1. The identity of the cloned insert was confirmed by direct sequencing, which was performed using the universal sequencing primer M13F (Dhanasekaran et al., 2010; Sun et al., 2010).

The standard curve was then generated using standard values obtained by 10 fold serial dilutions of the extract of the resulting plasmid harbouring the target insert. For this purpose, the amount of plasmid DNA was determined by a nanodrop spectrophotometer (Thermo Scientific, USA) at 260 nm. Then, 10 fold serial dilutions of the extract were prepared, ranging from 2×10^{8} to 2×10^{1} copies/ml based on the instruction available online at http://www.uri.edu/research/gsc/resources/cndna.html. Real time PCR of the standard dilution series was performed in triplicate as three separate tests. The standard curve was generated by plotting the threshold cycle (C_T) against the DNA amount (plasmid copies/ml) produced for the target sequence (Nicholson et al., 2000). Sensitivity was shown by applying these DNA dilution series of the reference strain to the real time PCR. For comparison of PCR amplification efficiencies and detection sensitivities among different experiments, slopes of standard curves were calculated by performing a linear regression analysis using the programme SPSS 12.0 for Windows (SPSS Inc., USA).

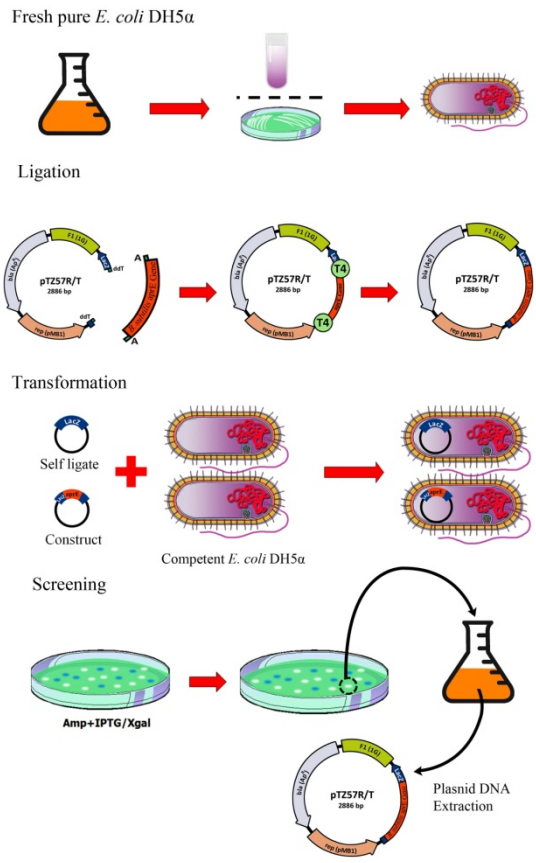

Figure 1. Schematic procedure of TA cloning used in this study for constructing the reference standard.

SYBR green real-time PCR amplification and melting curve analysis

Real time PCR was performed on the experimental samples and reference standards. The PCR was carried out using the Bio-RadCFX96 Touch™ machine (USA). Initially, primer pairs were run in PCR under the following conditions: Each 25 µl reaction mixture consisted of 12.5 µl Maxima SYBR Green/ROX qPCR Master Mix (Thermo Scientific, USA), 1 µl of forward and reverse primers (0.3 µM) and 2 µl of template DNA or extracted plasmid DNA from recombinant vector (100 ng). The standard protocol included one cycle at 95 ^{o}C for 10 min, followed by 40 cycles at 95^{o}C for 30 s, 54^{o}C for 30 s and 72^{o}C for 45 s. Fluorescence was measured at the end of each extension step. In order to allow subsequent melting temperature (T_m) analysis, PCR products were heated to 95^{o}C for 1 s, cooled to 65^{o}C for 5 s and then reheated to 95^{o}C at a rate of 0.01 ^{o}C/s. The correct size of PCR products was verified by 1.5% gel electrophoresis and visualized with UV transillumination after SYBR Safe staining. The specificity of the developed assay was assessed with mentioned *Bacillus* and non *Bacillus* bacterial species that may be naturally present in dough. The identity of the PCR product from a sample was also confirmed by performing a melting curve analysis and comparing its T_m with positive control (Kennedy and Oswald, 2011; Martínez et al., 2011; Nam et al., 2005; Postollec et al., 2011). The amount of fluorescence emission in real time PCR correlates to the initial amount of target template during exponential phase. The T_m peaks of the products were calculated based on initial fluorescence curves by plotting negative derivative of fluorescence over temperature (Levin, 2010; Nam et al., 2005; Postollec et al., 2011).

Results

Specificity evaluation of designed primers in conventional PCR

Fig. 2 shows the PCR results for specific detection of *B. subtilis*by conventional PCR. Extracted DNA from all bacterial species as described in materials and methods, were examined as templates. Specificity of primers and absence of nonspecific products or primer dimers were tested by analyzing PCR products on a 1.5% agarose gel stained with SYBR Safe. Only the expected 212 bpamplicon could be observed after electrophoresis and no other bands were visible. To confirm the identity of the amplicon and further characterize the detailed sequence of the gene, the PCR product was sequenced and the result was verified by with BLASTN search to find any sequence similarities. There were no known non-target strain DNA sequences in the BLASTN database with homology to the sequence. Many researchers used this procedure to confirm the specificity of designed primers before their use in SYBR green real time PCR such as Nam *et al.*(Nam et al., 2005), Fenicia*et al.*(Fenicia et al., 2007), Sun *et al.*(Sun et al., 2010) and Martínez-Blanch *et al.*(Martínez-Blanch et al., 2009). The proposed method was able to identify correctly the target pathogen both in bacterial cultures and dough samples. Furthermore, the use of related and unrelated species as negative controls for detection of any amplifiable bacterial DNA and sequencing results, confirmed the specificity of the developed assay.

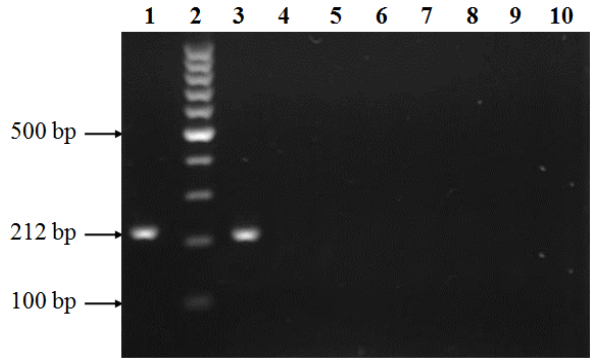

Figure 2. Agarose gel electrophoresis of PCR products obtained under optimized conditions for detection of *B. subtilis*(212 bp). Extracted DNA from cultured cells of *B. subtilis*in nutrient broth as positive control (lane 1), 100 bp DNA marker (lane 2), extracted DNA from inoculated dough with *B. subtilis*(lane 3), extracted DNA from dough artificially contaminated with B. amyloliquefaciens, B. cereus, B. licheniformis, Bacillus spp., S. aureus, E. coli and Lactobacillus spp., representing the negative controls with ca. 105 CFU/g of each bacterium (lanes 4 to 10, respectively).

Detection of *B. subtilis*by SYBR green based real time PCR

Nine samples tested with conventional PCR, including extracted DNA from cultured cells of *B. subtilis*in nutrient broth, extracted DNA from inoculated dough with *B. subtilis* and extracted DNA from dough artificially contaminated with *B. amyloliquefaciens*, *B. cereus, B. licheniformis, Bacillus* spp., *S.aureus*, *E.coli* and *Lactobacillus* spp., were analyzed for the presence of *B. subtilis* by real time PCR using SYBR green dye. DNA extracted from *B. subtilis* (cultured or artificially contaminated dough) yielded positive PCR products from the gene and all other samples were negative by both conventional and real time PCR. No false positive or false negative results were detected (Fig. 2 and Fig. 3). Specificity of the reaction was also confirmed by melting temperature analysis, which was constant for the amplicon obtained. *B. subtilis* evaluated in the present study, showed a constant T_m of 82.2 ± 0.2 ^oC equal to means ± standard deviation of ten separate tests (Fig. 3 b).

The unique T_m of some food bacterial pathogens such as *E. coli*(Jothikumar and Griffiths, 2002), *M. paratuberculosis*(O'Mahony and Hill, 2002), *S. enteritidis*, *S.typhimurium*, *Sh.sonnei*, *Sh.flexneri*, *Y. enterocolitica*, *Y. pseudotuberculosis*, *C. jejuni*, *V.cholerae*, *V. parahaemolyticus*, *V. vulnificus*, *A. hydrophila*, *A. trota*, *S. aureus*, *C. perfringens*, *B. cereus*(Fukushima et al., 2003), *L. monocytogenes*(Jothikumar et al., 2003), *E.*sakazakii(Liu et al., 2006), *C.botulinum*(Fenicia et al., 2007), *P.shigelloides*(Gu and Levin, 2008) and *K. pneumonia*(Sun et al., 2010) were used for their specific detection in designed SYBR green real time PCRs.

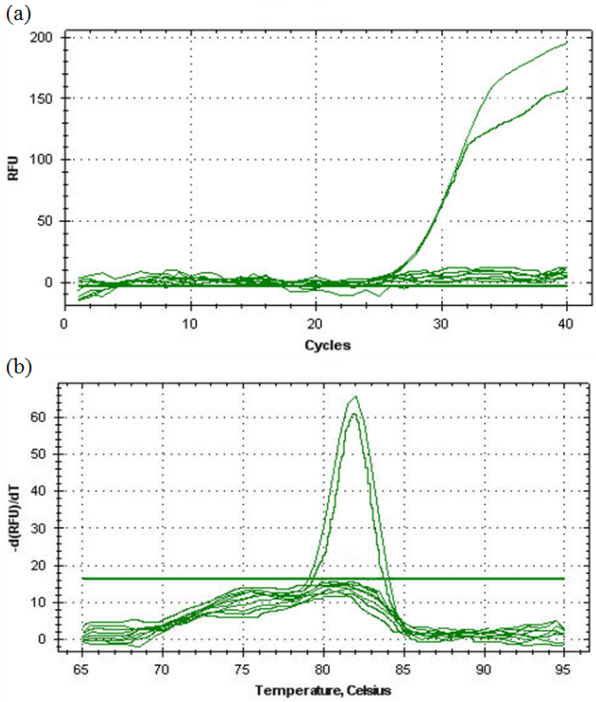

Figure 3. (a) Real time PCR amplification of *B. subtilis*aprE gene. (b) Melting curve analysis of SYBR green real time PCR product of *B. subtilis*(in broth culture as positive control and induced contaminated dough) after 40 cycles in presence of negative control bacterial species used for conventional PCR. The melting temperature is calculated as 82.2 oC. No non-specific peaks are present.

Generation of calibration curves

Identity of the cloned insert was confirmed by direct sequencing using the universal sequencing primer M13F and then reference standards of plasmid DNA were constructed. With these standards, real time PCR assay can be used to directly detect or accurately quantify the dough samples containing *B. subtilis*, which is usually the main pathogen in rope spoilage and also a potential source for foodborne illnesses. Fig. 4 (a) and Fig. 5 (a), show the typical amplification plot (ΔRn or RFU versus PCR cycle) constructed from fluorescence data generated from DNAs corresponding to 2×10^1–2×10^8 copies per ml or g, respectively for reference standards of cloned insert and *B. subtilis* cells in artificially contaminated dough.

In a real time PCR, fluorescence of reaction mixtures just before the denaturation step of each amplification cycle, and the cycle number at which fluorescence crosses a specific threshold value in the exponential phase of amplification are being monitored (designated as C_T or the threshold cycle). The C_T is thus a measure of the quantity of

transcript of interest, and target DNA copy number and C_T values are inversely related. The significant portion of each curve is the place along the C_T axis where each curve departs from the background. The angle and linearity of each curve is related to the efficiency of the PCR reaction with straight and nearly vertical slopes representing more nearly optimal PCR conditions (Bustin et al., 2009; Dhanasekaran et al., 2010). The calibration curve plotting C_T values against known serial dilutions of *B. subtilis* DNA, ranging from 2×10^1 to 2×10^8 copies per ml or g of samples is shown in Fig. 5 (b). The linear range of this real time PCR assay was 2×10^8 to 2×10^2 copies/ml with the best fit regression equation y= -3.0357x + 37.107, (R^2= 0.9993) for standard references of cloned insert. Standard curve also showed linear relationship between C_T and log CFU for serially 10 fold diluted *B. subtilis* cells in artificially contaminated dough with linear regression coefficient of R^2= 0.9887, (y= -3.1429x + 39.119). These results indicate that the reference standards were suitable for quantitative assay (Bustin et al., 2009; Martínez et al., 2011).

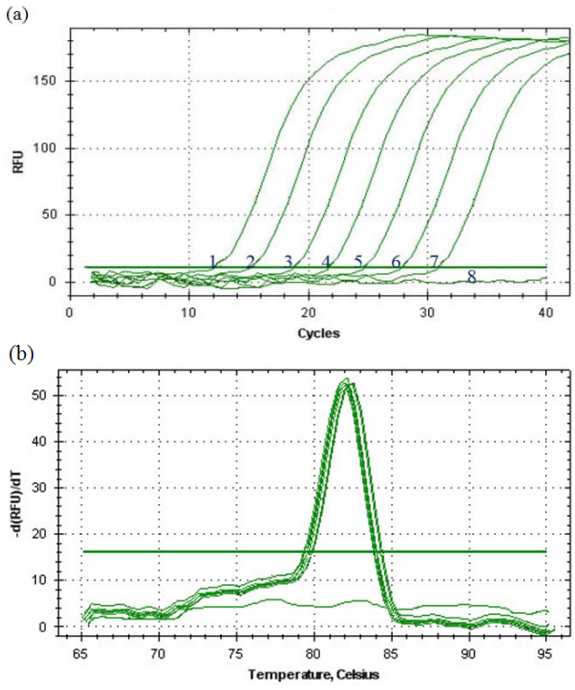

Figure 4. (a) The amplification profile of real time PCR of reference standards. The concentrations of cloning vector ranging from 2×10^8 to 2×10^1 copies/ml: (1) 2×10^8, (2) 2×10^7, (3) 2×10^6, (4) 2×10^5, (5) 2×10^4, (6) 2×10^3, (7) 2×10^2 and (8) 2×10^1. (b) The melting curve of amplification products.

Practical sensitivity of the real time PCR assay

The real time PCR assay was evaluated for practical sensitivity using artificially contaminated dough samples, as described before. The six inoculated samples ranging from 2×10^8 to 2×10^3 number of inoculated cells (CFUs), showed positive fluorescence signals with different C_T values (the last positive fluorescence signal was obtained at a C_T value of 29.5 cycles) and the expected melting temperature, was constant at approximately 82.2 ^oC, while one non-inoculated sample was tested negative by this method (Fig. 5 a). The detection limits of *B. subtilis* in standard references of cloned insert and artificially contaminated bread dough respectively, were determined as 200 CFU/ml and 2000 CFU/g, using SYBR green real time PCR and without the need for further enrichment steps.

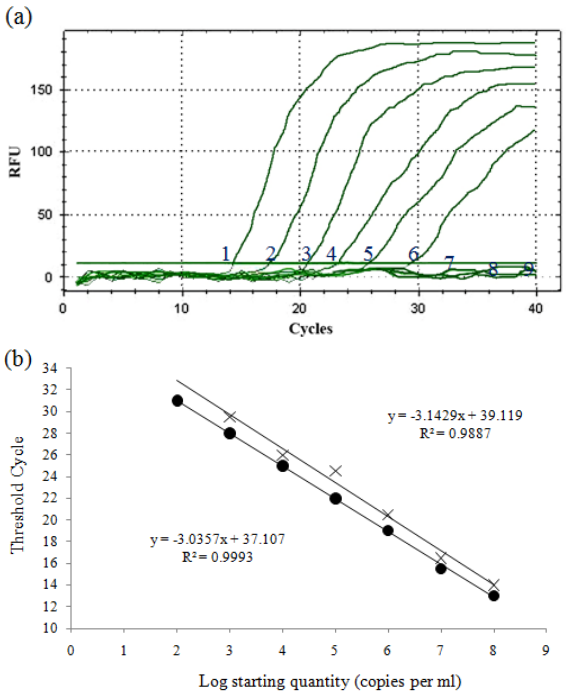

Figure 5. (a) Detection limit in model samples by SYBR green real time PCR assay without enrichment. The amplification profile of 10 fold serial dilutions of *B. subtilis*cells in artificially contaminated dough samples. The concentrations of bacteria inoculated in samples ranging from 2×108 to 2×101 CFU/g: (1) 2×108, (2) 2×107, (3) 2×106, (4) 2×105, (5) 2×104, (6) 2×103, (7) 2×102, (8) 2×101 and (9) negative control (no bacteria). (b) Standard curves as generated from threshold cycle (CT) numbers of a 10 fold dilution series of the new constructed reference standards (2×101–2×108 copies/ml). Standard curves showing the linear relationship between CT and log CFU *B. subtilis*cells in artificially contaminated dough (×) and reference standards of cloned insert (●).

Discussion

Molecular methods, such as conventional PCR and real time PCR, have been used to detect or quantify specific pathogens in food samples. In our procedure, a SYBR green real time PCR was developed with new primer pairs for detection and quantification of *B. subtilis* in dough used for bread making. Specificity of the reaction was confirmed

by melting temperature analysis, which was constant for the amplicon obtained (T_m of 82.2 ^oC). The linear range of this real time PCR assay was 2×10^8 to 2×10^2 copies/ml for standard references of cloned insert. Standard curve also showed the linear relationship between C_T and log CFU for serially diluted *B. subtilis* cells in artificially contaminated dough. This assay enabled us to differentiate *B. subtilis* from main related and unrelated bacterial species that may be naturally present in dough. The assay could detect approximately 2000 CFU/g dough without enrichment and showed potential for quantifying this bacterium with the new constructed reference standards. Since the typical cell counts of *B. subtilis*in rope spoilage have been reported about 10^5 CFU/g of dough (Rosenkvist and Hansen, 1995; Sorokulova et al., 2003), the samples can be processed and analyzed by this procedure, for detecting and quantification of mentioned pathogen in less than 3 h.

In recent SYBR green real time PCR studies for detection of *Bacillus* spp., in food samples, Fricker*et al.*(Fricker et al., 2007) showed that their developed assay, depending on the direct DNA isolation method is suitable for detection of 10^1 to 10^3 CFU/g emetic *B. cereus* in food samples without enrichment. Martínez-Blanch *et al.*(Martínez-Blanch et al., 2009)constructed calibration curves for different food matrices, and it had a wide quantification range of 6 log units using both serial dilutions of purified DNA and calibrated cell suspensions of *B. cereus*. The detection limit of that assay in artificially contaminated liquid egg and reconstituted infant formula was about 60 CFU/ml of food samples. The study of Wehrle*et al.*(Wehrle et al., 2010) showed that artificial contamination of three different food matrices including baby food cereal, rice pudding and carrot puree with distinct bacterial counts revealed a detection limit of 10^1 CFU/g enteropathogenic *B. cereus* cells after overnight enrichment. Although most real time PCR assays in themselves are characterized by high precision and reproducibility, the accuracy of the obtained data is largely depended on several other factors such as sample preparation and quality of the standards. The obtained absolute numbers are always calculated relative to the standard (RNA, cDNA, plasmid DNA, genomic DNA) and largely depend on the accuracy of used standard. Due to the lack of standardized reference material, the accuracy of the obtained data has to be checked during the establishment of the assay by comparison with other established assays. This is the major task for molecular diagnostics using real time PCR system (Dhanasekaran et al., 2010; Kennedy and Oswald, 2011; Martínez et al., 2011; Ponchel et al., 2003). As mentioned, reliable standards are essential for qPCR and it also has been found that the copy numbers vary (due to degradation of standards) over the period of time during storage at 4 °C and −20 °C, which affects PCR efficiency significantly. Based on the results obtained by Dhanasekaran*et al.*(Dhanasekaran et al., 2010) the cloned target sequences are noticeably more stable than PCR products. This could lead to substantial variance in results using standards constructed by different routes, and therefore, cloned insert was used for standard preparation in this study.

A number of fluorescent probe based real time PCR studies have been carried out to detect *Bacillus* spp., in foods or other samples using TaqMan probes or molecular beacons (Fernández-No et al., 2011; Fricker et al., 2007; Gore et al., 2003; Martínez-Blanch et al., 2009). These fluorescent probe based assays require availability of primers and probes that must be selected according to very rigid conditions, which cannot always be easily applied. Use of the double stranded DNA binding dye, SYBR green, for detection of PCR products has overcome this limitation by allowing real time PCR to be applied without the need for probes linked to fluorescent molecules. Protocols that are already in use for classic PCR can thus be used with only slight modifications (Aarts et al., 2001; Gibson et al., 1996). In the absence of probes, specificity of the reaction is determined by melting temperature of the amplicon obtained. SYBR green lacks the specificity of fluorescent DNA probes but has the advantage of allowing a DNA melting curve to be generated and software calculation of the $T_m$of the amplicon after the PCR. This allows identification of the amplified product and its differentiation from primer dimers, which also result in a fluorescent signal with SYBR green but usually have a lower $T_m$value. The fluorescent signal is measured immediately after the extension step of each cycle because thermal denaturation yielding single stranded DNA eliminates fluorescence. A software plot of the negative first derivative of the thermal denaturation plot yields a bell shaped symmetrical curve, the midpoint of which corresponds to the $T_m$value for the amplified product. Interference of the amplicon's signal by the signal resulting from primer dimer formation can be eliminated by raising the temperature to a critical point that is above the $T_m$of the primer dimer formed (resulting in thermal denaturation of the primer dimers) but below the $T_m$of the amplicons prior to measuring the intensity of fluorescence emission (Levin, 2010; Mackay, 2004).

In **conclusion**, this SYBR green real time PCR assay provides a rapid, highly sensitive tool for the detection of *B. subtilis*and quantification of the bacterium cells in a complex food matrix after suitable sample preparation. With further validation, this assay could be used by regulatory and food industry laboratories to rapidly screen for *B. subtilis*contaminations. Considering this bacterium association with foodborne illnesses and also its thermal resistance, especially to commercial baking conditions and spore forming ability indicates the importance of this assay. In contrast to the culture dependent methods, it offers significantly higher accuracy and speed, which are crucial criteria when comes to food safety and high volume of referred samples.

Acknowledgment

This investigation was supported by a grant (100171) from Institute of Biotechnology, Ferdowsi University of Mashhad, Iran.

References:

1. Aarts H.J., Joosten, R.G., Henkens, M.H., Stegeman, H. and van Hoek Angela, H. (2001) Rapid duplex PCR assay for the detection of pathogenic *Yersinia enterocolitica* strains. Journal of Microbiological Methods47: 209-217.
2. Blackburn C.W. (2006) Food spoilage microorganisms. CRC Press. USA, 194-209 pp.
3. Bustin S.A., Benes, V., Garson, J.A., Hellemans, J., Huggett, J., Kubista, M., Mueller, R., Nolan, T., Pfaffl, M.W. and Shipley, G.L. (2009) The MIQE guidelines: minimum information for publication of quantitative real-time PCR experiments. Clinical chemistry55: 611-622.
4. Dhanasekaran S., Doherty, T.M. and Kenneth, J. (2010) Comparison of different standards for real-time PCR-based absolute quantification. Journal of immunological methods354: 34-39.
5. Fenicia L., Anniballi, F., De Medici, D., Delibato, E. and Aureli, P. (2007) SYBR green real-time PCR method to detect *Clostridium botulinum* type A. Applied and Environmental Microbiology73: 2891-2896.
6. Fernández-No I., Guarddon, M., Böhme, K., Cepeda, A., Calo-Mata, P. and Barros-Velázquez, J. (2011) Detection and quantification of spoilage and pathogenic *Bacillus cereus*, *Bacillus subtilis* and *Bacillus licheniformis* by real-time PCR. Food microbiology28: 605-610.
7. Fricker M., Messelhäußer, U., Busch, U., Scherer, S. and Ehling-Schulz, M. (2007) Diagnostic real-time PCR assays for the detection of emetic Bacillus cereus strains in foods and recent food-borne outbreaks. Applied and Environmental Microbiology73: 1892-1898.
8. Fukushima H., Tsunomori, Y. and Seki, R. (2003) Duplex real-time SYBR green PCR assays for detection of 17 species of food- or waterborne pathogens in stools. Journal of Clinical Microbiology41: 5134-5146.
9. Fusco V., Quero, G.M., Morea, M., Blaiotta, G. and Visconti, A. (2011) Rapid and reliable identification of *Staphylococcus aureus*harbouring the enterotoxin gene cluster (*egc*) and quantitative detection in raw milk by real time PCR. International Journal of Food Microbiology144: 528-537.
10. Gibson U., Heid, C.A. and Williams, P.M. (1996) A novel method for real time quantitative RT-PCR. Genome research6: 995-1001.
11. Gore H.M., Wakeman, C.A., Hull, R.M. and McKillip, J.L. (2003) Real-time molecular beacon NASBA reveals hblC expression from *Bacillus* spp. in milk. Biochemical and biophysical research communications311: 386-390.
12. Gu W. and Levin, R.E. (2008) Innovative methods for removal of PCR inhibitors for quantitative detection of *Plesiomonasshigelloides* in oysters by real-time PCR. Food Biotechnology22: 98-113.
13. Inglis G.D. and Kalischuk, L.D. (2004) Direct quantification of Campylobacter jejuni and Campylobacter lanienae in feces of cattle by real-time quantitative PCR. Applied and Environmental Microbiology70: 2296-2306.
14. Jay J.M., Loessner, M.J. and Golden, D.A. (2005) Modern food microbiology. Springer. USA, 204-228 pp.
15. Jothikumar N. and Griffiths, M.W. (2002) Rapid detection of *Escherichia coli* O157: H7 with multiplex real-time PCR assays. Applied and Environmental Microbiology68: 3169-3171.
16. Jothikumar N., Wang, X. and Griffiths, M.W. (2003) Real-time multiplex SYBR green I-based PCR assay for simultaneous detection of *Salmonella serovars* and *Listeria monocytogenes*. Journal of Food

Protection66: 2141-2145.
17. Justé A., Thomma, B. and Lievens, B. (2008) Recent advances in molecular techniques to study microbial communities in food-associated matrices and processes. Food microbiology25: 745-761.
18. Kennedy S. and Oswald, N. (2011) PCR troubleshooting and optimization: the essential guide. Caister academic. USA, 139-149 pp.
19. Klein D. (2002) Quantification using real-time PCR technology: applications and limitations. Trends in molecular medicine8: 257-260.
20. Levin R.E. (2010) Rapid detection and characterization of foodborne pathogens by molecular techniques. CRC Press. USA, 8-20 pp.
21. Liu D. (2010) Molecular detection of foodborne pathogens. CRC Press. USA, 129-145 pp.
22. Liu Y., Cai, X., Zhang, X., Gao, Q., Yang, X., Zheng, Z., Luo, M. and Huang, X. (2006) Real time PCR using TaqMan and SYBR Green for detection of*Enterobactersakazakii* in infant formula. Journal of Microbiological Methods65: 21-31.
23. Mackay I.M. (2004) Real-time PCR in the microbiology laboratory. Clinical Microbiology and Infection10: 190-212.
24. Martínez-Blanch J., Sánchez, G., Garay, E. and Aznar, R. (2009) Development of a real-time PCR assay for detection and quantification of enterotoxigenic members of *Bacillus cereus* group in food samples. International Journal of Food Microbiology135: 15-21.
25. Martínez N., Martín, M.C., Herrero, A., Fernández, M., Alvarez, M.A. and Ladero, V. (2011) qPCR as a powerful tool for microbial food spoilage quantification: Significance for food quality. Trends in Food Science & Technology22: 367-376.
26. McMeekin T.A. (2000) Detecting pathogens in food. CRC press. USA, 347-350 pp.
27. Meroth C.B., Walter, J., Hertel, C., Brandt, M.J. and Hammes, W.P. (2003) Monitoring the bacterial population dynamics in sourdough fermentation processes by using PCR-denaturing gradient gel electrophoresis. Applied and Environmental Microbiology69: 475-482.
28. Nam H.-M., Srinivasan, V., Gillespie, B.E., Murinda, S.E. and Oliver, S.P. (2005) Application of SYBR green real-time PCR assay for specific detection of *Salmonella* spp. in dairy farm environmental samples. International Journal of Food Microbiology102: 161-171.
29. Nicholson W.L., Munakata, N., Horneck, G., Melosh, H.J. and Setlow, P. (2000) Resistance of *Bacillus* endospores to extreme terrestrial and extraterrestrial environments. Microbiology and Molecular Biology Reviews64: 548-572.
30. O'Mahony J. and Hill, C. (2002) A real time PCR assay for the detection and quantitation of *Mycobacterium avium* subsp. *paratuberculosis* using SYBR Green and the Light Cycler. Journal of Microbiological Methods51: 283-293.
31. Panicker G., Myers, M.L. and Bej, A.K. (2004) Rapid detection of *Vibrio vulnificus* in shellfish and Gulf of Mexico water by real-time PCR. Applied and Environmental Microbiology70: 498-507.
32. Pavic S., Brett, M., Petric, I., Lastre, D., Smoljanovic, M., Atkinson, M., Kovacic, A., centinic, E. and Ropac, D. (2005) An outbreak of food poisoning in a kindergarten caused by milk powder containing toxigenic *Bacillus subtilis* and *Bacillus licheniformis*. ArchivfürLebensmittelhygiene56: 20-22.
33. Ponchel F., Toomes, C., Bransfield, K., Leong, F.T., Douglas, S.H., Field, S.L., Bell, S.M., Combaret, V., Puisieux, A. and Mighell, A.J. (2003) Real-time PCR based on SYBR-Green I fluorescence: an alternative to the TaqMan assay for a relative quantification of gene rearrangements, gene amplifications and micro gene deletions. BMC biotechnology3: 18.
34. Postollec F., Falentin, H., Pavan, S., Combrisson, J. and Sohier, D. (2011) Recent advances in quantitative PCR (qPCR) applications in food microbiology. Food microbiology28: 848-861.
35. Rosenkvist H. and Hansen, Å. (1995) Contamination profiles and characterisation of *Bacillus* species in wheat bread and raw materials for bread production. International Journal of Food Microbiology26: 353-363.
36. Sadeghi A., Mortazavi, S.A., Bahrami, A.R. and Sadeghi, B. (2012) Design of multiplex PCR for simultaneous detection of rope forming *Bacillus* strains in Iranian bread dough. Journal of the Science of

Food and Agriculture92: 2652-2656.
37. Sorokulova I., Reva, O., Smirnov, V., Pinchuk, I., Lapa, S. and Urdaci, M. (2003) Genetic diversity and involvement in bread spoilage of *Bacillus* strains isolated from flour and ropy bread. Letters in applied microbiology37: 169-173.
38. Sun F., Wu, D., Qiu, Z., Jin, M. and Li, J. (2010) Development of real-time PCR systems based on SYBR Green for the specific detection and quantification of*Klebsiellapneumoniae* in infant formula. Food Control21: 487-491.
39. Wehrle E., Didier, A., Moravek, M., Dietrich, R. and Märtlbauer, E. (2010) Detection of *Bacillus cereus* with enteropathogenic potential by multiplex real-time PCR based on SYBR green I. Molecular and cellular probes24: 124-130.

Journal of Cell and Molecular Research (2014) 6 (2), 93-98

Research Article

Cytogenetic study and pollen viability of three populations of *Diplotaxis harra* (Brassicaceae) in Iran

Massoud Ranjbar[1,*] and Somayeh Karami[1]

1. *Department of Biology, Herbarium division, Bu-Ali Sina University, P. O. Box 65175/4161, Hamedan, Iran*

Received 21April 2014 Accepted 29 May 2014

Abstract

In this study, we examined the chromosome number, microsporogenesis, pollen fertility and distribution of cytotypes of *Diplotaxisharra* (Forssk.) Boiss. This is the first cytogenetic report of the taxon. Among three studied populations, two of them which belong to central regions of Iran showed aneuploid (x = 14) meiotic chromosome count while the other population existed at the diploid level (x = 13). It seems that the species with *x* = 14 are derived through aneuploid increase. The most prominent among these meiotic abnormalities was the chromatin stickiness which involved fragmented chromosome at different stages of meiosis. Consequently, these populations exhibited varying percentages of pollen sterility and pollen grains of smaller sizes. The aim of the present research was to study the male meiosis in detail, find the impact of chromatin stickiness in inducing meiotic aberrations and their consequent effects on pollen fertility and find out the distribution patterns of different cytotypes in Iran.

Keywords: Brassicaceae, Chromosome number, Cytotypes, *Diplotaxis*, Iran, Meiotic

Introduction

Diplotaxisharra is a genus of 2 species that belongs to the Brassicaceae in Iran, an economically important family with 321 genera and 3660 species (Al-Shehbaz, 2012; Hedge, 1968, 1980). The genus *Diplotaxis* belongs to tribe Brassiceae. The tribe consists of 46 genera and about 230 spp. characterized primarily by having conduplicate cotyledons, and segmented (heteroarthrocarpic) fruits, see Go´ mez-Campo, 1999, Appel and Al-Shehbaz, 2003, Warwick and Sauder, 2005). Most of cytological studies in the genus *Diplotaxis harra* have concerted on the chromosome counts, with a little work focused on detailed karyological criteria for taxonomic purposes. Results from cytological studies showed that there are three basic numbers and three ploidy level (*2n* = *2x* = 22, *2n* = *2x* = 26 and *2n* = *2x* = 38) in the genus *D. harra* (Warwick and Al-Shehbaz 2006; Al-Shehbaz 1978; Al-Shehbaz and Al-Omar 1982; Malallah and Attia 2003; Snogerup 1985).
The present study reports meiotic chromosome number and behavior of three populations belonging to genus *Diplotaxis*and aims to increase the knowledge about patterns of chromosome numbers and meiotic behavior in the three populations of *D. harra.*

Materials and methods

Cytogenetic

Material for male meiotic studies were analysed in three populations of *Diplotaxisharra*which were collected from the wild plants growing in different localities of Markazi and Fars provinces, provinces in Iran in the months of April-May the year 2012 (Table 1). The voucher specimens are deposited in the Herbarium, Department of Biology, Bu-Ali Sina University, Hamedan. The young developing floral buds from healthy plants were fixed in modified Carnoy's solution in ethyl alcohol (96%), chloroform and propionic acid (6:3:2) for 24 h at room temperature and then stored in 70% ethyl alcohol at 4°C until used.

Chromosome counts and male meiotic analysis

Developing anthers from floral buds were squashed in 1% acetocarmine and preparations were studied for chromosome counts, and detailed meiotic behavior of pollen mother cells (PMCs) at early prophase-I, metaphase-I/II (MI/II), anaphases-I/II

∗Corresponding authors E-mail:
massoud.ranjbar80@gmail.com

Table 1. Localities of the species used in this study.

Taxa	Voucher specimens	Altitude (m)	Location	Date	Collector name	Abbreviation
D. harra	30903	1400	Markazi: 35 km from Nubaran to Tafresh	26.5.2012	Ranjbar & Karami	HAR03
D. harra	30849	1434	Markazi: 30 km from Nubaran to Tafresh	26.5.2012	Ranjbar & Karami	HAR49
D. harra	29984	1450	Fars: Fasa, Azad university	27.4.2012	Ranjbar & Karami	HAR84

(AI/II), telophases-I/II (TI/II) and sporad stage (Wilson 1945). In populations with the normal meiotic course, a total of 95–127 PMCs were examined in determining the chromosome counts while in cytologically abnormal populations 20–50 slides prepared from different anthers/flowers (with 350–650 PMCs) were analysed in each case.

Pollenfertility

Pollen fertility was estimated through stainability tests for which anthers of mature flowers were squashed in glyceroacetocarmine mixture (1:1) dye. 800–1000 pollen grains were analysed in each case for pollen fertility and pollen size. Well-filled pollen grains with uniformly darkly stained cytoplasm were scored as fertile/viable while shrivelled pollen with unstained or poorly stained cytoplasm were counted as sterile/unviable. Pollen fertility was expressed as an average percentage of the stained pollen grains/total pollen grains analysed. Size of stained pollen grains was measured with occulomicrometer.

Photomicrographs

Chromosome spreads were analysed with Olympus light microscope and the best plates of chromosome counts, meiotic abnormalities, sporads and pollen grains (fertile, sterile) were photographed from the temporary mounts with an Olympus BX-51 microscope. Photographs of chromosomes were taken on an Olympus BX-51 photomicroscope at initial magnification of ×1000. Voucher specimens are kept at BASU, Hamedan, Iran (Table 1).

Results

Species Description

Diplotaxisharra (Forssk.) Boiss., Fig. 28.

Annual to perennial herbs. Stems erect, 10-60 cm, simple or many-stemmed, glabrous or scattered simple hairs at lower part. Basal leaves petiolate, ca . 2.8 × 0.3 cm, obovate or broadly ovate, more or less dentate, apex acute, sparsely covered hairs, ca.

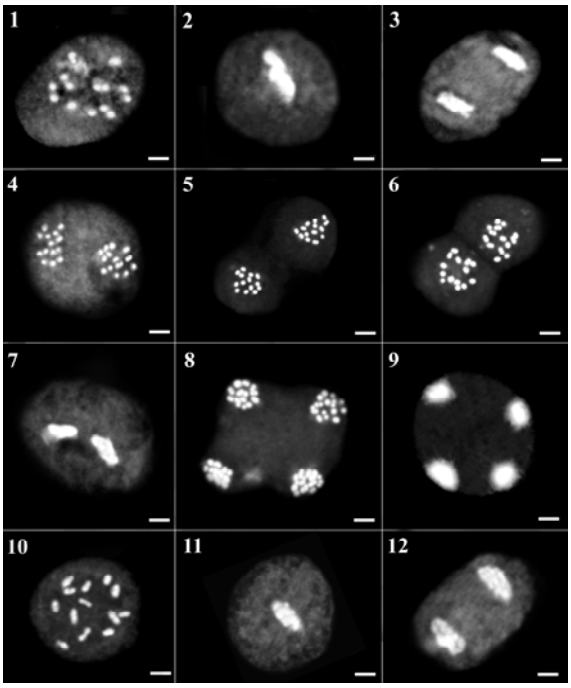

Figures 1-12. Representative meiotic cells in HAR49 and HAR84. (1) diakinesis (*2n = 2x* =28) HAR49, (2) chromosome stickiness in metaphase I HAR49, (3) chromosome stickiness in anaphase I HAR49, (4-6) telophase I HAR49, (7) chromosome stickiness in metaphase II HAR49, (8) anaphase II HAR49, (9) telophase II HAR49, (10) diakinesis (*2n = 2x* =26) HAR84, (11) chromosome stickiness in metaphase I HAR84, (12) chromosome stickiness in anaphase I HAR84. Scale bar = 1 µm.

1.2 mm long. Cauline leaves oblanceolate to oblong, 2.3–8.8 × 0.6–3.2 cm, apex acute, subsessile, entire. Inflorescence a raceme, up to 25 cm long, many flowered. Pedicels 10–15 mm long, erect to spreading, usually pendent when mature, becoming elongate in fruit and up to 24 cm long. Sepals spreading, inner not saccate, erect 4.8–6 × 0.8–2.2 mm, oblanceolate to oblong, acute, scarious margin, 0.2–0.4 mm long. Petals yellow or cream, distinctly longer than sepals, erect, 7–12.5 mm long, 2.5–5 mm broad, obovate, rounded at apex, claw differentiated from blade, shorter than sepals. Stamens 6, without appendages, slightly included,

erect; median filament pairs 4–6 mm long; anthers erect, linear, 2–3.2 mm long; lateral filament pair 3–5 mm long, anthers 2–2.7 mm long. Fruits 30–50 × 2.5–3 mm long, linear, compressed siliqua, 1-veined, beak very short or ca. 1 mm, terete, erect, gynophore ca. 2–3 mm long, glabrous. Stigma prominent, 2-lobed; style absent. Ovary with very many (up to 100) ovules. Seeds numerous, arranged in two rows in each cell. Cotyledons longitudinally folded.

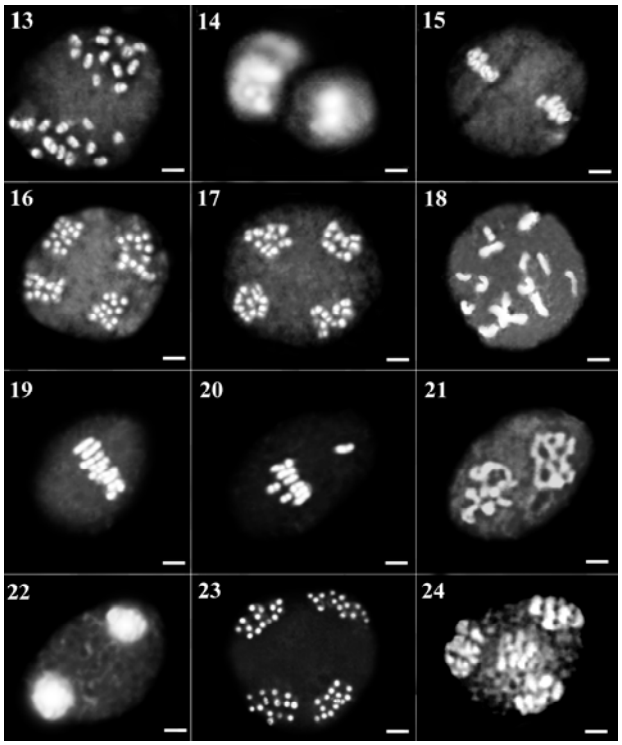

Figures 13-24: Representative meiotic cells in HAR84 and HAR03. (13-14) telophase I HAR84, (15) metaphase II HAR84, (16) anaphase II HAR84, (17) teloaphase II HAR84, (18) diakinesis (*2n = 2x* = 28) HAR03, (19) metaphase I HAR03, (20) metaphase I with fragmented chromosome HAR03, (21) anaphase I HAR03, (22) teloaphase I HAR03, (23) anaphase II HAR03, (24) teloaphase II HAR03. Scale bar = 1 µm.

Cytogenetics

Chromosome numbers and meiotic behavior were determined in three individuals belonging to three populations of one species. They were similar in life history, breeding system, ecology, and geographical distribution in Iran. A total of 542 diakinesis/metaphase I (D/MI); 318 anaphase I/telophase I (AI/TI); 27 metaphase II (MII) and 505 anaphase II/telophase II (AII/MII) cells were analyzed. Only one population growing in the Fars (1450 m) existed at diploid level (based on $x = 13$) as confirmed from the presence of 13 medium sized bivalents in the PMCs at MI (Fig. 10). These bivalents showed regular segregation during anaphase I. Further meiotic course was also regular resulting into normal tetrad formation, nearly percent pollen fertility and uniform sized pollen grains. The aneuploid cytotype has been found to be more common as confirmed from the presence of meiotic chromosome number of $x = 14$ in two out of the three populations scored presently from the different localities in the Iran. These aneuploid individuals in the populations unequivocally showed the presence of 14 bivalents in the PMCs (Figs. 1, 18). All taxa studied here displayed regular bivalent pairing and chromosome segregation at meiosis. However; some meiotic abnormalities were observed. The meiotic irregularities observed in different *D. harra* included the occurrence of varied degree of fragmented chromosome to poles and chromosome stickiness (Table 2).

Table2. Characterization of meiotic behavior and pollen viability in populations of *Diplotaxisharra*

Meiotic characters	HAR49	HAR84	HAR03
Cell number	360	507	628
D/MI	94	143	305
% D/MI	26.11	28.20	51.75
% Fragmented chromosome	0	0	5.27
AI/TI	32	183	103
% AI/TI	8.88	36.09	16.40
% Chromosome stickiness	60	11.18	0
MII	2	25	0
% MII	0.55	4.93	0
AII/TII	184	139	182
% AII/TII	51.11	27.41	28.98
N	14	13	14
% Pollen viability	46.37	54.21	49.37

Pollenviability

The results of the comparison between the meiotic behavior and pollen viability showed the highest (54.21) and lowest (46.37) percentages of the stained pollens in HAR84 and HAR49; respectively. This result indicates that irregularities observed at meiosis probably have a direct relation with species fertility. The pollen viability of examined species is described in Table 2 and illustrated in figures 25, 26 and 27. Chromosome stickiness coupled with associated meiotic abnormalities and consequent abnormal microsporogenesis resulted into high pollen sterility (Table 2) and smaller sized pollen grains (Fig. 25).

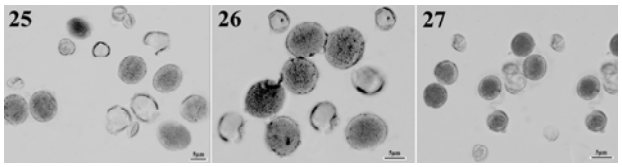

Figures 25-27: Pollen viability. (25) sterile pollen grains among fertile pollen grains in HAR49, (26) HAR84, (27) HAR03. Scale bar = 5 µm.

Discussion

Chromosomenumber and meiotic behavior

All populations are diploid and possess *2n* = *2x* = 26, *2n* = *2x* = 28 chromosome number, which is consistent with the proposed basic number of *x* = 13. The present diploid (*2n* = 26) and aneuploid (*2n* = 28) chromosome counts for the species from this region of the Iran, explored for the first time, agree with the earlier reports from other regions of Iran. Based on *x* = 13 another proposed basic number for

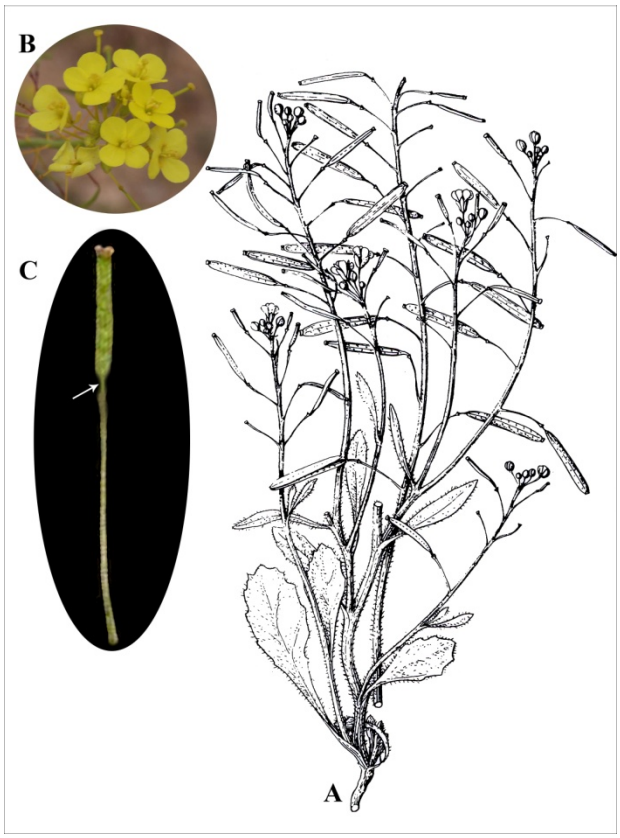

Figures 28. *Diplotaxisharra* (Forssk.) Boiss. (A) Plant, (B) Close up flowers, (C) Close up glabrous fruits and gynophore [illustration 28A through the courtesy of Flora of Iraq 4 (2): 860].

Diplotaxisharra a diploid (Warwick and Al-Shehbaz 2006). It is thus apparent that the species exhibits considerable degree of variability in chromosome number in the Iran. In addition to the presence of intraspecific cytotypes, the species also showed the existence of diploid and aneuploid chromosomal races (*2n* = 26, *2n* = 28) at basic number of *x* = 13 and *x* = 14. Consequently, the individuals of diploid and aneuploidy cytotypes of *D. harra* can't be distinguished from each other in the field. Meiosis is highly coherent and the process is genetically programmed, which comprises of pairing homologous chromosomes, crossing over, reduced in chromosome number, and lacking of S period between the two divisions. Similar to any other biological process, all the sequential steps involved in meiosis are controlled by a large array of genes (Ramana, 1974; Mok and Peloquin, 1975; Mok et al., 1976; Koduru and Rao, 1981; Falistocco et al., 1995). Mutation in any of these genes that govern micro or megasporogenesis from pre-meiotic to post meiotic events can lead to serious anomalies in the whole process resulting in the genetically aberrant end products having an adverse impact on fertility and overall reproductive efficiency of the species (Lattoo et al., 2006).

Stickychromosomes

Sticky chromosomes were observed in two studied populations with different frequencies (Figs. 2, 3, 7, 11, 12, Table 2). Chromosome stickiness may be caused by genetic and environmental factors, and several agents have been reported to cause chromosome stickiness (Pagliarini, 2000). Chromosome stickiness also resulted in the formation of pycnotic chromatin at earlier stages of prophase I and chromatin bridges at anaphase/telophase. The normal functioning of spindle apparatus is crucial for chromosome alignment during metaphase and correct segregation of chromosomes to poles (Shabrangi et al., 2010). Disturbed spindle apparatus orientation may have resulted in scattered and disoriented chromosomes in the meiocytes.

Genetic as well as environmental factors have been considered as the reason for chromosome stickiness in different plant species (Nirmala and Rao, 1996). They are characterized by their agglomeration in different stages of the cell cycle and can occur due to the presence of mutant genes or abiotic factors as X-rays (Steffensen, 1955; 1956), gamma irradiation (Rao and Rao, 1977; Al Achkar et al., 1989), temperature, herbicides (Badr and Ibrahim, 1987) and some chemical elements present in soil (Steffensen, 1956; Zanella, 1991; Caetano-Pereira et al., 1995). Another hypothesis is that chromosome stickiness may be caused by a failure or a bad functioning in one or two types of non-

histone chromosomal proteins (Peres Kiihl et al., 2011). The highest frequency of chromosome stickiness of anaphase I and telophase I cells was observed in population of HAR49 (Figs. 2, 3, 7, Table 2). The lowest degree of chromosome stickiness occurred in population of HAR84 (Figs. 11, 12, Table 2).

Fragmented chromosomes (Precocious migration)

There was another abnormality in metaphase I (Fig. 20). The highest frequency of fragmented chromosomes of metaphase I cells was observed in HAR03 population (Table 2). The highest and lowest abnormalities were seen in populations of HAR49 and HAR03, respectively.

Pollenviability

Furthermore, many abnormalities affecting plant fertility or causing total male sterility have been detected during the evaluation of meiotic behavior in some species. There is a difference in the pollen grain size of the diploid cytotype and in the two populations (Fig. 26) of the aneuploidy cytotype where the typical pollen grains were similar in smaller size as that of the diploid cytotype. So, the aneuploid increase can be concluded in the pollen grain size of populations in HAR49 and HAR03.

Different sized pollen grains in other populations of the aneuploidy cytotypes are the product of various meiotic abnormalities abnormal microsporogenesis. Consequently, very high pollen sterility and fertile pollen grains of two heterogeneous sizes were resulted. This result is predictable based on meiotic behavior data and of the lowest percentages of irregularities in these populations (Table 2). In contrast, a low percentage of pollen viability (46%) in population of HAR49 can be explained by having a high percent of sticky chromosomes. In this population a relatively high frequency of chromosome stickiness in different stages of meiosis and consequently, low pollen viability was observed. So, it can be concluded that sticky chromosomes affects the meiotic course considerably and results in reduced pollen viability, also showed that there is a direct relationship between occurrence of sticky chromosomes and reduced pollen viability. The pollen viability of examining populations is described in Table 2 and illustrated in figures 25, 26 and 27.

Acknowledgment

The field work in Iran was supported by the grants from the Bu-Ali Sina University.

References

1- Al Achkar W., Sabatier L. and Dutrillaux B. (1989) How are sticky chromosome formed? Annales de génétique 30: 10-15.
2- Al-ShehbazI. (1978) Chromosome number reports in certain Cruciferae from Iraq. Journal of Biological Sciences 6: 26-31.
3- Al-Shehbaz I. (2012) A generic and tribal synopsis of the Brassicaceae (Cruciferae). Taxon 61: 931-954.
4- Al-Shehbaz I. and Al-Omar M. (1982) In IOPB chromosome number reports LXXVI. Taxon 31: 587-589.
5- Appel O. and Al-Shehbaz I. (2003) Cruciferae. In: Kubitzki K. and Bayer C. eds., In: The families and genera of vascular plants. Springer, Berlin.
6- Badr A. and Ibrahim A. (1987) Effect of herbicide glean on mitosis, chromosomes and nucleic acids in *Allium cepa* and *Viciafaba* root meristems. Cytologia 52: 293-302.
7- Baptists-Giacomelli F., Pagliarini M. and Almeida J. (2000) Elimination of micronuclei from microspores in a Brazilian oat (*Avena sativa* L.) variety. Genetic Molecular of Biology 23: 681-684.
8- Caetano-Perira C., Pagliarini M. and Brasil E. (1995) Influence of aluminium in causing chromosome stickiness in *maize* microsporocytes. Maydica 40: 324-330.
9- Falistocco E., Tosti N. and Falcinelli M. (1995) Cytomixisin pollen mother cells of diploid *Dactylis*, one of the origins of 2n gametes. Cytologia 86: 448-453.
10- Gomez-Campo C. (1999) Taxonomy. In: Gomez-Campo C. ed., Biology of Brassica coenospecies. Elsevier, Amsterdam.
11- Hedge I. (1968) Brassicaceae. In: Rechinger K. H. ed., Flora Iranica, vol. 57.AkademischeDruck-u. Verlagsanstalt, Graz.
12- Hedge I., Lamond J. and Townsend C. (1980) Cruciferae. In: Flora of Iraq eds. Townsend C. and Guest E., Flora Iraq. 4(2). Ministry of Agriculture and Agrarian Reform, Baghdad.
13- Koduru P. and Rao M. (1981) Cytogenetics of synaptic mutant in higher plants. Theoretical and Applied Genetics 59: 197-214.
14- Lattoo S., Khan S., Bamotra S. and Dhar A. (2006) Cytomixis impairs meiosis and influences reproductive success in

Chlorophytumcomosum (Thunb) Jacq., an additional strategy and possible implications. Journal of Bioscience 31: 629-637.

15- Malallah G. and Attia T. (2003) Cytomixis and its possible evolutionary role in a Kuwaiti population of*Diplotaxisharra* (Brassicaceae). Botanical Journal of the Linnean Society 143(2): 169-175.

16- Mok D. and Peloquin S. (1975) The inheritance of three mechanism of diplandroid (2n pollen) formation in diploid potatoes. Heredity 35: 295-302.

17- Mok D., Peloquin S. and Mendiburu A. (1976) Genetic evidence for mode of 2n pollen formation and S-locus mapping in potatoes. Potato Research 19: 157-164.

18- Nirmala A. and Rao P. (1996) Genetics of chromosome numerical mosaism in higher plants. The Nucleus 39: 151-175.

19- Peres Kiihl P. (2011) Chromosome stickiness during meiotic behavior analysis of *Passifloraserrato-digitata* L. (Passifloraceae). Ciência Rural 41: 1018-1023.

20- Polatschek A. (1983) Chromosomenzahlen und hinweise auf systematik und verbreitung van Brassicaceae-Artenaus Europa, Nordafrika, Asien und Australien. Phyton (Horn) 23: 127–139.

21- Ramana M. (1974) The origin of unreduced microspores due to aberrant cytokinesis in the meiocytes of potato and its genetic significance. Euphytica 23: 20-30.

22- Rao P. and Rao R. (1977) Gamma-ray induced meiotic chromosome stickiness in tomato. Theoretical and Applied Genetics 50: 247-252.

23- Shabrangi A., Sheidai M., Majd A., Nabiuni M. and Dorranian D. (2010) Cytogenetic abnormalities caused by extremely low frequency electromagnetic fields in canola. Science Asia 36: 292-296.

24- Snogerup B. (1985) Chromosome Number Reports LXXXIX. Taxon 34: 727-730.

25- Steffensen D. (1955) Breakage of chromosomes in *Tradescantia* with calcium deficiency. Proceeding of Natural Academy Science of USA 41: 155-160.

26- Steffensen D. (1956) Effects of various cation imbalances on the frequency of x-ray induced chromosomal aberrations in *Tradescantia*. Genetics 42: 239-252.

27- Warwick S. and Al-Shehbaz I. (2006) Brassicaceae: chromosome number index and database on CD-Rom. Plant Systematics and Evolution 259: 237-248.

28- Warwick S. and Sauder C. (2005) Phylogeny of tribe Brassiceae (Brassicaceae) based on chloroplast restriction site polymorphisms and nuclear ribosomal internal transcribed spacer and chloroplast trnL intron sequences. Canadian Journal Botany 83: 467-483.

29- Wilson G. (1945) The venetian turpentine mounting medium. Stain Technology 20: 133-135.

30- Zanella C. (1991) Differential effect of soil acidity and lime treatment on the chromosomes of two wheat cultivars. Brazil journal Genetics 14: 1021-1032.

Journal of Cell and Molecular Research (2014) 6 (2), 99-102

Research Report

Genetic analysis of *ND4* and *ND4L* regions of mitochondrial genome in Khorasan native chickens

Morteza Hashemi Attar and Mohammadreza Nassiri*

Department of Animal Science, Ferdowsi University of Mashhad, Mashhad, Iran.

Received 14 Mar 2014 Accepted 25 Apr 2014

Abstract

Preserving genetic diversity of Iranian native chickens is significant in order to perform breeding programs and improved production. Genetic diversity among close populations can be determined by investigating their phylogenetic relations. Different approaches have been applied to determine the phylogenic relations from which genomic sequencing has been considered the most functional approach. In this project, we aimed to evaluate the phylogeny and genetic nucleotide sequences of *ND4* and *ND4L* regions in mitochondrial genome of Khorasan native chickens. Blood samples were collected from 6 random populations and their genomic DNAs were extracted. Results showed that there is no haplotype difference between the studied samples. Lowest genetic distance was observed between Khorasan native chicken and other Asian chickens i.e. Jiangbian, Lvenwv and Red jungle fowl for the *ND4* and *ND4L* genes indicating their close relationship.

***Keywords*:** Khorasan native chicken, *ND4L*, *ND4*, Mitochondrial DNA, Phylogeny tree

Introduction

There are more than 100 native fowl genetic masses in Iran adjusted to environmental conditions. They have obtained relative resistance to local diseases and are considered as important national wealth. These native chickens are genetic reserve and their protection for next generations needs an extensive study (Tavakolian, 1999). There are two hypotheses about the origin of domestic chickens, first, these are originated in gallus gallus or these were derived from several gallus subclass (Crwford1990). Mitochondrial genome sequencing has been considered the most functional method to determine the phylogeny relationship among their different populations and species (Bruforrd et al 2003). A lot of comparing tests have been conducted for different regions sequencing, genetic diversity and species developmental origin using mitochondrial genome. *ND4* (NADH dehydrogenase subunit 4) and *ND4L* (NADH-ubiquinone oxidoreductase chain 4L) are 459 and 98 amino acids containing proteins encoded by mitochondrial region's encoding genes to make NADH_COQ, the respiratory chain protein which is responsible to transfer electrons from NDAH to respiratory chain (Zhang et al 2000). The purpose of this project was phylogeny analyzes of *ND4* and *ND4L* regions of mitochondrial DNA of Khorasan native chickens.

Materials and Methods

Sampling:

Blood samples were collected from 6 Khorasan native chickens and unrelated chickens to ensuring their relationships. Blood samples were stored in EDTA containing tubes at -20^{0}C. DNA was extracted using commercial kit (Thermo, USA). Quantitative and qualitative assessment was done according to spectrometry method using nanodrop–ND 2000 spectrophotometer (Thermo, USA) and running on 1% agarose gel. *ND4* and *ND4L* regions were amplified using their specific primers as shown in table 1.

Polymerase chain reactions (PCR) were carried out to amplify *ND4* and *ND4L* using T-personal model Biometra thermo cycler according to the standard method. The components of PCR mix (25-µl)were as, 100 ng DNA, 0.2 unit *Taq* polymerase enzyme, 2 µl dNTP (10 mM), 1.5 µl MgCl2 and 1 pmol gene specific primers (50 mM). In order to confirm the amplification, samples were electrophoresed on 1% agarose gel. PCR program for*ND4L* fragment was adjusted as,94 ^{0}C for 30s (denaturation), 54^{0}C for 35s (annealing), 72^{0}C for

Corresponding authors E-mail:
* *E-mail: nassiryr@um.ac.ir*

30s (amplification) till 35 cycles, a primary step at 94°C for 10 min and a final amplifying stage at 72°C for 10 min, PCR program for *ND4* gene was adjusted as 94 °C for 30s (denaturation),56°C for 35s (annealing), 72 °C for 30s (proliferation) till 35 cycles, a primary step at 94°Cfor 10 min and a final amplifying stage at 72°C for 10 min. PCR products were electrophoresed on1% agarose gel which was strained by ethidium bromide (EtBr). ١٠٠ µl of PCR product was purified and sent for sequencing (Macro Gen company, South Korea) with 50 µl of each used primers. These samples were sequenced using the ABI3130 machine according to Sanger automated approach. The obtained sequences homology level was measured using accurate BLAST tool method in NCBI database. In order to study the phylogenetic relation between target breeds, we draw the phylogeny tree using the alignment sequences UPGMA approach by MEGA 5.1 software**.**

Table 1. Specific primers for *ND4L* and *ND4* region using Primer premier-5.

Primers	Sequence
Forward (*ND4L*)	5´- TTCACATTCAGCAGCCTAGGACT-3`
Reverse (*ND4L*)	5`- GCTTTAGGCAGTCATAGGTGTAGTC-3`
Forward (*ND4*)	5`- ACCTACCTGCCTCCTGAACAA-3`
Reverse (*ND4*)	5`-TCTGGTTTGAGGATGAGTGTTAGTA-3`

Results

The quality of extracted DNA was confirmed by spectrophotometery. Electrophoresis of amplified fragments on 1% agarose resulted in the bands of *ND4* and *ND4L* fragments as 913bp and 802 bp respectively, showed the correct size of *ND4* and *ND4L* fragments as shown in figure 1. Sequencing of *ND4* and *ND4L* regions was performed for 6 samples. After sequencing, their alignment was compared using Glusta multiplie alignment tool of Bio Edit 7.2.2 software. The 891and 707 fragments were used in all the samples as the consensus sequence for *ND4L*, *ND4* regions respectively. Comparative analysis of the obtained sequences by these tools revealed that there is no difference between the studied sequences (p=0).Probably it was resulted from few samples or homogenization of the mass because of permanent selection according to commercial goals for several generations.*ND4L* sequence nucleotide compound was calculated as A 30%, C 36%, G 10% and T 24%, indicating the 46% and 54% frequency for G+C and A+T respectively (figure 3).

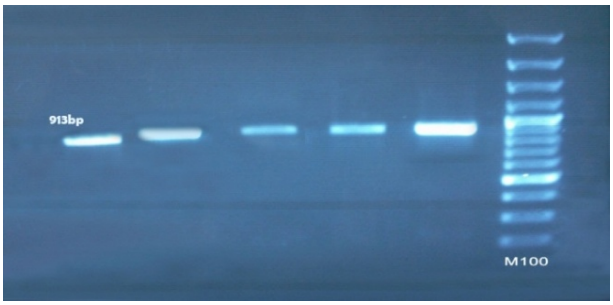

Figure 1A. Electrophoresis of 913 bp PCR Products on 1 % agarose gel

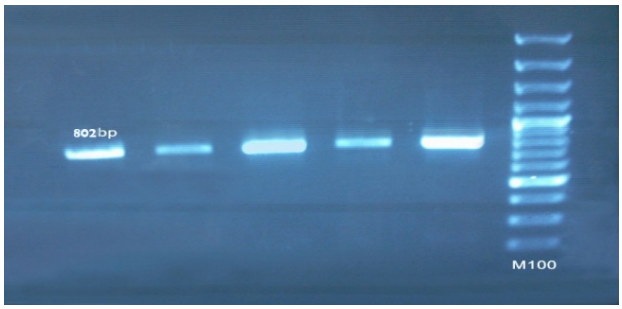

Figure 1B. Electrophoresis of 802 bp PCR Products on 1 % agarose gel

A+T and G+C frequencies were calculated for *ND4* as 23%, 12%, 36%, 29, and the 48, 52% frequency in relation to G+C and A+T, respectively (figure 4).

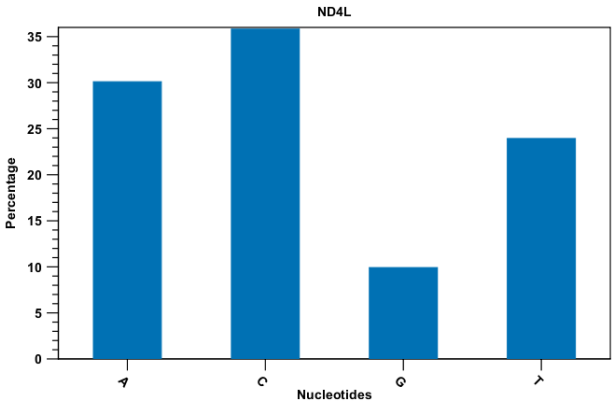

Figure 3. Frequency percentage for constituent nucleotides at *ND4* Lconsensus sequences in Khorasan native chickens.

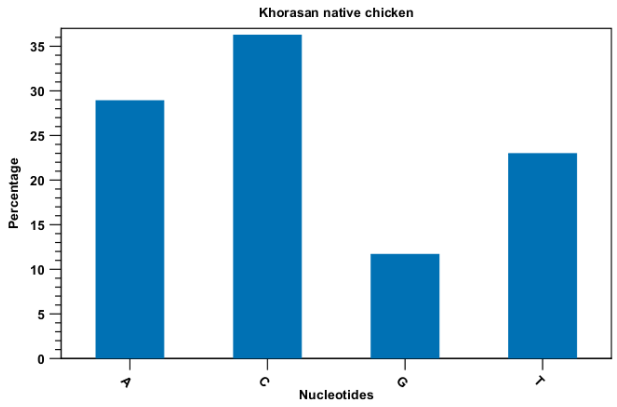

Figure 4. Frequency percentage for constituent nucleotides at *ND4* consensus in Khorasan native chickens.

The constructed phylogenetic tree revealed that *ND4L* region's sequence of Khorasan native chickens comparing with Asian chicken breeds was close to Jiangbian, Lvenue, Red and jungle fowl. Furthermore, results showed that all of them are belonging to the same group except of Nixi breeds (figure 5).

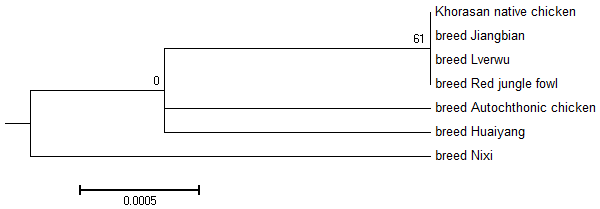

Figure 5. Phylogenetic tree of *ND4L* consensus sequence of Khorasan native chicken and other breeds

Furthermore, the results of *ND4* gene phylogenetic tree showed that mitochondrial genome of Khorasan native chickens are close to Autochtonic, jiangbian, Lvenwva and red jungle fowl, and belonged to the same group but differences were observed with Tulufan and Huaiyang gushi breeds(figure 6).

Studying the *ND4L* region's genetic matrices of mitochondrial genome of Khorasan native chickens indicated that there was lowest genetic distance between Khorasan native chickens and Jiangbian, Lvenwv, Red jungle fowl and Autochthonic chickens. Genetic distance between Khorasan native chickens with Nixi and Huaiyang chickens was also observed (Table 2).

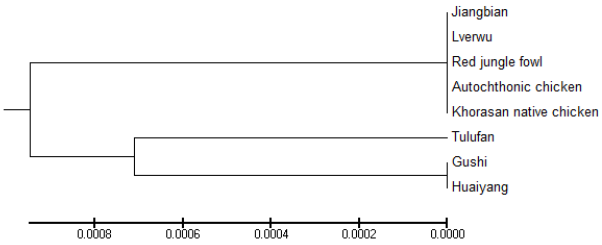

Figure 6. Phylogenetic tree of *ND4* consensus sequence of Khorasan native chicken and other breeds

Table 2. Nucleotide similarities and differences matrix of *ND4L* gene in Khorasan native chickens in relation to other breeds

	1	2	3	4	5	6	7
Khorasan native chicken 1		0	0	0	2	3	2
breed Jiangbian 2	100.00		0	0	2	3	2
breed Lv'erwu 3	100.00	100.00		0	2	3	2
breed Red jungle fowl 4	100.00	100.00	100.00		2	3	2
breed Autochthonic chicken 5	99.78	99.78	99.78	99.78		3	2
breed Nixi 6	99.66	99.66	99.66	99.66	99.66		3
breed Huaiyang 7	99.78	99.78	99.78	99.78	99.78	99.66	

Matrix of *ND4* region's genetic distances of mitochondrial genome indicated that there is a little genetic distance between Khorasan native chickens and Authochthonic, Jiangbian, Lvenwv and Red jungle fowl chickens. A huge distance was observed between them with Tulufan and Huaiyang Gushi (Table 3).

Table 3. Nucleotide similarities and differences matrix of NDL gene in Khorasan native chickens in relation to other breeds

	1	2	3	4	5	6	7	8
Khorasan native chicken 1		1	1	2	2	1	1	3
Autochthonic chicken 2	99.86		0	1	1	0	0	2
Red jungle fowl 3	99.86	100.00		1	1	0	0	2
Gushi 4	99.72	99.86	99.86		0	1	1	1
Huaiyang 5	99.72	99.86	99.86	100.00		1	1	1
Jiangbian 6	99.86	100.00	100.00	99.86	99.86		0	2
Lv`erwu 7	99.86	100.00	100.00	99.86	99.86	100.00		2
Tulufan 8	99.58	99.72	99.72	99.86	99.86	99.72	99.72	

Discussion:

As we find out the genetic conservation of Khorasan native chickens, this genetic reserver may be helpful to enhance production capacity of native chickens and to increase their ability against variable environmental conditions and relative resistance to local diseases. Import of foreign modified breed may lead in the reduction of native chickens production which are the national asset themselves. It should be noted that using the

mentioned sequences and their registration in the world gene bank would be regarded as an indicator to determine native chicken breeds in the Khorasan regions of Iran.

Results showed nucleotide relative frequency in consensus sequences in *ND4* and *ND4L* regions of Khorasan native chickens is very close to nucleotides percentage with the registered domestic chicken mtDNA in NCBI database. Comparison of these obtained sequences with the registered sequences indicated that there are high overlapping and homology among these sequences. These findings showed that the sequenced regions in this study were same as in other studies.

The phylogeny tree of different Asian chicken breeds and genetic analysis of *ND4* and *ND4L*, lead us to the conclusion that these genes are very important to study the breeds and the genetic distances between the Khorasan native chicken. Also results are comparable with the findings of Silvia et al., 2008; Oluwabukola et al., 2005; Pirany et al., 2005 and Siming, 2011. Zardoya et al., 1996 suggested *ND4* as an ideal gene to analyze the mitochondrial proteins. They also considered the *ND4L* gene as a weak gene in phylogeny analysis. Our results indicated the genetic diversity among these populations.

References:

1. Bruford M. W., Bradley D. G. and Luikart G. (2003) DNA markers re-veal the complexity of livestock domestication. Nature Reviews Genetics 4: 900–10.
2. Chinnery P. F., Schon E. A. (2003). Mitochondria. J Neurol Neurosurg Psychiatry 74: 1188–1199.
3. Crawford R. D. (1990) Origin and history of poultry species. In: Poultry Breedingand Genetics. Ed. By RD Crawford. Elsevier, Amsterdam
4. Hong Y., Arpit M., Gaofeng W., William W., Hauswirth, V. C., Sanford L., Boye J. G. (2013) Next-generation sequencing of mitochondrial targeted AAV transfer of human *ND4* in mice. Molecular Vision 2013; 19:1482-1491.
5. Lolai P. (2001) Study of genetic diversityof Barbuscapito fish in Mazandaran and Gilan Province. M.Sc. Thesis. University of TarbiatModares, Tehran, Iran.
6. Mirhosseini S. Z. (1998) Study genetic diversity of Iranian Silkworm using protein and DNA Markers. Thesis. Ph.D. Tarbiat Modarres University
7. Mohammadipestebik F., Pirani N., Shoja J., Mohammadhashemi A. (2011) Determination the mtDNA D-loop Sequence in Marandi Native Chicken Population and Its Phylogenic Relationships with Other Breeds.ResearchJournal ofAnimal Sciences 21(2): 1-9.
8. Pirany N., Mohammadhashemi A., Alijani S., RezazadehGoli R., Ghanbari S. (2011) MolecularAnalysis of Mazandrani native chicken population based on HVR-I region of Mitochondrial DNA. Journal of Agricultural Biotechnology 1: 53-65
9. Silva P., Guan X., Ho-Shing O., Jones J., Xu J., Hui D., Notter D. and Smith E. (2008). Mitochondrial DNA-based analysis of genetic variation and relatedness among Sri Lankan indigenous chickens and the Ceylon jungle fowl (Gallus lafayetti). International Society for Animal Genetics, Animal Genetics 40: 1–9.
10. Tavakolian J. (1999) A look at livestock and chicken genetic pool of Iran. Animal Research Institute of Iran.
11. Zardoya R. and Meyer A., (1996) Phylogenetic Performance of Mitochondrial Protein-Coding Genes in Resolving Relationships among Vertebrates. Mol. Biol. Evol. 13(7): 933-942. 1996
12. Zhang S., Zhang Y., Zheng X., Chen Y., Deng H., Wang D., Wei Q., Zhang Y., Nie L., Wu Q. (2000) Molecular phylogenetic systematics of twelve species of Aci-penseriformes based on mtDNA *ND4L* — *ND4* gene sequence analysis.SCIENCE IN CHINA: Vol. 43 No. 2:129-139.

Journal of Cell and Molecular Research (2014) 6 (2), 103-104

Letter to Editor

Impact of MTHFR and RFC-1 gene in the development of neural tube defect

Rinki Kumari[1]*, Aruna Agrawal[1], Om Prakash Upadhyaya[2], Gur Prit InderSingh[3], Govind Prasad Dubey[1]

1. Dept. of Kriya Sharir, Faculty of Ayurveda Institute of medical Sciences, Banaras Hindu University, Varanasi UP, India
2. Health center, Institute of medical Sciences, Banaras Hindu University, Varanasi UP, India
3. Adesh University, Bhatinda, Punjab, India

Received 03 Jun 2014 Accepted 07 Jul 2014

Summary

Neural tube defects (NTDs) are complex problem of central nervous system including brain and spinal cord. Anencephaly and myelomeningocele are the two most common forms of NTDs. Epidemiological studies reveal that genetic and environmental factors are responsible for the development of NTDs. During embryogenesis large numbers of extrinsic and intrinsic factors are responsible for the closure of neural tube which is responsible to maintain the three germ layers including neural ectoderm. The role of MTHFR and RFC-1 gene in etiopathology of NTDs has not been clearly defined in Indian population. Hence, the curiosity has been developed with the aim to evaluate folate metabolism and folate regulatory gene in clinically diagnosed NTDs by using PCR based DNA analysis with selected specific forward/reverse primers. Interestingly, the highest frequency (12.5%) of CT has been appeared of MTHFR C677T gene noticed in NTDs mother. We also observed the similar frequency of heterozygous AG genotype in NTDs of A80G RFC-1 gene. Therefore, C and A allele have high prevalence among than other genotype. However, the mutation in MTHFR partially have protective effect of embryo and these selected candidate folate markers are responsible to influence the cells of neural crest confirming the folding of neural tube associated with severity of disease in NTDs.

***Keywords*:** NTDs, MTHFR, RFC-1, Folate, Homocystine

Dear Editor…

Low folate intakes and impaired folate metabolism play major role in the etiology of neural tube defects (NTDs), which is complex problem of central nervous system including brain and spinal cord. Anencephaly and myelomeningocele are the two most common forms of NTDs. Epidemiological studies reveal that genetic and environmental factors are responsible for the development of NTDs1. Periconceptional folic acid supplementation diminishes the risk of NTDs in new born baby. Mutation in 5, 10 methylenetetrahydrofolatereductase (MTHFR; 677→CT) gene, reduced enzymatic activity and results in increased plasma homocysteine levels. Such defects can be lowered by supplementing folic acid in the diet. Another gene, reduced-folate carrier-1 (RFC-1), has a critical role in anti-folate transport with resistance and higher affinity to reduce the folate, including the physiological substrate 5-methyltetrahydrofolate and oxidized folic acid 2-3. Still it is not absolutely clear how genetic and epigenetic factors regulate neural tube folding during neurogenesis. We studied the genotypic distributions and allele frequencies of MTHFR C677T and RFC-1 A80G with level of folic acid, RBC and homocysteine in the clinically diagnosed NTDs and in their mothers.

Blood for mutation analysis was obtained after written informed consent from study subjects NTDs and their mothers. The study was approved by ethical committee of the Institute medical sciences, Varanasi, India. The study population comprised of 50 subjects with NTDs, and their mothers (n=50). The control group consisted of 59 healthy infants with their mothers (n=59). Genotype analysis of the blood samples were done using polymerase chain reaction based DNA analysis with selected specific forward/reverse primers and allele specific restriction digestion(Hinf-I and HhaI; MTHFRC677T andRFC-1 A80G respectively), according to the method described by Frosst et al4 and Chang et al 20005. The total homocysteine

∗Corresponding author E-mail: *rinkiv3@gmail.com*

(tHcy) and folic acid in the NTDs cases from the plasma was determined by HPLC and fluorescence detector 6 and RBC investigated from central collection investigation laboratory, S.S. Hospital Varanasi.

Our data showed evidence for an association between the 677→C and A80G-RFC-1, with the occurrence of NTDs (table 1). The average concentration of plasma homocysteine are in higher (8.87 µmol/L) in the NTDs case as compared to the controls (5.65 µmol/L) whereas the level of folic acid and RBC are higher in controls than the cases. Interestingly, the highest frequency (12.5%) of CT has been appeared of MTHFR C677T gene noticed in NTDs mother and the similar frequency of heterozygous AG genotype in NTDs of A80G RFC-1 gene. Therefore, C and A alleles have high prevalence than other genotype. On the other hand, the mutations in MTHFR have partial protective effect on embryo and these selected candidates. Folate markers are responsible to influence the cells of neural crest, confirming the folding of neural tube associated with severity of disease in NTDs. Therefore, NTDs have multifactor origin of CNS disorders with common variant in more than one gene involved in folate and tHcy could interact to increase in infant's NTDs risk.

Table 1. Genotype and allele frequencies of MTHFR 677CT and RFC-1 in Indian subjects

Gene	**Genotype % frequency**			**Allele frequency**	
MTHFR C677T	***CC***	***CT***	***TT***	***C***	***T***
NTDs Cases	10	9.0	6.0	0.58	0.42
NTDs Mother	7.5	12.5	5.0	0.55	0.45
Control Child	24.7	7.0	2.9	0.81	0.18
Control Mother	27.1	6.4	1.1	0.87	0.12
RFC-1	***AA***	***AG***	***GG***	***A***	***T***
NTDs Cases	9	12.5	5.0	0.61	0.45
NTDs Mother	9	9.5	6.5	0.45	0.55
Control Child	7.0	6.4	1.1	0.29	0.06
Control Mother	25.3	7.0	2.3	0.83	0.16

Earlier studies have implicated susceptibility to NTDs due to the MTHFR and RFC-1 gene polymorphism. Folate supplement has potential effect in prevention and management of NTD and reduces the risk of the RFC-1 carrying variant. This study has important implications in the assessment of potential "risk factor" either due to folate deficient diet (nutritional factor) or unknown environmental factor responsible for NTDs and has been proven that mutant genotype has impact on the pregnancy outcome with possible maternal-foetal interaction. The results of this study indicate that 677→CT and RFC-1 mutation are responsible for NTDs in Indian patients.

References:

1. Botto L. D. and Yang Q. (2000) 5,10-Methylenetetrahydrofolate reductase gene variants and congenital anomalies: A HuGE review. Am J Epidemiol 151: 862–877.
2. Chango A., Emery-Fillon N., de-Courcy G. P. (2000) A polymorphism (G80-A) in the reduced folate carrier gene and its associationswith folate status and homocysteinemia. Mol Genet Metab 70: 310–315.
3. Fiskeratrand T., Refsum H., Kvalheim G., Ueland P. M. (1993) Homocysteine and other thiols in plasma and urine: automated determination and sample stability. Cli Chem 39:263-71.
4. Frosst P., Blom H. J., Milos R., Goyette P., Sheppard C. A., Matthews R. G. (1995) A candidate genetic risk factor for vascular disease: a common mutation in methylenetetrahydrofolate reductase. Nat Genet 10: 111–3.
5. Goldman I. D., Lichtenstein N. S., Oliverio V. T. (1988) Carrier-mediated transport of the folic acid analogue, methotrexate, in L1210 leukemia. J Biol Chem 243: 5007–5017.
6. Wald N., Sneddon J., Densem J., Frost J., and Stone J. (1991) Prevention of neural tube defects: results of the Medical Research Council Vitamin Study. Lancet 338: 131-137.

Scientific Reviewers

MANUSCRIPT PREPARATION

Manuscripts should be prepared in accordance with the uniform requirements for Manuscript's Submission to **"Journal of Cell and Molecular Research".**

Language: Papers should be in English (either British or American spelling). The past tense should be used throughout the results description, and the present tense in referring to previously established and generally accepted results. Authors who are unsure of correct English usage should have their manuscript checked by somebody who is proficient in the language; manuscripts that are deficient in this respect may be returned to the author for revision before scientific review.

Typing: Manuscripts must be typewritten in a font size of at least 12 points, double-spaced (including References, Tables and Figure legends) with wide margins (2.5 cm from all sides) on one side of the paper. The beginning of each new paragraph must be clearly indicated by indentation. All pages should be numbered consecutively at the bottom starting with the title page.

Length: The length of research articles should be restricted to ten printed pages. Short communication should not exceed five pages of manuscript, including references, figures and tables. Letters should be 400-500 words having 7-10 references, one figure or table if necessary. Commentaries and news should also be 800-1000 words having 7-10 references and one figure or table if necessary.

Types of Manuscript: JCMR is accepting original research paper, short communication reports, invited reviews, letters to editor, biographies of scientific reviewers, commentaries and news.

GENERAL ARRANGEMENT OF PAPERS

Title: In the first page, papers should be headed by a concise and informative title. The title should be followed by the authors' full first names, middle initials and last names and by names and addresses of laboratories where the work was carried out. Identify the affiliations of all authors and their institutions, departments or organization by use of Arabic numbers (1, 2, 3, etc.).

Footnotes: The name and full postal address, telephone, fax and E-mail number of corresponding author should be provided in a footnote.

Abbreviations: The Journal publishes a standard abbreviation list at the front of every issue. These standard abbreviations do not need to be spelled out within paper. However, non-standard and undefined abbreviations used five or more times should be listed in the footnote. Abbreviations should be defined where first mentioned in the text. Do not use abbreviations in the title or in the Abstract. However, they can be used in Figures and Tables with explanation in the Figure legend or in a footnote to the Table.

Abstract: In second page, abstract should follow the title (no authors' name) in structured format of not more than 250 words and must be able to stand independently and should state the Background, Methods, Results and Conclusion. Write the abstract in third person. References should not be cited and abbreviations should be avoided.

Keywords: A list of three to five keywords for indexing should be included at bottom of the abstract. Introduction should contain a description of the problem under investigation and a brief survey of the existing literature on the subject.

Materials and Methods: Sufficient details must be provided to allow the work to be repeated. Correct chemical names should be given and strains of organisms should be specified. Suppliers of materials need only be mentioned if this may affect the results. Use System International (SI) units and symbols.

Results: This section should describe concisely the rationale of the investigation and its outcomes. Data should not be repeated in both a Table and a Figure. Tables and Figures should be selected to illustrate specific points. Do not tabulate or illustrate points that can be adequately and concisely described in the text.

Discussion: This should not simply recapitulate the Results. It should relate results to previous work and interpret them. Combined Results and Discussion sections are encouraged when appropriate.

Acknowledgments: This optional part should include a statement thanking those who assisted substantially with work relevant to the study. Grant support should be included in this section.

References: References should be numbered and written in alphabetical order. Only published, "in press" papers, and books may be cited in the reference list (see the examples below). References to work "in press" must be accompanied by a copy of acceptance letter from the journal. References should not be given to personal communications, unpublished data, manuscripts in preparation, letters, company publications, patents pending, and URLs for websites. Abstracts of papers presented at meetings are not permissible. These references should appear as parenthetical expressions in the text, e.g. (unpublished data). Few example of referencing patterns are given as follows:

Bongso A., Lee E. H. and Brenner S. (2005) Stem cells from bench to bed side. World Scientific Publishing Co. Singapore, 38-55 pp.

Irfan-Maqsood M. (2013) Stem Cells of Epidermis: A Critical Introduction. Journal of Cell and Molecular Research 5(1): 1-2.

Note: All the reference should be in EndNote format (JCMR EndNote Style is available on JCMR's web site, Author's Guideline)

Tables and Figures: Tables and Figures should be numbered (1, 2, 3, etc.) as they appear in the text. Figures should preferably be the size intended for publication. Tables and Figures should be carefully marked. Legends should be typed single-spaced separately from the figures. Photographs must be originals of high quality. Photocopies are not acceptable. Those wishing to submit color photographs should contact the Editor regarding charges.

Black Page Charges: There is no black page charges for publication in the Journal of Cell and Molecular Research.

Color Page Charges: All color pages being printed in color will cost 1,000,000 Iranian Rials/page.

شرکت داروسازی
پارس تک رخ

Pars Tech Rokh
Pharmaceuticals
Reconciliation Between
Technology & Nature

- Herbs & Extracts
- Biotech Products
- Finished Products
- Natural & Biotech Based Cosmeticts

Lets join hand with us
To reconcil the Nature

www.parstechrokh.com

Adress: Hossein Yazdi St. 17
Kilometers of Asian Highway
Mashhad-Iran
Tel: +98 513 5420014-5
Fax: +98 513 5420014

کنگره سلول های بنیادی و پزشکی بازساختی

Stem Cells & Regenerative Medicine Congress

پژوهشگاه رویان
مرکز تحقیقات علوم سلولی

دانشگاه فردوسی مشهد

جهاد دانشگاهی
واحد خراسان رضوی

۳۰ اردیبهشت تا ۱ خردادماه ۱۳۹٤
مشهد مقدس-سالن همایش های
دانشکده علوم دانشگاه فردوسی مشهد

May 20-22, 2015
Conference Centre-
faculty of science-
Ferdowsi University of Mashhad, Mashhad, Iran

Stem Cells-2015

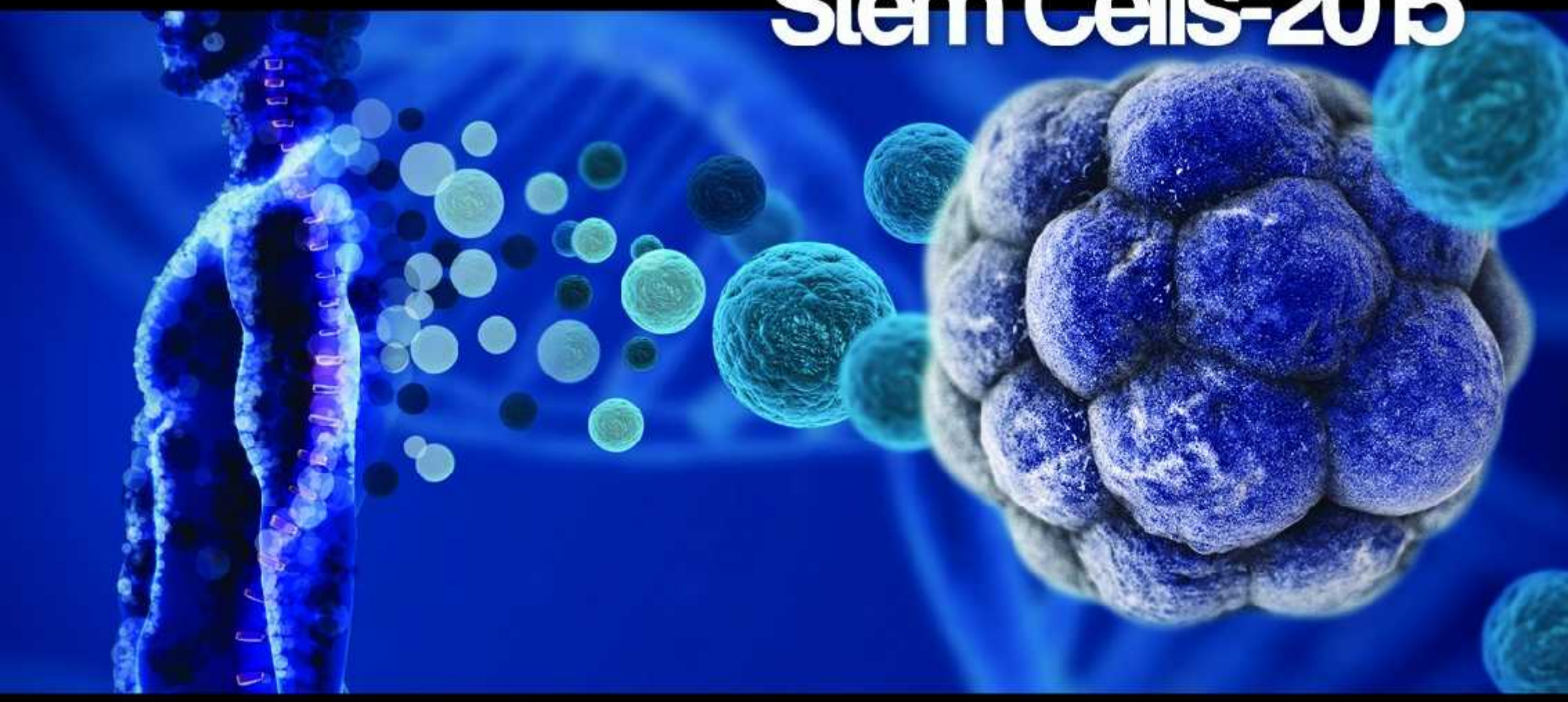

Main Topics of The Congress

- Reprogramming
- Epigenetics
- Stem Cells and Cancer
- Stem Cells Differentiation
- Immunology & Stem Cells
- Disease Modelling
- Migration and Engraftment
- Stem-Cells-Based Tissue Engineering
- Road to the Clinic
- Regulations of Stem-Cell-Based Therapies in IRAN
- Ethical & Moral Issues

- دارای امتیاز آموزش مداوم برای گروه‌های مختلف پزشکی
- همراه با برگزاری کارگاه های آموزشی تخصصی

با همکاری و حمایت:

آغاز پذیرش خلاصه مقالات: ۷ دی ماه ۱۳۹۳
مهلت ارسال خلاصه مقالات: ۱۵ اسفندماه ۱۳۹۳
شروع ثبت نام در کنگره: ۷ دی ماه ۱۳۹۳
پایان زمان ثبت نام زودهنگام: ۲۵ فروردین ماه ۱۳۹٤

Call for abstracts starts: Dec 28, 2014
Abstract submission deadline: Mar 6, 2015
Registration opens: Dec 28, 2014
Early registration deadline: Apr 14, 2015

دبیرخانه کنگره:
مشهد مقدس، پردیس دانشگاه، سازمان مرکزی جهاددانشگاهی خراسان رضوی
گروه پژوهشی سلولهای بنیادی و پزشکی ترمیمی
تلفکس: ۳۸۸٤۲۹۸۱-۰۵۱
www.mashhadstemcell.com